ROLE OF INDO-PACIFIC OCEAN IN REGULATING THE REGIONAL VARIABILITY OF INDIAN SUMMER MONSOON RAINFALL

Thesis submitted to the

University of Calicut

in partial fulfillment of the requirements for the award of the degree of

Doctor of Philosophy in Physics

Under the Faculty of Science

By

HRUDYA P. H.

Post Graduate and Research Department of Physics

Sree Krishna College, Guruvayur

Kerala

March 2021

Dedicated to

My Father and Mother

For their endless love, support, and encouragement

CERTIFICATE

This is to certify that the thesis entitled **'Role of Indo-Pacific Ocean in regulating the regional variability of Indian summer monsoon rainfall'** is an authentic record of the research work carried out by **Mrs. Hrudya P. H** under our supervision and guidance in the Department of Physics, Sree Krishna College, Guruvayur, in partial fulfillment of the requirements for the award of the degree of **Doctor of Philosophy in Physics**. We also certify that this is her original contribution and has not been submitted for the award of any degree or diploma in any other University or Institution.

Dr. Vishnu R
(Research guide)
Assistant Professor
Department of Physics
Sree Krishna College, Guruvayur

Dr. Hamza Varikoden
(Research co-guide)
Scientist-E, CCCR
Indian Institute of Tropical Meteorology
Pune

SREE KRISHNA COLLEGE GURUVAYOOR
ARIKANNIYUR
Date.....

DECLARATION

I hereby declare that the thesis entitled **'Role of Indo-Pacific Ocean in regulating the regional variability of Indian summer monsoon rainfall'** is a genuine record of research work done by me under the supervision and guidance of Dr. Vishnu R, Assistant Professor, Department of Physics, Sree Krishna College, Guruvayur, and under the co-guidance of Dr. Hamza Varikoden, Scientist-E, Indian Institute of Tropical Meteorology, Pune, in partial fulfillment of the requirements for the award of the degree of Doctor of Philosophy in Physics. I also declare that no part of this work has been previously submitted for the award of any degree or diploma in any other University or Institution.

Guruvayur
23/3/2021

HRUDYA P. H.

ACKNOWLEDGEMENTS

I wish to record my sincere thanks to all who supported me for the successful completion of this thesis entitled 'Role of Indo-Pacific Ocean in regulating the regional variability of Indian summer monsoon rainfall'.

Primarily, I express my sincere gratitude to my research guide Dr. Vishnu R, Assistant Professor, Department of Physics, Sree Krishna College, Guruvayur, for his valuable support and guidance provided throughout the research. My gratitude also extends to my research co-guide Dr. Hamza Varikoden, Scientist, IITM, Pune, who deserves special thanks, as this thesis would not have been possible without his kind support and help. His dedication, expert guidance, and encouraging suggestions have helped me to complete this work successfully.

I would like to thank Dr. Lovely M. R, Principal, Sree Krishna College, Guruvayur, and Dr. Ravi Nanjundiah, Director, IITM, Pune, for their support and providing necessary facilities for conducting this research.

I am very grateful to Prof. D. Jayaprasad, former Principal, Sree Krishna College, Guruvayur, for giving me permissions to carry out the research work at the Department of Physics, Sree Krishna College, and also for proving facilities and support.

I wish to thank Dr. Geetha K, HOD, Department of Physics, Sree Krishna College, Guruvayur, for her support and encouragement. I extend my thanks to all teaching and non teaching staff members of the Department of Physics, Sree Krishna College, for their corporation. I am also thankful to the research advisory committee members, whose continuous monitoring and support has helped a lot for the improvement of the research work.

My special thanks to Dr. Usha. K, Assistant Professor, Department of Physics, E. K. N. M. Govt. College, Elerithattu, Mrs. Vijayasree Haridas, Research scholar, Department of Chemistry, Govt. College, Pattambi, and Mrs. Sheema Dharmapal, Research scholar,

Department of Botany, Sree Krishna College, Guruvayur, for extending a helping hand whenever I needed. I also thank Mrs. Remani K. C, Assistant Professor, Department of Chemistry, Govt. College, Pattambi, for her valuable help, especially during the time of thesis submission. I am indebted to Dr. M. Nasser, Head of Directorate of Research, University of Calicut, and all staff members of Directorate of Research for their valuable help during different stages of research.

Most importantly, I wish to thank my parents Haridas and Sobha, and my sister Haritha, who have always been a constant source of energy, support, and love throughout my life. I would like to extend my thanks to my husband Vipin, for his love, patience, and support. Lastly, I thank my co-workers, friends, and all well wishers from the bottom of my heart for supporting me for the successful completion of this work.

HRUDYA P. H.

PREFACE

The livelihood of a large portion of Indian society depends on the monsoon. The term 'monsoon' has been a topic of research in the scientific community for the last few decades due to its inevitable role in agriculture and economic areas of the country. The Indian monsoon system is one of the important and most studied monsoon systems among all the global monsoons since it has significant teleconnections with the climate all over the tropics. The summer monsoon (southwest monsoon) over India from June-September contributes about 70-80% of annual rainfall over India and exhibits significant variations in temporal as well as regional scale. The influencing mechanisms for these variabilities include topography, different convective systems of the atmosphere, ocean-atmosphere interactions in the tropical oceans, etc. Since, most of the agricultural activities and water management of the country depend on the summer monsoon, understanding its variabilities and influencing mechanisms, particularly in regional scale is important. This thesis entitled the **'Role of Indo-Pacific Ocean in regulating the regional variability of Indian summer monsoon rainfall'** tries to explore the regional characteristics of Indian summer monsoon rainfall (ISMR), by identifying its influences from different oceanic and atmospheric parameters.

The structure of the thesis is as follows. **Chapter 1** gives the basic introduction to the Indian summer monsoon and its features, convective systems of atmosphere, ocean-atmosphere interactions in the tropical oceans, and the future projections of monsoon variability. The description of data and methodologies adopted for the thesis is given in **Chapter 2**. **Chapter 3** analyzes the variation of summer monsoon rainfall over different regions of India during the period 1950-2015, by analyzing its influence from different convective systems of the atmosphere. The relationship between lower tropospheric stability (LTS), cloud cover, and convective available potential energy (CAPE) with ISMR during the study period is analyzed separately for the west coast, northeast, northwest, and the central Indian regions. The interannual variations and trends of ISMR and convective parameters are analyzed together with their relationship with the El Niño Southern Oscillation (ENSO) in the tropical Pacific.

In **Chapter 4,** the influence of the tropical Pacific Ocean on the ISMR variability is analyzed by studying the ENSO-ISMR relationship and its changes from early to recent

decades. The influence of sea surface temperature (SST) and circulations during ENSO events on the ISMR variability is analyzed separately for the onset, peak, and withdrawal phases of ISMR. Since the ocean-atmosphere interactions in the tropical Indian Ocean are also an important driver of ISMR variability, the impact of Indian Ocean dynamics on ISMR is analyzed in **Chapter 5,** through the analysis of the teleconnections between the Indian Ocean Dipole (IOD) and ISMR. For this analysis also, the teleconnections were studied separately for onset, peak, and withdrawal phases of ISMR, and their changes were analyzed from early to recent decades. The features of SST, circulation features, and moisture transport over the Indian Ocean and the Indian region during different IOD events are also studied.

Numerical models are widely being used in the study of monsoon systems and their future projections. The future projections of ISMR variability are now widely carried out using Coupled Model Inter Comparison Project Phase 5 (CMIP5). This thesis has also used CMIP5 models to analyze the ISMR variability and ENSO-ISMR relationship in future decades in **Chapter 6**. The changes in ENSO-ISMR teleconnections in future decades and their influence from the tropical Pacific Ocean are analyzed under different warming scenarios. **Chapter 7** summarizes the findings of the thesis and describes future prospects of the work.

LIST OF PUBLICATIONS

1. **Hrudya PH**, Varikoden H, Vishnu R (2021) Changes in the relationship between Indian Ocean dipole and Indian summer monsoon rainfall in early and recent multidecadal epochs during different phases of monsoon. Int J Climatol 41:305-318. http://doi.org/10.1002/joc.6685

2. **Hrudya PH**, Varikoden H, Vishnu R, Kuttippurath J (2020) Changes in ENSO-monsoon relations from early to recent decades during onset, peak and withdrawal phases of Indian summer monsoon. Clim Dyn 55:1457-1471 http://doi.org/10.1007/s00382-020-05335-x

3. **Hrudya PH,** Varikoden H, Vishnu R (2020) A review on the Indian Summer Monsoon Rainfall, Variability and their Association with ENSO and IOD. Meteorol Atmos Phys 133:1-14. http://doi.org/10.1007/s00703-020-00734-5

4. **Hrudya PH**, Varikoden H, Vishnu R. Regional variabilities of rainfall and convective parameters during the summer monsoon period: Their linkage with El Niño Southern Oscillation. Meteorol Atmos Phys **(Revision submitted).**

5. Hamza Varikoden, **Hrudya PH**, Vishnu R, Kuttippurath J. Changes in the ENSO-ISMR relationship in the historical and future projection periods based on coupled models. Int J Climatol **(under review).**

CONFERENCE PRESENTATIONS

1. **Hrudya, P. H.**, Varikoden, H., Vishnu, R. (2018, September). Lower tropospheric stability and its influence on the Indian Summer Monsoon regional variability. National seminar on 'Advances in Applied Physics and Applications', Department of Physics, Sree Krishna College, Guruvayur.

2. **Hrudya, P. H.**, Varikoden, H., Vishnu, R. (2019, February). Regional variability of summer monsoon rainfall over India and its association with lower tropospheric stability. 31st Kerala Science Congress, Fathima Matha National College, Kollam.

3. **Hrudya, P. H.**, Varikoden, H., Vishnu, R. (2020, December). Changes in the relationship between El Niño Southern Oscillation and Indian summer monsoon rainfall in future decades. TROPMET 2020: National virtual Symposium on 'Weather and Climate Services over Mountainous Regions', NESAC, Shillong, Meghalaya.

4. **Hrudya, P. H.**, Varikoden, H., Vishnu, R. (2021, January). Impact of ENSO on the onset, peak and withdrawal phases of Indian summer monsoon rainfall and their changes from early to recent decades. Annual Monsoon E-Workshop and National E-Symposium on 'Cloud and Precipitation Processes', Indian Meteorological Society, Pune (**Paper was selected for best poster award**).

CONTENTS

LIST OF FIGURES

LIST OF TABLES

ABBREVIATIONS

AMO	Atlantic Multi-decadal Oscillation
APHRODITE	Asian Precipitation-Highly Resolved Observational Data Integration Towards Evaluation of Water Resources
AZM	Atlantic Zonal Mode
CAPE	Convective Available Potential Energy
CINE	Convective Inhibition Energy
CMIP5	Coupled Model Inter Comparison Project Phase 5
CRU	Climate Research Unit
DMI	Dipole Mode Index
ECMWF	European Centre for Medium-Range Weather Forecast
ENSO	El Niño Southern Oscillation
ERSST	Extended Reconstructed Sea Surface Temperature
ESGF	Earth System Grid Federation
HadISST	Hadley Centre Sea Ice and Sea Surface Temperature
HCC	High Cloud Cover
ICOADS	International Comprehensive Ocean-Atmosphere Dataset
IMD	India Meteorological Department

IOD	Indian Ocean Dipole
IPCC	Inter-governmental Panel on Climate Change
ISMR	Indian Summer Monsoon Rainfall
ITCZ	Inter Tropical Convergence Zone
LCC	Low Cloud Cover
LLJ	Low Level Jet
LTS	Lower Tropospheric Stability
MCC	Medium Cloud Cover
NCEP	National Centre for Environmental Prediction
NCEP	National Centre for Atmospheric Research
nIOD	negative IOD
NOAA	National Oceanic and Atmospheric Administration
PDO	Pacific Decadal Oscillation
pIOD	positive IOD
RCP	Representative Concentration Pathways
SST	Sea Surface Temperature
TCZ	Tropical Convergence Zone
VIMT	Vertically Integrated Moisture Transport
WCRP	World Climate Research Programme

CHAPTER 1

INTRODUCTION

CHAPTER 1

INTRODUCTION

1.1 Global monsoon: an introduction

The word ‘monsoon’ was derived from the Arabic word 'mausam' which means season. In the meteorological aspect, monsoon is considered as the seasonal reversal of winds and the associated precipitation. The changes in precipitation occur as a result of the differential heating of continental regions and the adjacent oceans, which drives the corresponding monsoonal winds from high pressure to low pressure areas in different seasons. The vorticity of the monsoonal winds due to the earth's rotation and the moist processes in the atmosphere are also considered as the driving mechanisms for the global monsoon system (Chandrasekar 2010). Monsoon is widely accepted as a global scale phenomenon rather than a regional phenomenon. As per the criteria given by Trenberth et al. (2000), the global monsoon system is a seasonally varying overturning circulation throughout the tropics. As per the definition given by the World Climate Research Programme (WCRP), the global monsoon domain is distributed over all tropical continents, and over the tropical oceans including the tropical western North Pacific, eastern North Pacific, and southern Indian Oceans. Monsoon is also manifested as a seasonal migration of Inter Tropical Convergence Zone (ITCZ)/monsoon trough (Gadgil 1988, 2003), which is simply defined as a band of convective clouds located near the equator. Since the livelihood of a large portion of the world’s population depends upon monsoon, its better understanding and prediction are important for better hydrological balance and water management. Extensive research has been carried out for the last few decades on monsoon systems. However, its complete understanding and prediction exist as a challenging problem, since it involves several internal and external dynamics including the complex interactions between ocean, atmosphere, and land.

1.2 Asian monsoon

The Asian monsoon system is considered as a large-scale coupled ocean-atmosphere phenomenon and is associated with distinct seasonal precipitation and circulation patterns (Meehl 1994; Wang and Fan 1999; Hu et al. 2000; Wang 2006; Hernandez et al. 2015). The climate variations in Asia are closely related to the Asian summer

monsoon variabilities (Hu et al. 2000). Different weather systems such as ITCZ, monsoon depressions, subtropical high and mid-troposphere cyclones affect the Asian monsoon variability (Wang 2006). The south Asian summer monsoon system (June-September) is a component of the Asian monsoon system and one of the most developed and studied monsoon systems among all other monsoons. Figure 1.1 shows the synoptic-scale weather system associated with the south Asian summer monsoon. These systems are responsible for the onset of summer monsoon during June, peak distribution of rainfall during July and August, and the withdrawal from mid-September to mid-October (Wang 2006).

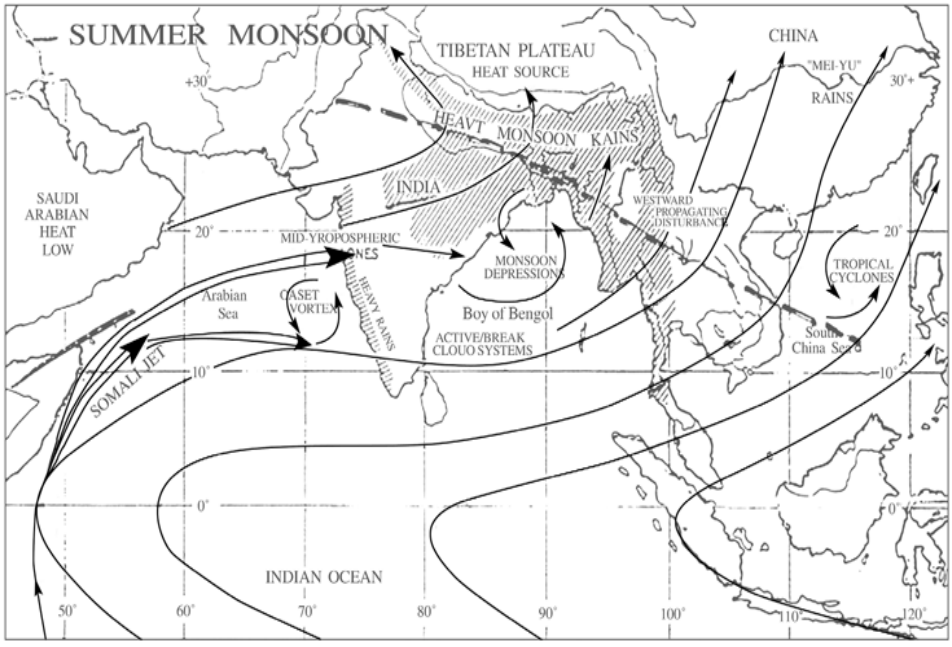

Figure 1.1: Major synoptic-scale weather systems associated with the south Asian summer monsoon (Wang 2006)

1.2.1 Annual cycle of monsoon

According to the study of Webster et al. (1998), the annual cycle of the Asian monsoon system is divided into 'wet' and 'dry' phases which correspond to the excess and deficit rainfall conditions, respectively, over the Asian domain. Gadgil (2003) has defined the annual cycle of the monsoon as a manifestation of the seasonal migration of ITCZ between the northern and southern hemispheres. ITCZ is a zone of low pressure near the equator, where the trade winds from both hemispheres converge. The northward

migration of ITCZ with seasons influences the weather conditions and circulation features of the Asian monsoon domain since a strong (weak) continental ITCZ provides wet (dry) conditions over the Indian region (Chandrasekar 2010).

1.3 The Indian monsoon system

The Indian region is identified as one of the most convectively active regions of the tropics (Jain et al. 2013). The Indian monsoon system, which is a component of the Asian monsoon system (Ghosh et al. 2009) is a large-scale tropical phenomenon (Jayakumar et al. 2017). The India Meteorological Department (IMD) has classified the monsoon systems in India into four major categories; Pre-monsoon (March-May), summer monsoon (June-September), post-monsoon (October-December), and winter monsoon (January-February). Since the summer monsoon rainfall is the major source of precipitation over India and has significant impacts on the agricultural and economic areas of the country, the present work has mainly focused on the Indian summer monsoon and its variability.

1.4 Indian summer monsoon

In India, most of the annual rainfall is contributed by the summer monsoon (southwest monsoon) which is from June-September. It is mainly driven by the differential heating of the Indian Ocean and the adjacent Asian landmass. When the land becomes warmer than the surrounding ocean, low-level winds carrying moisture blows from nearby oceans into land areas and result in precipitation over the Asian landmass including the Indian region. The summer monsoon rainfall over India is associated with synoptic-scale convective systems generating over the oceans that surround the Indian subcontinent, which propagates into the landmass (Gadgil 2003). I. e, the westward propagation of synoptic systems from the Bay of Bengal and the northward propagation of synoptic systems from the equatorial Indian Ocean maintain the continental Tropical Convergence Zone (TCZ) over the Indian region and hence sustain the summer monsoon rainfall over the region. The summer monsoon mean circulation is characterized by a low-level cyclonic vorticity (and convergence) and upper-level anti-cyclonic vorticity (and divergence) over the region (Goswami 2005a). The changes in Indian summer monsoon rainfall (ISMR) are associated with several teleconnections

that can affect the climate all over the world apart from the Indian region (Webster et al. 1998).

1.5 Features of Indian summer monsoon rainfall (ISMR)

1.5.1 Onset and withdrawal of ISMR

As per the criteria given by IMD, summer monsoon rainfall over India begins from Kerala on 1st June (known as the monsoon onset over Kerala) and the rainfall covers the entire country by the 1st July every year. Similarly, the withdrawal starts from northwest of India on 1st September and the rainfall withdraws from the country by the end of the season. Hence, the onset and withdrawal phases of the summer monsoon are usually considered as the months of June and September, respectively. Between these two phases, the maximum precipitation occurs over most of the Indian region during the months of July and August, which is called the peak phase of the summer monsoon. Figure 1.2 shows the normal onset and withdrawal dates of the Indian summer monsoon as defined by IMD.

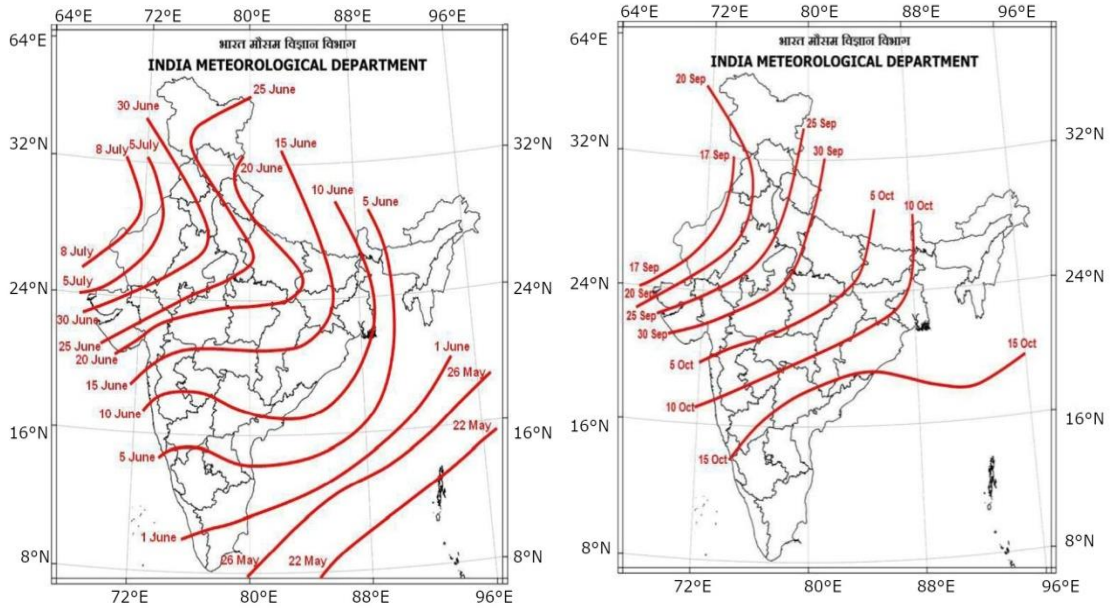

Figure 1.2: Normal onset (base period 1961-2019) and withdrawal (base period 1971-2019) dates of summer monsoon rainfall over India. Credit: https://mausam.imd.gov.in.

1.5.2 ISMR variability

The summer monsoon rainfall over India exhibits high variabilities in spatial and temporal scales. The mechanisms behind these variabilities include internal dynamics, the influence of land and oceans, and teleconnections to climate variability in other regions (Krishnamurthy and Kinter 2003). A detailed explanation of the spatio-temporal variabilities of ISMR is provided in the following sections.

1.5.2.1 Temporal variability

The temporal variation of ISMR includes variabilities in diurnal, interannual, intraseasonal, and interdecadal scales. However, the interannual and intraseasonal variabilities are more explored (Eg: Goswami and Ajayamohan 2001a; Sengupta et al. 2001; Goswami and Xavier 2005; Suhas et al. 2012). The year-to-year variability of ISMR is referred as the interannual variability whereas the variability within a season is called intraseasonal variability.

The predictability of the mean seasonal rainfall depends mainly on the interannual variability of the ISMR (Goswami et al. 2006a; Pillai and Chowdary 2016). The interannual variability of ISMR is mainly contributed by an externally forced component and an internal intraseasonal component (Krishnamurthy and Shukla 2000, 2007). Goswami and Ajayamohan (2001b) reported that the internal component arises from the interaction between the intraseasonal oscillations and the annual cycle. The intraseasonal variability is associated with active (periods of high rainfall) and break (periods of deficient rainfall) spells during the season (Goswami et al. 2006a; Taraphdar et al. 2010; Sinha et al. 2011). The intraseasonal variations are mainly composed of oscillations of 10 to 20 days (Chatterjee and Goswami 2004; Goswami 2005b) and 30 to 60 days time scales (Annamalai and Slingo 2001; Suhas and Goswami 2008). The 10 to 20 days oscillation is associated with the westward propagating convective systems entering the Indian region from the Bay of Bengal and the 30 to 60 days oscillation is associated with the northward propagation of convective systems to the Indian region from the equatorial Indian Ocean (Achuthavarier and Krishnamurthy 2011).

Since intraseasonal variability plays an important role in agriculture, economy, and water resource management, the prediction of active and break spells, their duration,

and intensities are highly relevant (Maharana and Dimri 2015). Goswami and Ajayamohan (2001b) indicated that the poor predictability of the ISMR is due to the contributions to interannual variability by the internal low-frequency variations. A clear understanding of the mechanisms responsible for the internal interannual variability is useful for improving seasonal mean prediction (Goswami and Xavier 2005). However, it remains as a challenging problem since the mechanisms behind the low-frequency internal variations have not been fully understood.

1.5.2.2 Spatial variability

The spatial variability of ISMR is associated with variations in precipitation from one region to another over the Indian domain. Previous works have shown that the summer monsoon rainfall shows high variabilities over different regions of India for the past few decades. From Figure 1.3, it is clear that during the summer monsoon, high values of precipitation are observed along the west coast and northeast regions of India, moderate values over the foothills of Himalayas and central Indian regions, and least values over the northwest and southeast regions.

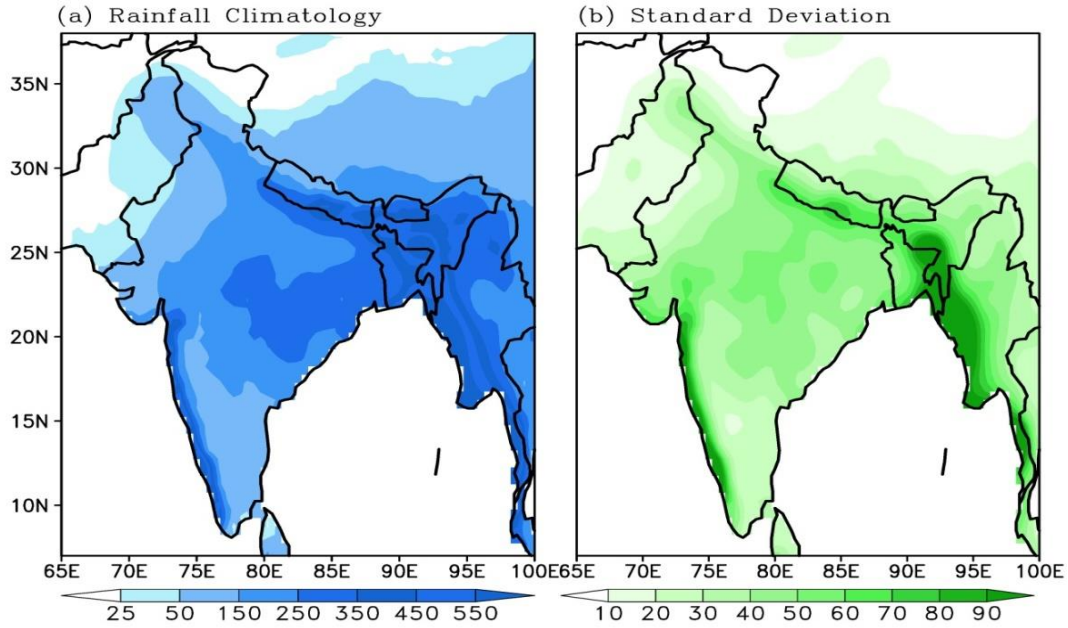

Figure 1.3: (a) ISMR climatology (mm) during the period 1901-2015 and (b) standard deviation (Figure plotted based on the precipitation data from climate research unit (CRU))

The amount of rainfall during the southwest monsoon varies spatially from 160 to 1800 mm $year^{-1}$ from the northwest to the northeast and from the far north to the extreme south (Kishore et al. 2015). The variations in ISMR over the Western Ghats, the Ganges basin, the Bay of Bengal, and Bangladesh-northeastern India were studied by Cash et al. (2015). They reported that ISMR varies independently in these four regions since the correlation in rainfall between the regions is not significant. A similar analysis was carried out by Kishore et al. (2015), but the regions considered were the west coast, east coast, interior peninsula, northeast, north-central, northwest, and the western Himalayas. They also reported significant incoherent variabilities from one region to region. Guhathakurtha and Rajeevan (2008) reported that ISMR showed large variations in regional scale during the period 1901-2003. In a similar study, Guhathakurtha et al. (2014) found multidecadal variability in ISMR over the northwest, central, northeast and peninsular India.

Konwar et al. (2012) observed asymmetry in trends of summer monsoon rainfall over the western (eastern) parts of India and found that the trends of low and moderate rainfall events are increasing (decreasing) in recent decades. They attributed it to the changes in vertically integrated moisture transport (VIMT) over the Arabian Sea and the Bay of Bengal. Varikoden et al. (2019) found an increasing (decreasing) trend in summer monsoon rainfall in the northern (southern) Western Ghats. They attributed that this contrasting trend is basically due to the shift of low-level westerlies over the region. Ghosh et al. (2016) reported that the trends in the spatial variability of mean summer monsoon rainfall are decreasing but that of extremes are increasing in recent decades.

The northeast regions of India show an increase in high-intensity rain events and a decrease in low-intensity rain events in recent years (Varikoden and Revadekar 2019). Ramesh and Goswami (2007) reported decreasing trends in summer monsoon rainfall over India and increasing trends in pre-monsoon and post-monsoon rainfalls. Das et al. (2014) found that the southern region of the Indian peninsula covering the Deccan plateau and east coast shows positive trends both in ISMR and rainy days. They reported a negative trend in both the parameters over the west coast (Kerala, coastal Karnataka), the eastern part (Jharkhand, Arunachal Pradesh), and the western desert region (east and west Rajasthan).

1.6 Internal and external drivers of ISMR variability

The spatio-temporal variability of ISMR is influenced by many internal as well as external drivers, such as the topography, convective systems in the atmosphere, and the influence from tropical oceans. However, the present study mainly focuses on the regional variability and its influencing factors since they were less explored in the previous works. The topography (influence from Tibetan Plateau, Himalayas, Western Ghats, etc.) of India plays an important role in the regional variations of summer monsoon rainfall. Apart from these, different convective systems of the atmosphere, such as cloud cover, lower tropospheric stability (LTS), and convective available potential energy (CAPE) also make significant impacts on ISMR variability.

Considering the case of external drivers, the mutual interactions between ocean and atmosphere over the tropical oceans are considered as one of the major external drivers of ISMR variability. The impacts of different tropical oceans on ISMR have been widely proved since the sea surface temperature (SST) and circulation features over the tropical oceans are well related to the variability of ISMR. Even though there are several internal and external drivers of ISMR regional variability, the present work mainly focuses on the analysis of the influence from the convective systems of the atmosphere, and the different ocean-atmosphere interactions in the tropical oceans, particularly from the Pacific and Indian Oceans.

1.7 ISMR and stability parameters

Atmospheric stability plays an important role in meteorological analyses since the stability conditions are closely related to cloud formation and convective precipitation. If an air parcel is warmer than the surrounding environment, it will be less dense than the environment and thus it will rise from the surface. Thus, the air is called unstable and helps to form convective clouds and storms. The opposite condition is observed in the case of stable air in which the air parcel is denser than the surrounding environment which leads the air parcel to sink. The third phase is neutral air, in which the air parcel has the same temperature as that of the environment so that it will not rise from the surface. These stability conditions are determined using the concept of lapse rate, which is the rate of change of temperature with respect to height in the atmosphere. It has been

proved that different convective parameters (stability parameters) of the atmosphere make significant impacts on the summer monsoon rainfall over India (Mani et al. 2009; Varikoden et al. 2011; Jayakumar et al. 2017; Jain et al. 2019). However, the present study has focused mainly on three convective parameters; cloud cover, LTS, and CAPE.

(a) Cloud cover

Clouds are an inevitable part of the earth's weather system and essential for the radiative balance of Earth (Zhang et al. 2009). The total cloud cover in the atmosphere is usually classified as low, medium, and high cloud covers (LCC, MCC, and HCC, respectively) depends upon their vertical extend. The vertical extent of LCC, MCC, and HCC is usually taken as 2000 m, 6000 m, and 12,000 m, respectively from the surface. Pokhrel and Sikka (2013) reported that about 99% of the total rainfall during the summer monsoon season is contributed by the stratiform and convective clouds. However, Sreekanth et al. (2019) classified the clouds as stratiform, convective, transition, and mixed clouds based on disdrometer and micro rain radar observations at Thiruvananthapuram, Kerala. They reported that the stratiform and convective clouds together contribute only about 65 % of the total rainfall during the summer monsoon, and the remaining rainfall is contributed by the transition and mixed clouds.

(b) Lower tropospheric stability (LTS)

LTS is defined as the difference in potential temperature between 700 h Pa and the surface (Slingo 1987; Klien and Hartmann 1993; Wood and Hartmann 2006; Varikoden et al. 2011), where potential temperature is the temperature that an air parcel would have attained if it is adiabatically brought to a standard reference pressure (usually the surface pressure, 1000 h Pa). LTS is considered as a measure of the strength of inversion that caps the planetary boundary layer (Wood and Bretherton 2006) and its variations have a major impact on low cloud fraction and thus the regional rainfall (Zhang et al. 2009). As LTS increases, it causes more moisture to be trapped within the lower troposphere (boundary layer) which enhances the cloud cover and thus the rainfall. The low-level stratiform cloud frequency has a significant positive correlation with LTS during the Indian summer monsoon (Varikoden et al. 2011). Sun et al. (2011) has proved that LTS can be used as a meaningful predictor of low cloud amount. In the

present climate scenario, there is a large increase in global warming and global SST, which decreases the stability of the lower troposphere and hence the low cloud amount (Ceppi and Gregory 2017).

(c) Convective available potential energy (CAPE)

CAPE is considered as a measure of how much energy an air parcel would have gained by being raised to a specific height in the atmosphere. In other words, CAPE is the positive buoyancy to be available for an air parcel to rise. The consumption of CAPE is associated with convective activity (Jain et al. 2019) and is essential for the formation of convective clouds**.** The association between CAPE and summer monsoon rainfall over central India and the Bay of Bengal in diurnal scale was studied by Jain et al. (2019). They found that the maximum CAPE occurs six hours prior to the precipitation over central India and 3 hours prior to the precipitation over the Bay of Bengal. Mani et al. (2009) reported a significant increase in CAPE during the summer monsoon over central India during the period 1901-2004 and they attributed this to the increase in convective instability of the atmosphere.

1.8 Role of Indo-Pacific Oceans on ISMR variability

Tropical oceans play an important role in maintaining global climate variability. Different coupled ocean-atmosphere phenomena generated in tropical oceans affect the global circulation changes and thus the regional climate variability (Yamagata et al. 2004). The ocean-atmosphere interactions have an important role in monsoon variability in which the ocean and atmosphere interact with each other through the exchange of heat and momentum. Therefore, it is highly relevant to understand the impact of different coupled ocean-atmosphere processes in the tropical Oceans on the variability of ISMR. The El Niño Southern Oscillation (ENSO), Indian Ocean Dipole (IOD), Atlantic multi-decadal oscillation (AMO), Atlantic zonal mode (AZM), Pacific decadal oscillation (PDO), etc. are widely recognized as the major coupled ocean-atmosphere processes in the tropical Oceans. ENSO and IOD phenomena are considered as the two major coupled ocean-atmosphere interactions in the tropical Pacific Ocean and the Indian Ocean, respectively, and also the most important external

drivers of ISMR variability. Details of the two processes are provided in the following sections**.**

Even though many studies have analyzed the link between ocean-atmosphere interactions and ISMR, the most robust results were observed in the studies focusing particularly on the ENSO-ISMR and IOD-ISMR relationships. The previous studies have provided evidence regarding how the SST conditions and circulation features over the Indian and Pacific Oceans affect the variability of ISMR, especially in the decadal and interdecadal scales. However, the present work mainly focuses on teleconnections in regional scale. I. e, it analyzes how the changes in the ocean-atmosphere processes in the Indo-Pacific domain (usually taken as, 40°E-300°E, 30°S-30°N) affect the summer monsoon rainfall over different regions of India separately.

1.8.1 SST variabilities over the tropical Pacific Ocean

SST is usually considered as a fundamental climate variable. The ISMR is controlled by the tropical pacific SST through an equatorial zonal circulation called Walker circulation (Shukla and Paolino 1983) and regional meridional circulation over the south Asian domain called Hadley circulation. The Walker and Hadley circulations are considered as the world's two prominent and important atmospheric zonal and meridional circulations, respectively. Walker circulation is an east-west zonal circulation in the lower atmosphere with ascending (descending) regions of air over the western (eastern) Pacific Ocean. On the other hand, Hadley circulation is manifested as the rising of heated air at the equator, and when it moves poleward, it cools, sinks, and moves to the equator. This circulation is modified by the earth's rotation and is associated with the propagation of trade winds. The impact of tropical Pacific Ocean SST on the ISMR variability can be studied by exploring the relationship between ENSO and ISMR.

1.8.2 El Niño Southern Oscillation (ENSO)

The ENSO phenomenon arises due to the mutual interactions between ocean and atmosphere over the tropical Pacific Ocean (Sikka 1980; Cherchi and Navarra 2013; Feba et al. 2018; Nair et al. 2018; Hrudya et al. 2020a; Seetha et al. 2020). The oceanic component of ENSO is called El Niño, whereas southern oscillation refers to the

atmospheric component. The term ‘El Niño’ refers to the unusual warming of the central and eastern equatorial Pacific Ocean relative to the west, whereas the southern oscillation refers to the corresponding changes happening in the atmospheric pressure conditions over the tropical Pacific Ocean. Figure 1.4 shows the three phases of ENSO; neutral, El Niño (positive phase), and La Niña (negative phase).

Under normal conditions (neutral phase), the western Pacific Ocean is characterized by high SST, high sea level pressure, and thus high cloud formation. However, opposite conditions are observed over the eastern Pacific Ocean. Under this condition, the easterly trade winds are strong and move warm water from the equatorial region to the western Pacific which leads to high SST, cloud formation, and convective precipitation over the region. This east-west zonal circulation in the equatorial Pacific is called the Walker circulation as explained in section 1.8.1. The El Niño and La Niña phases occur as a result of the changes in Walker circulation. An unusual warming or above-average SST conditions in the central and eastern tropical Pacific Ocean is called El Niño (means ‘Christ child’) which is the positive phase of ENSO. During an El Niño event, the low-level easterly surface winds weaken, and the Walker circulation is shifted eastward towards the eastern Pacific. The shift in Walker circulation produces corresponding changes in the regional Hadley circulation which causes enhanced subsidence and below normal rainfall over the Indian region.

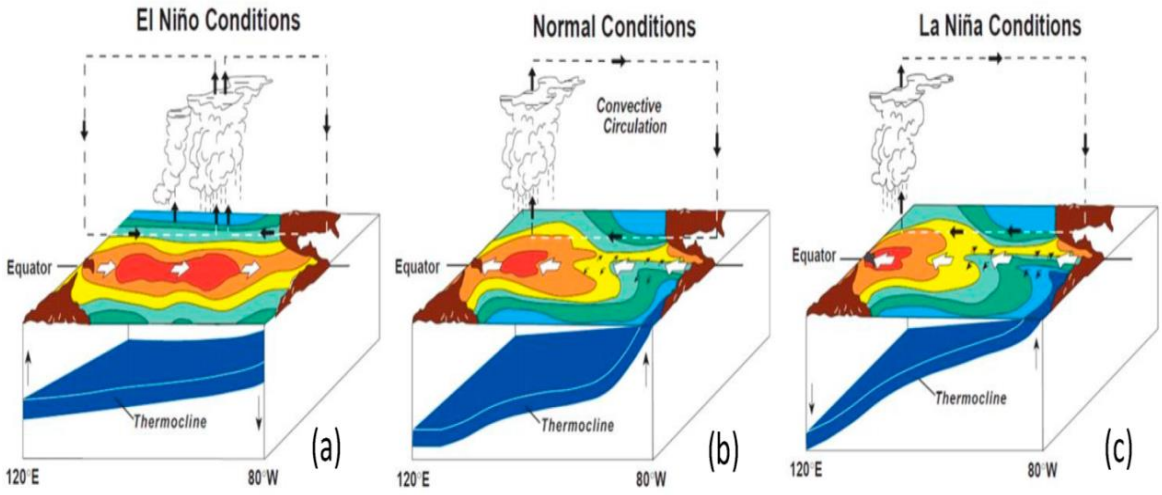

Figure 1.4: Schematic representation of El Niño, La Niña, and neutral phases of ENSO. Credit: https://www.pmel.noaa.gov.

On the other hand, the La Niña event (negative phase of ENSO) refers to the below-normal SST in the central and eastern tropical Pacific Ocean. During La Niña events, the low-level easterly surface winds strengthen and it enhances the ascending motion of air over the Indian region and thus the rainfall.

1.8.3 Impacts on ISMR

Previous works have proved significant relationships between ISMR variability with ENSO and thus with the tropical Pacific Ocean. It does not mean that the ENSO is the only driver of ISMR variability in the Pacific Ocean. However, the existence of ENSO as a major coupled ocean-atmosphere phenomenon in the tropical Pacific and its strong impact on ISMR variability was widely proved. Several studies have been undertaken in the last few years to understand ENSO and its impacts on ISMR variability (Slingo and Annamalai 2000; Lau and Nath 2000; Annamalai and Liu 2005; Guilyardi 2006; Xavier et al. 2007; Mishra et al. 2012; Ashok et al. 2019; Hrudya et al. 2020b). In most of the studies, the ENSO-ISMR relationship has been studied by connecting the ISMR anomalies to the SST anomalies over the tropical Pacific (Wang et al. 2003), since the SST anomalies act as intermediate to ocean-atmosphere coupling (Rao et al. 2002). Even though ENSO originates in the tropical Pacific Ocean, it affects the weather events across the globe (Guilyardi et al. 2009) and may be influenced by the ocean-atmosphere processes in other tropical oceans and extratropics (Liu and Alexander 2007). El Niño events are accompanied by a deficit Indian monsoon rainfall due to anomalous subsidence associated with a shift in the zonal Walker circulation (Ummerhofer et al. 2011). On the other hand, La Niña events are associated with excess rainfall conditions in the Indian region**.**

It is well observed that the changes in the Walker and Hadley circulations are linked to ENSO (Power and Smith 2007; Stachnik and Schumacher 2011). ENSO affects the Indian monsoon through an interaction between equatorial Walker circulation and the regional Hadley circulation (Bjerknes 1969). In general, large-scale circulation changes due to spatial shift in the zonal direction of the ascending/descending limbs of Walker circulation influence the monsoon circulation over the Indian domain. Moreover, coupled air-sea feedbacks in the Indian Ocean also alter the meridional circulation

during the ENSO events and thus make impacts on the ISMR variability (Wu and Kirtman 2004).

The observed inverse relationship between ENSO and ISMR was weakened after the 1980s (Kumar et al. 1999). Kumar et al. (1999) proposed two possible reasons for this weakened ENSO-ISMR relationship. One is the southeastward shift in the Walker circulation anomalies during ENSO events, which produce normal summer monsoon rainfall in the Indian region. The second reason is the increased surface temperatures over Eurasia during the winter and spring, which enhances the land-sea gradients favorable to a strong monsoon. Ashrit et al. (2001), however, attributed the enhanced concentration of greenhouse gases as a reason for the weakened ENSO-ISMR relationship. Another possible reason was found as the enhanced impact of the IOD (Saji et al. 1999; Webster et al. 1999; Ashok et al. 2001, 2004).

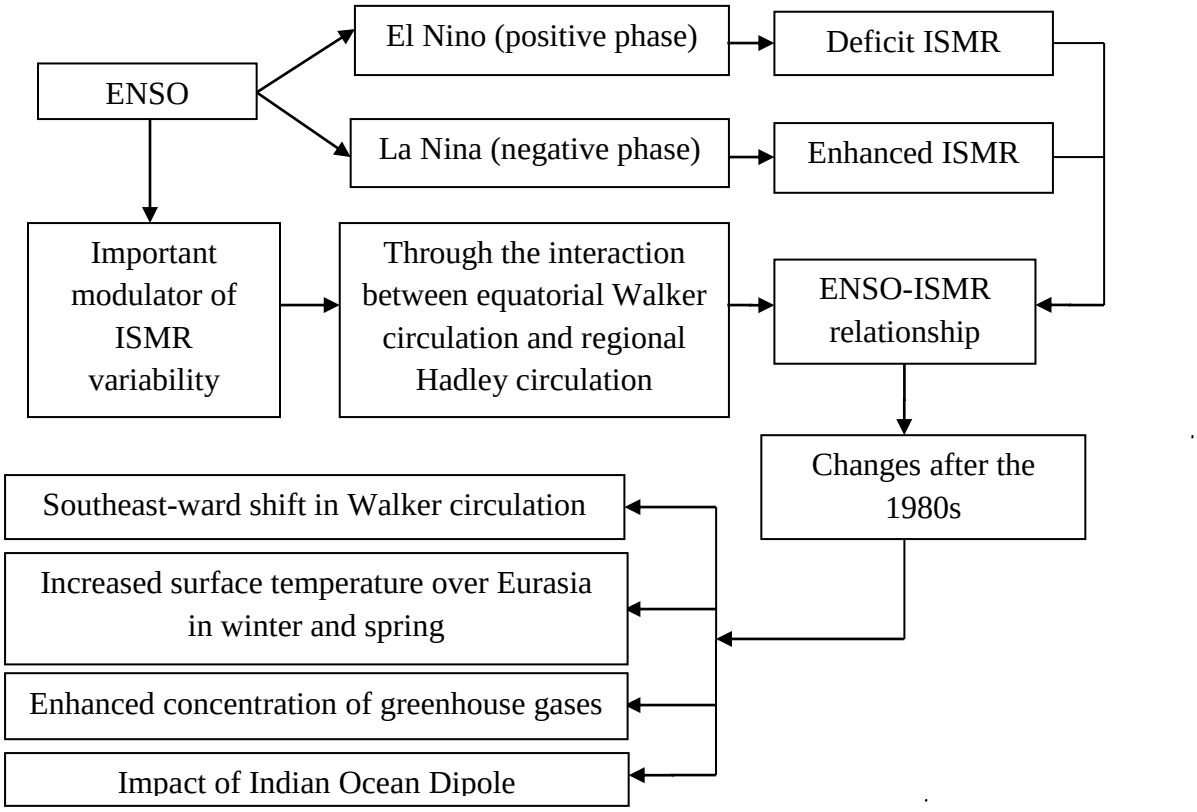

Figure 1.5: Schematic representation of the ENSO-ISMR relationship

The study of Kumar et al. (2006) showed that India is more prone to drought when the El Niño events shifted westward in the tropical Pacific. They also found that the El

Niño events with the warmest SST in the central equatorial Pacific are associated with Indian droughts than the events with the warmest SST in the eastern equatorial Pacific. In a similar type of analysis carried out by Ratnam et al. (2010), the role of Pacific SSTs on the ISMR failure during 2009 was explored. They reported that the unusual warming of the central Pacific altered the regional Walker circulation over tropical and subtropical Pacific, which lead to deficit rainfall in the Indian region. All these analyses indicate the inevitable role of Pacific Ocean SST on the modulation of ISMR variability since ENSO plays as an important modulator of ISMR variability. A schematic representation of the ENSO-ISMR relationship is given in Figure 1.5.

1.9 Impact of Indian Ocean dynamics on ISMR variability

In contrast to the Pacific Ocean, the Indian Ocean is bounded by the Asian landmass in the north so that the heating of the land during the boreal summer season produces a strong meridional pressure gradient that drives the summer monsoon (Han et al. 2014). The deep convection over the equatorial Indian Ocean is critical for monsoon since the cloud bands generated over the equatorial Indian Ocean propagate northward and cause precipitation in India during the summer monsoon (Gadgil et al. 2003). However, the role of the tropical Indian Ocean on the ISMR variability is still uncertain (Chowdary et al. 2015), even though it is an important modulator of tropical climate variability **(**Ashok et al. 2003). Apart from Pacific Ocean SST, SST in the Indian Ocean also plays a major role in ISMR variability (Ummerhofer et al. 2011). The moisture availability in the Indian region is related to the ocean-atmosphere conditions in the Indian Ocean (Ajayamohan and Rao 2008). So, analyzing the convective systems and the ocean-atmosphere interactions in the Indian Ocean are also important as much as that in the Pacific to understand the ISMR variability.

The ENSO phenomenon was considered as the most important driver of ISMR variability, and a major focus of the scientific community was to explore the mechanisms behind ENSO until a dipole mode was discovered in the Indian Ocean called IOD (Saji et al. 1999; Webster et al. 1999). After the discovery of IOD, it was recognized that the coupled ocean-atmosphere processes in the Indian Ocean also can make significant climate fluctuations all over the globe (Han et al. 2014).

1.9.1 Indian Ocean Dipole (IOD)

IOD is defined as the difference in SST between the western equatorial Indian Ocean and the eastern equatorial Indian Ocean (Saji et al. 1999). The positive IOD event is characterized by warm (cold) SST anomalies in the west (southeast) equatorial Indian Ocean. The conditions are reversed for a negative IOD event (Vinayachandran et al. 2002; Rao et al. 2007).

Figure 1.6 shows a schematic representation of positive and negative IOD events. A positive IOD event modulates the Hadley circulation over the Indian region by inducing convergence patterns over the Bay of Bengal, which leads to above normal rainfall over the monsoon core zone (Ashok et al. 2004). However, below normal rainfall is observed over the monsoon core zone of India due to the divergence pattern over the Bay of Bengal during negative IOD events.

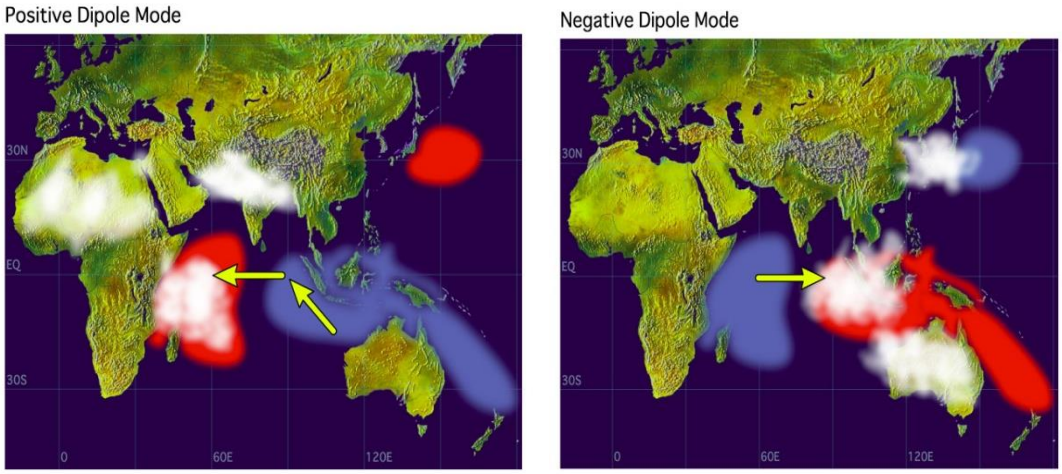

Figure 1.6: Schematic representation of positive IOD and negative IOD events. The red and (blue) shades indicate warm (cold) SST anomalies. White patches indicate the areas with increased convective activities and arrows indicate the trade wind directions. Credit: http://www.godac.jamstec.go.jp/catalog/data_catalog/e/index.html.

1.9.2 Impacts on ISMR

After the discovery of IOD, several studies were conducted to understand its characteristics, relationship with ISMR, ENSO, and with the climate of other tropical regions (Yamagata et al. 2004; Behera et al. 2005; Abram et al. 2008; Luo et al. 2010;

Behera and Ratnam 2018; Hrudya et al. 2021). Ashok et al. (2001) pointed out that the surplus rainfall over the monsoon core zone of Indian during the summer monsoon is associated with positive IOD events, whereas, negative IOD events lead to the weakening of ISMR. IOD can also modulate the number of extreme rain events in India by transporting moisture from the southeastern equatorial Indian Ocean to the Bay of Bengal (Ajayamohan and Rao 2008). The study of Ajayamohan and Rao (2008) suggested that the ongoing warming of the Indian Ocean in recent decades enhances the occurrence of extreme rain events in central India. The warming trend of Indian Ocean SST in recent decades was also reported by Ihara et al. (2008). Thus, IOD is found to have an important role in seasonal and interannual climate variations (Yamagata et al. 2004) and makes impacts on several remote regions apart from the Indian Ocean such as Europe, North and South America, South Africa, and Australia (Saji and Yamagata 2003). A positive IOD event causes deficit rainfall in Indonesia and surplus rainfall in India, Africa, Bangladesh, and Vietnam (Yamagata et al. 2004).

1.9.3 Linkage between the Indian Ocean and the Pacific Ocean variabilities

Since the Indian Ocean and the Pacific Ocean variabilities are interlinked (Ummerhofen et al. 2011), it is important to check how the coupled ocean-atmosphere phenomena in these two basins are connected and how the Indian Ocean influences the climate conditions in the Pacific and vice versa. The influence of the Indian Ocean on the ENSO events in the Pacific can be mainly associated with the relationship between IOD and ENSO events. Ashok et al. (2001) found that IOD and ENSO have complimentary impacts on ISMR. They found that the ENSO induced subsidence over the Indian region during a pure ENSO (ENSO events that occur without IOD events) year is replaced by the IOD induced convergence and causes normal summer monsoon rainfall even during a strong El Niño year. Similarly, the negative IOD events can reduce the impact of La Niña on ISMR and provide deficit monsoon rainfall. They reported that the co-occurrence of IOD with ENSO reduces the impacts of ENSO on ISMR.

IOD can make significant influences on the atmospheric pressure variations of the Indo-Pacific domain (Behera and Yamagata 2003). The study of Behera and Yamagata (2003) demonstrated the role of IOD in the pressure swings of the Asia- Pacific sector. In contrast, Li et al. (2003) reported that ENSO is one of the forcing mechanisms that

trigger the IOD events. It was supported by Behera et al. (2006), who found that the interannual variability of IOD events is affected by the changes in the Walker circulation, induced by ENSO in the tropical Pacific. Krishnaswami et al. (2015) found that the influence of IOD on ISMR and extreme rainfall events is strengthening but that of ENSO is weakening during recent decades. While the IOD-ISMR relation is mainly confined to the summer and autumn seasons, on the other hand, ENSO-ISMR relation extends beyond these seasons (Cherchi and Navarra 2013). Even though a positive IOD event is said to be associated with above normal rainfall in most of the Indian region, an unusual case was occurred in the summer monsoon season of 2008, in which the central Indian region was witnessed a below normal rainfall (Rao et al. 2010). Rao et al. (2010) reported that during the summer monsoon period of 2008, abnormal SST warming was observed in the southern tropical Indian Ocean, which resulted in enhanced convection over the southern tropical Indian Ocean and anti-cyclonic circulation over the Bay of Bengal and Central India. Thus, it resulted in a suppressed rainfall over the central Indian region. Since the warming was so strong that it nullified the influence of IOD on ISMR. In other words, the combined Indian Ocean warming and IOD related warming could make significant impacts on ISMR.

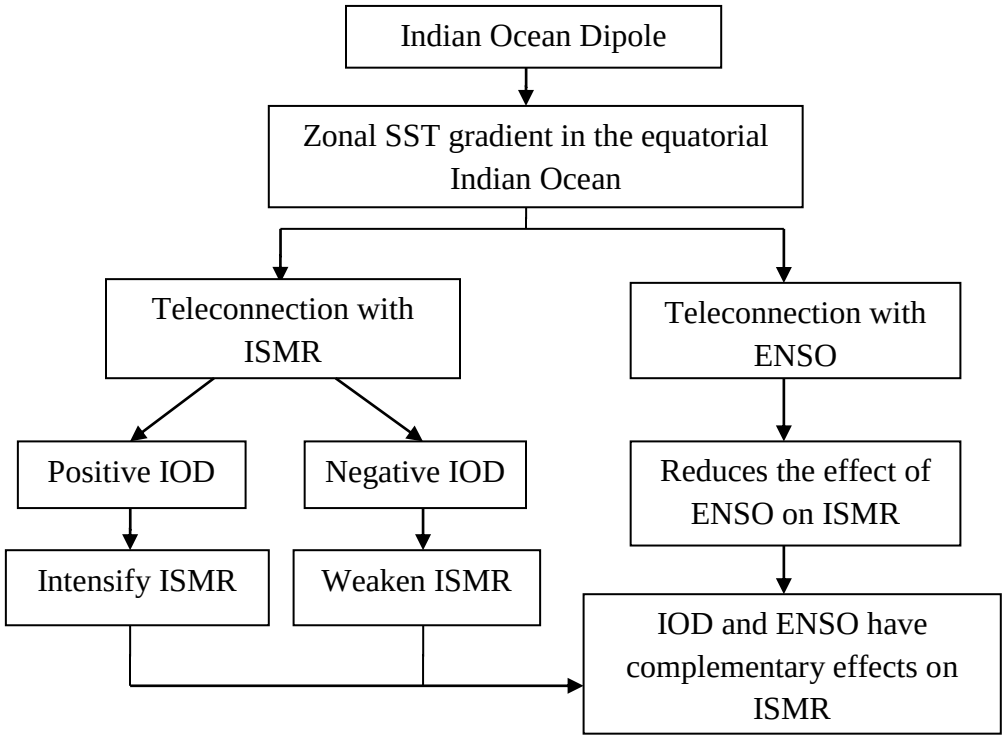

Figure 1.7: Schematic representation of the IOD-ISMR and IOD-ENSO relationships

The impact of ENSO and IOD on the regional variability of ISMR was investigated by Ashok and Saji (2007). They found that ENSO has a significant impact on the rainfall variability of 19 sub-divisions of India, while IOD has an impact on 8 sub-divisions out of 29 sub-divisions considered. They showed that the impact of ENSO is distributed more widely since the correlation between ENSO and regional rainfall is stronger than that of IOD. There have been several different arguments put forward by the scientific community regarding the existence of IOD, especially its dependence on ENSO and ISMR. However, the research on IOD has raised new possibilities in the prediction of seasonal and interannual climate variations all over the tropics (Yamagata et al. 2003, 2004). Figure 1.7 is a schematic representation of the IOD-ENSO and IOD-ISMR relationships.

1.10 Influence from other tropical oceans on ISMR variability

Apart from ENSO and IOD, other coupled ocean-atmosphere phenomena in the tropical oceans also play an important role in determining the spatio-temporal variability of ISMR. Atlantic multi-decadal oscillation (AMO) is considered as a basin-wide oscillation of North Atlantic SST, with a period of about 65-80 years (Kerr 2000). A positive (warm) phase of AMO is associated with the enhanced SST over the North Atlantic, which strengthens the low-level jets and thus the monsoon circulation over the Indian region (Li et al. 2008). It can also affect the variability of ISMR by inducing changes in the tropospheric temperature over Eurasia (Goswami et al. 2006b; Lu et al. 2006). I. e, positive (negative) AMO can produce stronger (weaker) ISMR by inducing positive (negative) tropospheric temperature over Eurasia. The study by Feng and Hu (2008) reported that the North Atlantic SST affects the surface temperature of the Tibetan Plateau, which influences the monsoon circulation over the Indian region. The link between ISMR and Atlantic Zonal Mode (AZM; Kucharski et al. 2008) is also carried out in many studies, where AZM is considered as a dominant mode of interannual variability in the equatorial Atlantic (Sabeerali et al. 2019). Nair et al. (2018) reported that the summer monsoon rainfall over different regions of India (northeast, northwest, north-central, west-central, and peninsular regions) is influenced by the AZM variability. Sabeerali et al. (2019) showed that the observed inverse relationship between ISMR and AZM has strengthened in recent decades. They

identified the increase of SST over the eastern equatorial Atlantic Ocean as the reason for this strengthened relationship.

Apart from the Atlantic Ocean, another important external forcing of ISMR variability is the Pacific Decadal Oscillation (PDO), which is an important mode of climate variability in the North Pacific Ocean (Vishnu et al. 2018). It is inversely linked to the ISMR, with the warm (cold) phases related to the decrease (increase) of rainfall over the Indian subcontinent (Krishnan and Sugi 2003). It can also amplify the impact of ENSO on ISMR (Roy et al. 2003). When El Niño events co-occur with the positive phase of PDO, drought conditions are likely to occur over the Indian region. On the other hand, when La Niña events co-occur with the negative phase of PDO, it produces wet conditions.

1.11 Future projections of ISMR variability

Numerical models are widely used in meteorological applications, particularly in weather prediction systems. A model simply describes a system using mathematical equations and concepts. Various modeling studies have been carried out in the last few years to understand the ISMR variability in both the historical and future decades (Eg: Meehl and Washington 1993; Kripalani et al. 2007; Cherchi et al. 2011; Kumar et al. 2010, 2011; Preethi et al. 2010; DelSole and Shukla 2012; Wang et al. 2015; Sudeepkumar et al. 2018; Varikoden et al. 2018). Recently, such projections are being widely carried out using Coupled Model Inter Comparison Project Phase 5 (CMIP5).

1.11.1 Coupled Model Inter Comparison Project Phase 5 (CMIP5)

CMIP5 was organized in 1995 by the World Climate Research programme (WCRP) and was released in the Inter-governmental Panel on Climate Change fifth assessment report (IPCC-AR5) (Taylor et al. 2012; Sabeerali et al. 2015; Sudeepkumar et al. 2018). CMIP5 is a collaborative framework designed to improve the understanding of climate and to provide estimates of future climate change. CMIP5 models are of higher spatial resolution comparing with the earlier phases (Taylor et al. 2012) and are well in representing the Asian-Australian monsoon matrices (Wang et al. 2014). In CMIP5, the future projections are usually carried out in four Representative Concentration Pathways

(RCPs 2.6, 4.5, 6, and 8.5), where RCPs provide an estimate of the radiative forcing in the year 2100 (Taylor et al. 2012; Menon et al. 2013; Sarthi et al. 2015).

Many studies have analyzed the changes in ISMR in future decades using CMIP5 models (Chaturvedi et al. 2012; Jourdain et al. 2013; Sabeerali et al. 2015; Sharmila et al. 2015; Jena et al. 2016). Most of these studies have reported significant changes in ISMR in future warming scenarios. Sabeerali et al. (2015) has analyzed the future projections of ISMR and its large-scale thermodynamic drivers using 23 CMIP5 models. They reported that most of the models project an increase in ISMR and a weakening of tropospheric temperature gradient over the south Asian summer monsoon domain in a future warming scenario (RCP 4.5 and 8.5). A similar study was carried out by Jayasankar et al. (2015) who observed an enhancement in ISMR by the end of the century (2070-2099) in RCP 2.6 and 8.5 scenarios using 26 CMIP5 models. Menon et al. (2013) has also reported an increase in ISMR during the same period using different scenarios and found that the ISMR shows a large increasing trend in RCP 8.5 than that in other RCPs. A study by Sarthi et al. (2015) projected an enhanced (deficit) summer monsoon rainfall over northwest, northeast, west-central, and peninsular Indian (north-central) regions in both the RCP 4.5 and 8.5 scenarios during the period 2006-2050. Sharmila et al. (2015) reported a moderate increase in ISMR over the monsoon core zone of India by the end of the 21st century using 20 CMIP5 models. They also found an increase of the interannual variability and extreme wet and dry rain events in a future warming scenario.

Apart from the ISMR projections, researches have been undergoing on the future projections of ENSO-ISMR relationship using models (Eg: Kumar et al. 2010; Preethi et al. 2010; Ramu et al. 2016; Roy 2017). Roy (2017) has analyzed the ENSO-ISMR correlations in both the historical and RCP scenarios using CMIP5 models by focusing on some specific regions around central India. They reported that ENSO showed a negative correlation with ISMR in both the historical and RCP scenarios in all models they considered. A similar result has also been reported by Azad and Rajeevan (2016), but with different CMIP5 models. The changes in the ENSO-ISMR relationship in future decades were analyzed separately for canonical and Modoki ENSO events by Roy et al. (2019). They found that the relationship is strengthening (weakening) for

canonical (modoki) ENSO events, particularly over north-central India. Jourdain et al. (2013) analyzed the future changes in the relationship between Indo-Australian monsoon and ENSO using CMIP5 models and found that the relationship between ENSO and Indian monsoon in future decades strongly depends upon the seasonal cycle of ENSO.

1.12 Objectives

From the literature review, it is understood that many works have been carried out in the last few years to explore the ISMR variability and its influence from different internal and external climate factors. Most of the works have focused on the temporal variability of ISMR and its influencing mechanism; however, the regional variability is less explored. For a country like India, where a large portion of society depends on agriculture, a better understanding and prediction of summer monsoon rainfall in regional scale is very important for water management and economic development. Also, the studies analyzing the spatio-temporal variability of ISMR have considered the summer monsoon season as a whole and none of them have focused on the analysis during different phases of summer monsoon separately. I. e, onset phase, peak phase, and withdrawal phase. Since the characteristics of ISMR during different phases and their influencing mechanisms are highly different from one another; it's highly relevant to analyze the ISMR variability during different phases separately, rather than considering the summer monsoon season as a whole.

Moreover, several studies have been undertaken to analyze the changes in ISMR variability and ENSO-ISMR relationships in future decades using models. However, the studies analyzing the ENSO-ISMR relationships have not given much focus to the analysis in regional scale. I. e, they have not much focused on how the ENSO-ISMR teleconnections over different Indian regions will be projected in future decades.

By considering these gap areas, in this thesis, the regional variability of ISMR is explored by identifying its relationship with different oceanic and atmospheric parameters. The regional variations and trends of summer monsoon rainfall over different regions of India are analyzed separately. The influence of different convective parameters of the atmosphere on these regional variations is also explored. Further, the

impact of coupled ocean-atmosphere interactions in the tropical Indian and Pacific Oceans on the ISMR variability is also analyzed. The influence of Pacific Ocean and Indian Ocean dynamics on ISMR variability is analyzed separately for the onset, peak, and withdrawal phases of the summer monsoon. Further, the study also analyzes the modulation of ISMR variability and ENSO-ISMR relationships in future decades using CMIP5 models.

More precisely, the main objectives of the present thesis are:

- To explore the regional variability of ISMR such as the variability over the west coast, foothills of Himalaya, northeast, northwest, and the central Indian regions.
- To analyze the impact of different convective systems in the atmosphere on the regional variations of ISMR.
- To find out the influence of El Niño Southern Oscillation on the modulation of ISMR variability during the onset (June), peak (July-August), and withdrawal (September) phases of ISMR.
- To find out the changes in the ENSO-ISMR relationship from early (1951-1980) to recent decades (1986-2015) and their influencing mechanisms from the tropical Pacific Ocean (changes in SST, low-level winds, Walker circulation, etc.).
- To find out the role of Indian Ocean dynamics on the modulation of ISMR variability during onset, peak, and withdrawal phases.
- To estimate the changes in the IOD-ISMR relationship from early to recent decades and their influencing mechanisms from the tropical Indian Ocean.
- To estimate the modulation of regional variability of ISMR in the future decades using CMIP5 models.
- To analyze the changes in the ENSO-ISMR relationship in future decades under different RCP scenarios
- To analyze the future impacts of SST and circulation features over the tropical Indo-Pacific Ocean on the ISMR variability in future decades during El Niño and La Niña events separately.

The data and methodologies adopted to address these objectives are presented in Chapter 2. The analysis of the regional variations and trends of ISMR and the impact of convective systems of the atmosphere on the ISMR variability is included in Chapter 3. Chapters 4 and 5 describe the role of Indo-Pacific Oceans on ISMR variability during the onset, peak, and withdrawal phases of ISMR. The future projections of ISMR regional variability and ENSO-ISMR relationship are presented in Chapter 6, followed by conclusions in Chapter 7.

CHAPTER 2

DATA AND METHODOLOGY

CHAPTER 2

DATA AND METHODOLOGY

2.1 Introduction

In this chapter, the description of datasets and methodologies adopted for the present thesis are included. Different observational, reanalysis, and model datasets were used for the analysis, whose descriptions are given in section 2.2. The methodologies adopted for the analysis are described in section 2.3.

2.2 Description of datasets

For the present thesis, different reanalysis datasets were used. Reanalysis is a systematic approach to produce datasets for climate research, in which the datasets are constructed to provide a consistent estimate of climate state at each time step. Apart from reanalysis datasets, model data from CMIP5 was also used in the study to understand the projected changes in ISMR and ENSO-ISMR relationships in future decades. The description of different datasets and indices used for the study are given below.

1. NCEP/NCAR reanalysis data

NCEP/NCAR (National Centre for Environmental Prediction/National Centre for Atmospheric Research) dataset is high quality research data with a spatial resolution of 2.5° latitude × 2.5° longitude used for meteorological studies (Kalnay et al. 1996). The NCEP/NCAR reanalysis project is using a data assimilation system using past data from 1948 to the present. In this project, all the atmospheric field variables are classified into four different categories depending upon the degree to which they are influenced by the observation/models. In the present study, the monthly NCEP/NCAR data for potential temperature, wind velocity (zonal, meridional, and vertical), and specific humidity for the period 1950-2015 were used. The data was accessed from the website of NOAA (National Oceanic and Atmospheric Administration) (https://psl.noaa.gov/data/gridded/data.ncep.reanalysis.html).

2. ERA-Interim reanalysis data

ERA-Interim is the latest global atmospheric reanalysis dataset with 0.75° × 0.75° grid spatial resolution. It describes the surface and oceanic field variables (Dee et al. 2011),

provided by the European Centre for Medium-Range Weather Forecast (ECMWF). The present study has utilized the ERA-Interim monthly data for cloud cover (low, medium, and high), and CAPE for the period 1979 to 2015, accessed from the website of ECMWF (https://www.ecmwf.int/en/forecasts/datasets/reanalysis-datasets/era-interim)

3. CRU precipitation data

CRU (Climate Research Unit) datasets contain high resolution data ($0.5^o \times 0.5^o$ grid spatial resolution) for precipitation, cloud cover, temperature, etc. covering the land areas of Earth (Harris et al. 2014). For the present study, the monthly precipitation data from CRU is used for the period 1950-2015 (www.cru.uea.ac.uk). The CRU monthly rainfall datasets were formed by interpolating the rainfall anomalies (base period: 1961 to 1990) observed at different meteorological stations across the world's land areas into a $0.5^o \times 0.5^o$ grid cell and combined with the existing rainfall climatology.

4. HadISST SST data

HadISST (Hadley Centre Sea Ice and Sea Surface Temperature) dataset is a combination of monthly global SST and sea ice concentration ($1^o \times 1^o$ grid spatial resolution) available from 1871 onwards (Rayner et al. 2003). The present study has utilized the monthly HadISST data version 1.1 for SST for the period 1951-2015, accessed from the website of NCAR (https://climatedataguide.ucar.edu/climate-data/sst-data-hadisst-v11).

5. ERSST SST data

Extended Reconstructed Sea Surface Temperature (ERSST) dataset, version 5 (Huang et al. 2017) is a global monthly SST dataset provided by the International Comprehensive Ocean-Atmosphere Dataset (ICOADS) with 2° latitude × 2° longitude spatial resolution. This dataset is available from January 1854 to the present and contains SST anomalies computed with respect to the monthly climatology of the period 1971–2000. The present study has utilized the ERSST data for SST for the period 1951-2005 accessed from the website of NOAA (https://www.ncdc.noaa.gov/data-access/marineocean-data/extended-reconstructed-sea-surface-temperature-ersst-v5).

6. APHRODITE precipitation data

Asian Precipitation–Highly Resolved Observational Data Integration Towards Evaluation of Water Resources (APHRODITE) dataset (Yatagai et al. 2012) is a gridded precipitation dataset with 0.25° latitude × 0.25° longitude spatial resolution. This dataset is formed based on the rain-gauge data from Asia including the Himalayas, South and Southeast Asia, and mountainous areas in the Middle East. The present study has utilized the APHRODITE dataset for precipitation for the period 1951-2005, accessed from the website of NCAR (https://climatedataguide.ucar.edu/climate-data/aphrodite)

7. CMIP5 model dataset

The present study has utilized the monthly data from 25 CMIP5 models for precipitation, wind velocity (zonal, meridional, and vertical), and SST for the period 1951-2005 (historical period), and future projection data for the same variables for the period 2050-2099 (future period). The model output data were accessed from the website of Earth System Grid Federation (ESGF, https://esgf-node.llnl.gov/projects/cmip5/). For the future projection analysis, RCP 4.5 and RCP 8.5 scenarios were used, as RCP 4.5 and 8.5 scenarios represent the radiative forcing of 4.5 and 8.5 Wm^{-2}, respectively, by the year 2100 (Taylor et al. 2009, 2012; Thomson et al. 2011; Van-Vuuren et al. 2011). A brief description of CMIP5 models selected for the study is given in Table 2.1.

Model	Institution	Horizontal resolution (°lat × °lon)
ACCESS-1.0	Commonwealth Scientific and Industrial Research Organization (CSIRO) and Bureau of Meteorology,(BOM), Australia	1.25×1.875
ACCESS-1.3	Commonwealth Scientific and Industrial Research Organization (CSIRO) and Bureau of Meteorology,(BOM), Australia	1.25×1.875
CNRM-CM5	Centre National de Recherches Meteorologiques/Centre Europeen de Recherche et Formation Avancees en Calcul Scientifique (CNRM-CERFACS)	1.4 ×1.4
CSIRO-Mk3-6-0	Commonwealth Scientific and Industrial Research Organization and the Queensland Climate Change Centre of Excellence (CSIRO-QCCCE), Australia	1.875×1.875

HadGEM2-AO	National Institute of Meteorological Research/Korea Meteorological Administration (NIMR/KMA), Korea	1.25×1.875
INMCM4	Institute for Numerical Mathematics (INM), Russia	1.5×2
IPSL-CM5A-LR	Institut Pierre-Simon Laplace, France	1.875×3.75
IPSL-CM5A-MR	Institut Pierre-Simon Laplace, France	1.25×2.5
IPSL-CM5B-LR	Institut Pierre-Simon Laplace, France	1.875×3.75
MIROC5	Atmosphere and Ocean Research Institute (The University of Tokyo), National Institute for Environmental Studies, and Japan Agency for Marine-Earth Science and Technology	1.4×1.4
MIROC-ESM	National Institute for Environmental Studies, and Japan Agency for Marine-Earth Science and Technology (MIROC)	2.8×2.8
MPI-ESM-LR	Max Planck Institute for Meteorology (MPI-M), Germany	1.875×1.875
MPI-ESM-MR	Max Planck Institute for Meteorology (MPI-M), Germany	1.875×1.875
MPI-ESM-P	Max Planck Institute for Meteorology (MPI-M), Germany	1.875×1.875
MRI-CGCM3	Meteorological Research Institute (MRI), Japan	1.125×1.125
MRI-ESM1	Meteorological Research Institute (MRI), Japan	1.125×1.125
MIROC-ESM-CHEM	Japan Agency for Marine-Earth Science and Technology, Atmosphere and Ocean Research Institute(The University of Tokyo), and National Institute for Environmental Studies, Japan	2.81×2.81
CMCC-CESM	Centre Euro-Mediterraneo sui Cambiamenti Climatici, Italy	3.75×3.75
GISS-E2-H	NASA Goddard Institute for Space Studies (NASA GISS), USA	2×2.5
GISS-E2-H-CC	NASA Goddard Institute for Space Studies (NASA GISS), USA	2×2.5
GISS-E2-R	NASA Goddard Institute for Space Studies (NASA GISS), USA	2×2.5
GISS-E2-R-CC	NASA Goddard Institute for Space Studies (NASA GISS), USA	2×2.5
HadGEM2-CC	Met Office Hadley Centre (MOHC), UK	1.25×1.875
NorESM1-M	Norwegian Climate Centre, Norway	1.875×2.5
NorESM1-ME	Norwegian Climate Centre, Norway	1.875×2.5

Table 2.1: Details of CMIP5 models used for the study.

8. Niño 3.4 index

Different indices are being used to study the ENSO characteristics over the tropical Pacific Ocean, out of which, the most commonly used index is the Niño 3. 4 index, which is the average of SST anomalies over the Niño 3.4 region (5°N-5°S, 170°-120°W). Figure 2.1 shows different Niño regions in the tropical Pacific Ocean. The Niño 3.4 index was used in the present study to analyze the linkage between convective parameters and ISMR with ENSO, changes in ENSO-ISMR relationship during different phases, and the historical and future projections of the ENSO-ISMR relationship. The index values were obtained from the website of NOAA (https://www.ncdc.noaa.gov/teleconnections/enso/indicators/sst).

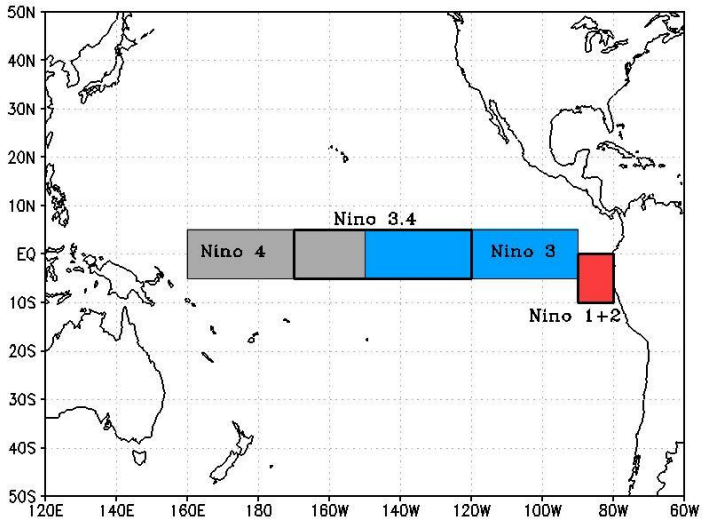

Figure 2.1: Different Niño regions in the tropical Pacific Ocean.

9. Dipole Mode Index (DMI)

DMI is the commonly used index to study the IOD characteristics over the tropical Indian Ocean. DMI is calculated as the difference in SST anomalies between the tropical western Indian Ocean (50°E-70°E, 10°S-10°N) and the tropical southeastern Indian Ocean (90°E-110°E, 10°S-Equator) as defined by Saji et al. *(*1999). For the present study, DMI was obtained from the website of Earth System Research Laboratory, NOAA *(*http://www.ersl.noaa.gov).

2.3 Methodology

In the present thesis, the regional variability of ISMR and its association with convective parameters (LTS, cloud cover, and CAPE) were analyzed. For that, different regions of India were selected based on the rainfall characteristics over these regions during the summer monsoon. The trends and variabilities of ISMR and convective parameters in each region were separately studied. To identify the role of Indo-Pacific Oceans on ISMR variability, the early and recent decades for the analysis were selected based on sliding correlations. The classification of different ENSO and IOD years was carried out based on Niño 3.4 index and DMI, respectively. For the analysis of the changes in ISMR variability and ENSO-ISMR relationships in future decades, the selection of CMIP5 models was carried out by using the Taylor diagram. A detailed description of the methodologies adopted in the present thesis is given below.

2.3.1 Calculation of LTS and CAPE

For the analysis of the linkage between ISMR and convective parameters, calculation of LTS and CAPE was carried out. Following the previous studies (Slingo 1987; Klien and Hartmann 1993; Wood and Hartmann 2006), LTS was calculated as the difference in potential temperature between 700 h Pa and the surface (1000 h Pa).

$$LTS = \Theta_{700} - \Theta_{1000}, \text{ where } \Theta \text{ is the potential temperature.}$$

The calculation of CAPE was carried out using the below equation given by Emanuel (1994).

$$CAPE = \int_{LFC}^{EL} g\frac{(Tp - Te)}{Te}dz$$

Where LFC is the level of free convection, EL is the equilibrium level, T_p is the temperature of the air parcel, and T_e is the temperature of the environment.

2.3.2 Calculation of Vertically Integrated Moisture Transport (VIMT)

VIMT (Q) is usually calculated by integrating the product of wind velocities and specific humidity from the surface (1000 h Pa) to 300 h Pa (Murukami et al. 1984).

$$Q = \frac{1}{g}\int_{1000}^{300} q\,\vec{V}\,dp$$

Where q is the specific humidity, and $\vec{V}$ is the wind velocity vector

2.3.2 Selection of regions

To explore the regional characteristics of ISMR, four different regions of India; west coast (WC: 73°E-76°E, 10°N-20°N), central India (CI: 77°E-86°E, 18°N-26°N), northeast (NE: 88°E-94°E, 22°N-28°N), and northwest (NW: 66°E-75°E, 24°N-31°N) regions were selected based on the difference in rainfall characteristics. The four rainfall regions selected are highlighted as rectangular boxes in Figure 2.2.

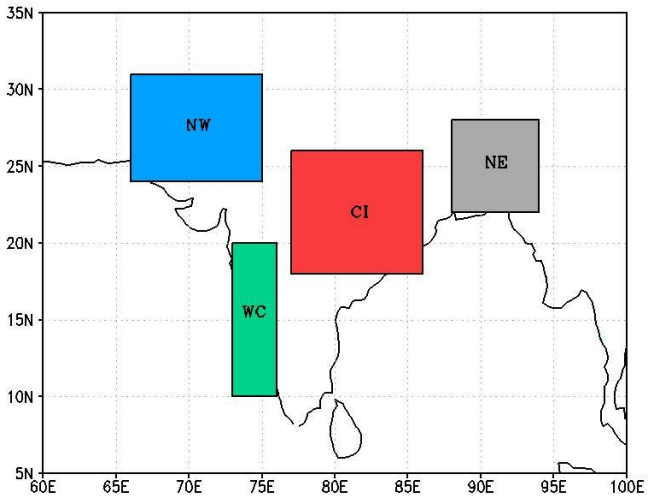

Figure 2.2: Different regions of India selected for the study

Since the analysis based on the entire country does not reveal the regional characteristics (Dash et al. 2009), the entire analysis was carried out separately for each region. The analysis of ISMR and LTS was carried out during the period 1950-2015. Since the ERA-Interim data is available from 1979 onwards, the analysis of cloud cover and CAPE was carried out during the period 1979-2015.

2.3.4 Selection of onset, peak, and withdrawal phases

The analyses of ENSO-ISMR and IOD-ISMR relationships were carried out separately for three phases of the summer monsoon season; onset phase (June), peak phase (July-

August), and withdrawal (September) phases. The three phases were chosen by following the criteria given by IMD, as described in Chapter 1.

2.3.5 Selection of early and recent decades

The changes in the ENSO-ISMR relationships were studied for the early (1951-1980) and recent (1986-2015) decades during onset, peak, and withdrawal phases. The early and recent decades were chosen based on a 31-year sliding correlation between Niño 3.4 index and ISMR (Figure 2.3).

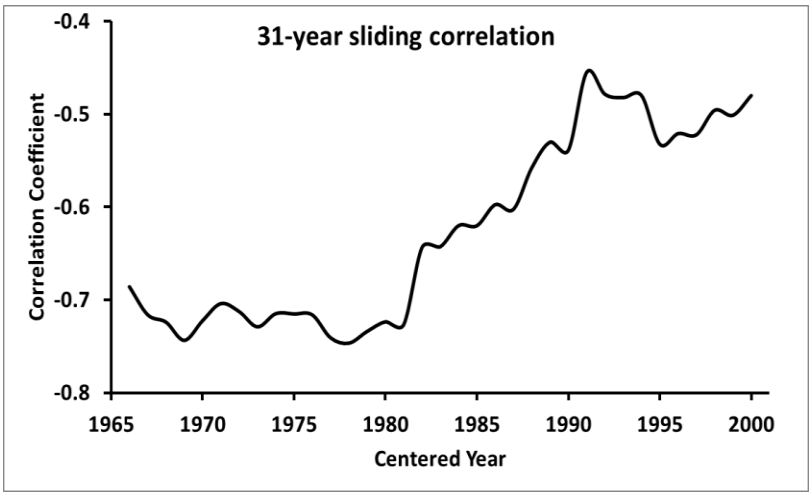

Figure 2.3: 31-year sliding correlation between Niño 3.4 index and ISMR during the period 1951-2015.

The sliding correlation is consistent in the early decades (up to 1980) with a value of more than -0.7. However, this relationship weakens in the recent decades (after 1985). During the recent decades, the value of sliding correlation is less than -0.6, which is less significant than in the early decades. Moreover, the values of sliding correlation in the recent decades are more fluctuating. Based on these changes in sliding correlation, the early and recent decades were selected as 1951-1980, and 1986-2015, respectively. Since the period between the two multi decades (1981 to 1985) shows a transition from high and consistent correlation to a low and inconsistent correlation, it was kept away from the analysis.

A similar criterion was applied to study the changes in the IOD-ISMR relationship during different phases. The early and recent decades were chosen based on a 21-year

sliding correlation between DMI and ISMR during the period 1951-2015 (Figure 2.4). The sliding correlation is negative (positive) in the early (recent) decades, which indicates a phase change in the relationship. IOD and ISMR show a consistent out-of-phase (negative correlation) relationship during the period 1951-1980, and an in-phase (positive correlation) relationship during the period 1986-2015. Hence, the two multi decades were chosen as the early and recent decades, respectively. The change from negative correlation to positive correlation is almost sudden from 1981 to 1985 and therefore, this period was considered as a transition period and kept away from the analysis.

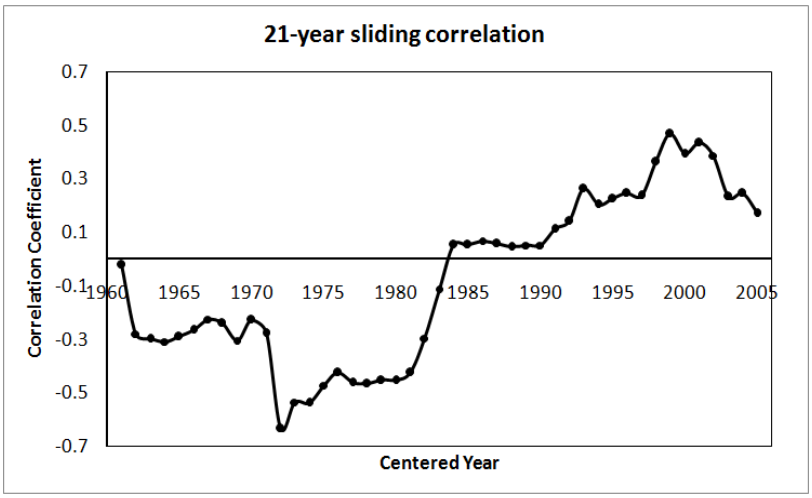

Figure 2.4: 21-year sliding correlation between DMI and ISMR during the period 1951-2015.

The early period 1951-1980 includes a climate shift in the year 1976/77 observed in the tropical Pacific (Miller et al. 1994; Trenberth and Hurrel 1994). It has made noticeable impacts on the onset (Sahana et al. 2015) and withdrawal (Sabeerali et al. 2012) dates of ISMR. As per Figure 2.4, a significant IOD-ISMR negative correlation is also observed during 1976/77. It indicates that the climate shift of 1976/77 has not affected the observed IOD-ISMR relationship in the early decades. Hence, the entire analysis was carried out without considering the impact of the 1976/77 climate shift.

2.3.6 Selection of models in CMIP5

Since the CMIP5 models differ from one another in many aspects (Sudeepkumar et al. 2018), it is not necessary that all the models can represent the ISMR variability and

their future projections accurately. To select the models that well capture the observational characteristics, the Taylor diagram was used. The performance of each model was compared with the CRU observational data set by using the Taylor diagram, in which the model performance is evaluated using pattern correlation and normalized variance (Taylor 2001). Based on the Taylor diagram, five models (CNRM-CM5, GISS-E2-R, GISS-E2-R-CC, HadGEM2-CC, and IPSL-CM5A-MR) that well simulate the ISMR variability over the Indian region were selected out of 25 models. The future projections were carried out based on the selected models for the period 2050-2099 in RCP 4.5 and RCP 8.5 scenarios. The consistency of selected models was analyzed using sliding correlation. A detailed description of model selection using the Taylor diagram and the evaluation of model consistency is provided in Chapter 6.

2.3.7 Classification of El Niño and La Niña years

For the present thesis, the El Niño and La Niña years for the historical and future periods were classified based on Niño 3.4 index. A year is classified as an El Niño (La Niña) year when the Niño 3.4 index exceeds the threshold value of 0.4 (-0.4).

2.3.8 Classification of positive IOD and negative IOD years

The classification of positive IOD (pIOD) and negative IOD (nIOD) years was carried out using DMI. A year is classified as a pIOD (nIOD) year if the DMI for that phase exceeds a threshold value of 0.75 (-0.75**)** times the standard deviation (Guo et al. 2015).

2.3.9 Correlation analysis

In the present thesis, the strength of the relationship between different variables was examined using correlation analysis. Correlation analysis is a statistical method used to measure the linear correlation between two variables. The strength of the relationship between variables is expressed using the correlation coefficient (commonly known as Pearson correlation coefficient), given by the following formula.

$$r = \frac{\sum (x_i - \bar{x})\,(y_i - \bar{y})}{\sqrt{\sum (x_i - \bar{x})^2\,(y_i - \bar{y})^2}}$$

Where xi = values of x-variable

y_i= values of y-variable

$\bar{x}$ = mean of the values of x-variable

$\bar{y}$ = mean of the values of y-variable

For the correlation analysis and trend analysis, the statistical significance of the results was calculated using the *student's t-test* and *F-test*, respectively.

In the next chapter, the regional variations and trends of ISMR over different regions of India are analyzed. The association between ISMR with convective parameters and ENSO is also analyzed for all the selected regions separately.

CHAPTER 3

REGIONAL VARIABILITY OF ISMR AND ITS LINKAGE WITH CONVECTIVE PARAMETERS AND ENSO

CHAPTER 3

REGIONAL VARIABILITY OF ISMR AND ITS LINKAGE WITH CONVECTIVE PARAMETERS AND ENSO

3.1 Introduction

The summer monsoon rainfall over India is associated with mesoscale convective systems having high spatio-temporal variability (Revadekar et al. 2016; Jayakumar et al. 2017). This chapter analyzes the variability of summer monsoon rainfall over different regions of India during the period 1950-2015, by identifying its relationship with different convective parameters, such as lower tropospheric stability (LTS), low cloud cover (LCC), medium cloud cover (MCC), high cloud cover (HCC), and convective available potential energy (CAPE). The spatio-temporal variabilities of ISMR and convective parameters are analyzed over the west coast (WC), northeast (NE), central India (CI), and northwest (NW) regions. Further, the linkage between convective parameters and ISMR with ENSO is also analyzed in this chapter.

3.2 Climatology of ISMR and convective parameters

The climatology of ISMR, LTS, CAPE, LCC, MCC, and HCC during the period of study (1950-2015) is shown in Figure 3.1. The climatology of ISMR (Figure 3.1a) shows maximum rainfall over the northeast and west coastal regions, moderate rainfall over the foothills of Himalayas and central India, and the least amount of rainfall over the northwest and southeast regions. It is consistent with the results of the previous studies (Rajeevan et al. 2006; Kishore et al. 2015; Nair et al. 2018; Suthinkumar et al. 2019). High values of LTS are observed over most of the Indian region during the summer monsoon season, with a noticeable increase of about 14-15 K over the northeast and peninsular regions (Figure 3.1b). However, relatively low LTS values are observed over the northwest region. The climatology of LTS over the northeast, northwest, and west coast regions is similar to that of ISMR, which indicates the one-to-one relationship between LTS and ISMR over these regions.

High values of CAPE (about 700-800 J Kg^{-1}) are observed over most of the Indian regions, particularly over the northeast, northwest, and central Indian regions (Figure

3.1c). Usually, the convection is likely to occur in the regions with a high value of CAPE (Jain et al. 2019). This is evident from Figure 3.1c, that the regions with high values of CAPE are associated with a high amount of ISMR as shown in Figure 3.1a. This association does not hold good in the case of the west coast region, in which relatively low values of CAPE and high values of LTS and ISMR are observed. This contradictory characteristic may be due to the stratiform nature of rainfall over the western Ghats regions (Sreekanth et al. 2019) and the convective nature of rainfall in other regions due to the less orographic influences (Jayakumar et al. 2017).

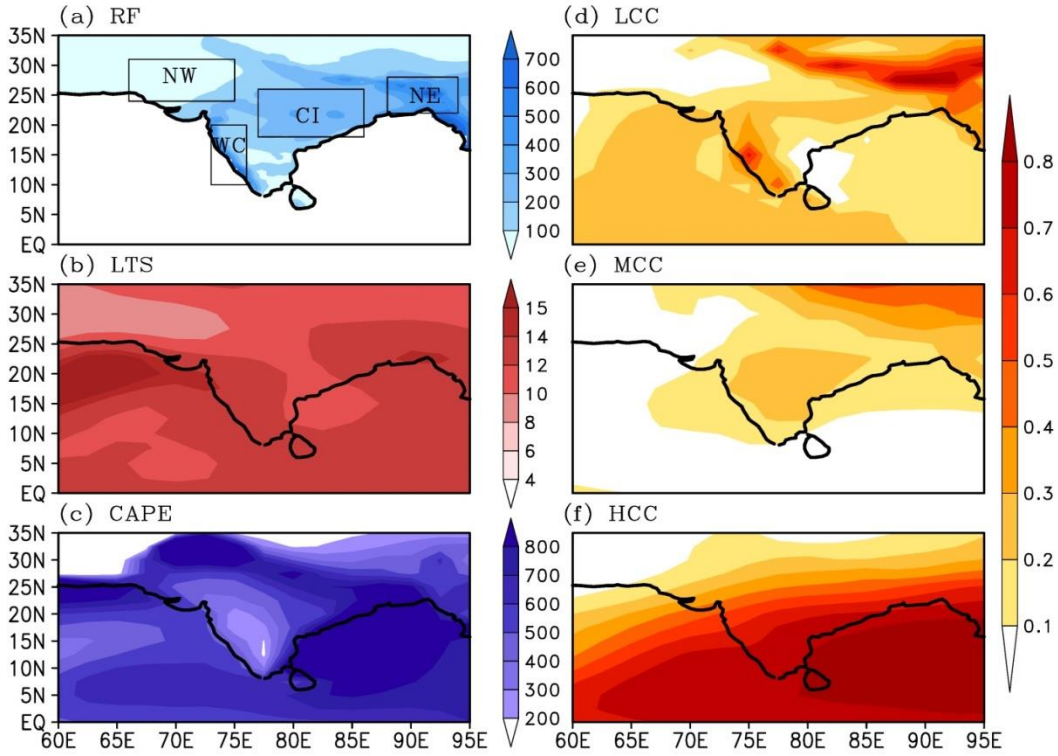

Figure 3.1: Climatology of (a) rainfall (mm), (b) LTS (K), (c) CAPE (J Kg^{-1}), (d) LCC (Okta), (e) MCC (Okta), (f) HCC (Okta) during summer monsoon. Climatology of rainfall and LTS were plotted for the period 1950-2015 and that of cloud covers and CAPE were plotted for the period 1979-2015.

The climatology of LCC shows a good association with ISMR and LTS since the regions with high values of LCC are related to enhanced ISMR and LTS and vice versa (Figure 3.1d). It is also related to the spatial pattern of CAPE, except over the west coast region. In contrast to LCC, the values of MCC are not dominant over most of the Indian regions; however, considerable variability is observed over central India (Figure

3.1e). Altogether, the analyses show a good relationship between LCC, MCC, LTS, and CAPE with the ISMR over different regions of India. Since HCC does not show a good relationship with spatial variation of ISMR and does not contribute to the regional rainfall characteristics (Figure 3.1f), it was excluded for further analyses.

3.3 Annual cycle of ISMR and convective parameters

The monthly time series/annual cycle of ISMR, LTS, and CAPE over the WC, CI, NE, and NW regions are shown in Figure 3.2. The analysis of the annual cycle is important since the convective systems of the atmosphere can make significant impacts on the ISMR during all other seasons apart from the summer monsoon season. The monthly variations of all the parameters during the pre-monsoon (March-April-May), post-monsoon (October-November-December), and winter (January-February) seasons are analyzed in addition to the summer monsoon season.

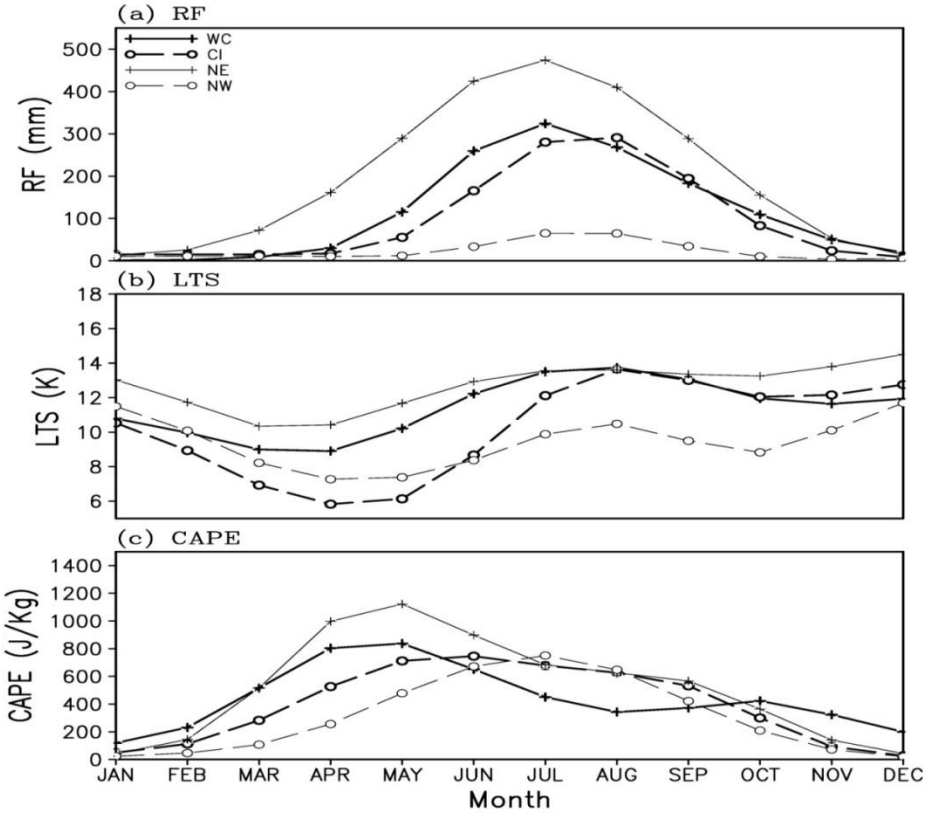

Figure 3.2: Annual cycle of (a) rainfall (mm), (b) LTS (K), and (c) CAPE (J Kg^{-1}) over WC, CI, NE, and NW regions. The annual cycle of rainfall and LTS were plotted for the period 1950-2015 and that of CAPE was plotted for the period 1979-2015.

The annual cycle of ISMR shows a common trend in all four regions even though the precipitation amounts vary from one region to another (Figure 3.2a). The amount of ISMR is minimum during pre-monsoon, becomes maximum during the summer monsoon, and thereafter decreases during post-monsoon season. In the WC region, the least amount of rainfall is observed during winter and pre-monsoon seasons. However, high values are observed during the summer monsoon months, with the peak value of precipitation in July (~325 mm). The rainfall decreases after September through the post-monsoon season. A similar annual cycle is seen in the CI region but with slightly reduced magnitude, and peak rainfall is observed in August (~ 290 mm). The variation of rainfall over the NE region is almost similar to that of WC. But, an increase in the precipitation amount (peak value of ~460 mm during July) is observed throughout the year, except in November and December. The amount of precipitation over the NW region is less while comparing with the other three regions. A relatively high amount of rainfall is observed only during the summer monsoon season.

In the case of LTS also (Figure 3.2b), a common trend in the distribution is observed over all the regions. The least values of LTS are observed over the NW region while comparing with the other three regions. The peak values of LTS are observed during the summer monsoon in all regions. The annual cycle of LTS during the summer monsoon season is almost similar to that of rainfall in all the regions, but, it is different during other seasons as observed in Figure 3.2a.

In the case of CAPE, it is more prominent over the WC and NE regions during the pre-monsoon period (Figure 3.2c). It may be due to the local convective systems developed by the convective instability of the atmosphere during the pre-monsoon season (Murugavel et al. 2012). Over the CI region, CAPE shows peak values during May-June, and over the NW region, peak values are observed during July. The annual cycle of CAPE is consistent with that of rainfall in the NW region, which indicates the dominance of convective rainfall over the NW region. The variation of CAPE over the WC region during the summer monsoon season is almost opposite to that of rainfall. Therefore, the rainfall in this region may be contributed more from the stratiform clouds than from the convective clouds.

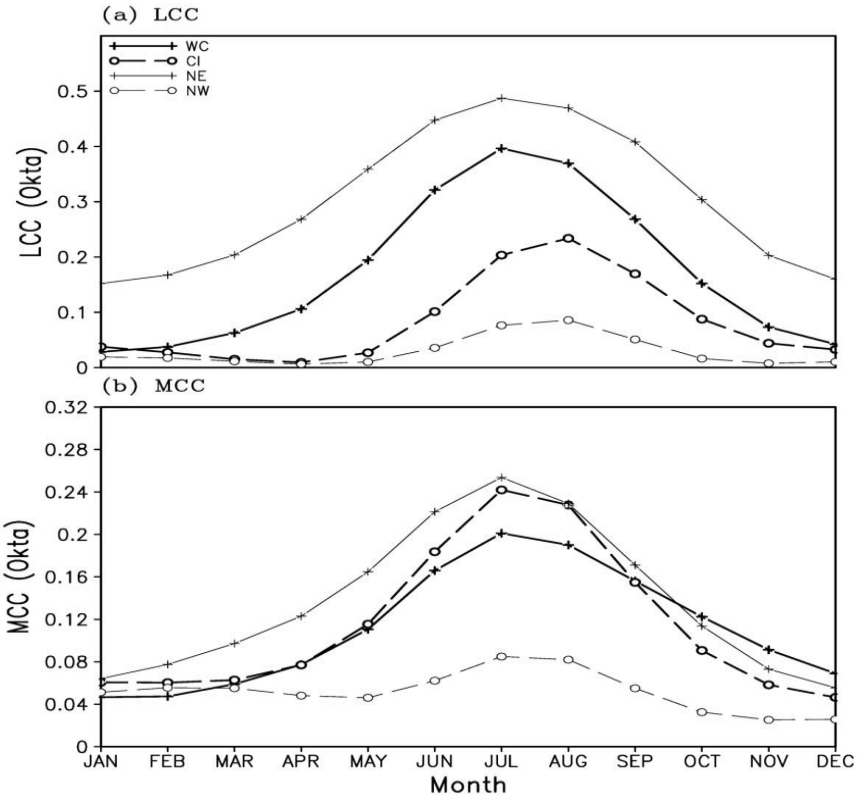

Figure 3.3: Annual cycle of (a) LCC (Okta) and (b) MCC (Okta) over WC, CI, NE, and NW regions for the period 1979-2015.

The annual cycle of LCC (Figure 3.3a) shows a similar trend as that of rainfall over all the regions. During the summer monsoon, high values of LCC are observed over WC (peak value of ~0.4 Okta in July) and NE (peak value of ~0.5 Okta in July) regions. However, moderate values are observed over the CI region (peak value of ~0.24 Okta in August) and least values over NW (peak value of ~0.09 Okta in August) region. These trends are directly related to the annual cycle of rainfall (Figure 3.2a) and thus the ISMR climatology (Figure 3.1a). The annual cycle of MCC (Figure 3.3b) shows a similar trend as that of LCC over all the regions, but with a decrease in their magnitudes. During the summer monsoon, the MCC values are high over the NE and CI regions, slightly decrease in the WC region, and becomes the minimum in the NW region. The annual cycle of MCC is also coherent with the climatology of MCC shown in Figure 3.1e. For all the four regions, the peak values of MCC are observed during the month of July (~ 0.2, 0.24, 0.25, and 0.09 Okta for WC, CI, NE, and NW regions, respectively).

3.4 Interannual variability and linear trends

Figure 3.4 shows the year-to-year variations of ISMR, LTS, and CAPE over WC, CI, NE, and NW regions during the summer monsoon season. Their trend values (per decade) along with that of LCC and MCC are given in Table 3.1. The ISMR shows high interannual variability over all the four regions with standard deviations of 57.5, 30.4, 51.5, and 17.4 mm over the WC, CI, NE, and NW regions respectively (Figure 3.4a).

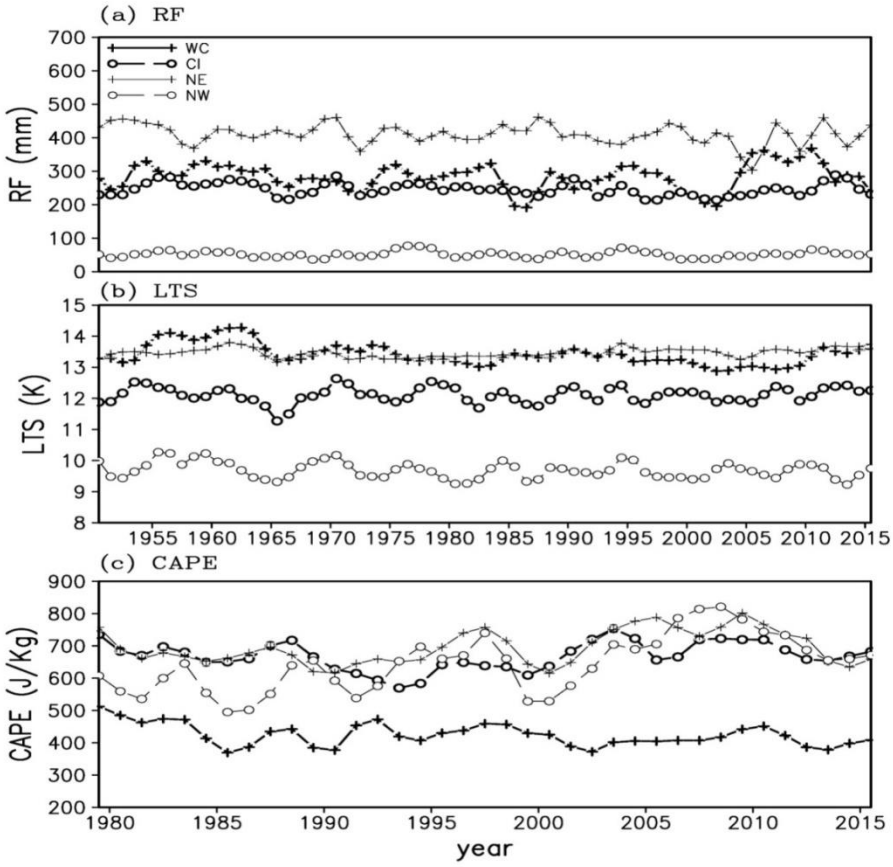

Figure 3.4: Interannual variability of (a) rainfall (mm), (b) LTS (K), and (c) CAPE (J Kg^{-1}) over WC, CI, NE, and NW regions during the summer monsoon. The interannual variability of rainfall and LTS were plotted for the period 1950-2015 and that of CAPE was plotted for the period 1979-2015.

It is noted that the ISMR shows a significant decreasing trend with 4.2 mm $decade^{-1}$ (at 15% significant level) in the NE region. Similarly, other regions also show decreasing trends but they are insignificant. The significant decreasing trend of ISMR in the NE region after the 1950s was also reported by Guhathakurtha et al. (2014). However,

Varikoden et al. (2013, 2019) reported an increasing trend in the NE region and that may be due to the different temporal period they considered. The decreasing trend of ISMR over the WC and CI regions was also reported by Varikoden et al. (2013). A negative trend in LTS is observed over the WC (at 0.01% significant level) and NW regions (at 15% significant level) and a positive trend over the other two regions, with a significant increase (at 12% significant level) over the NE region (Figure 3.4b).

An increasing trend in CAPE is observed in all the regions except in the WC (Figure 3.4c), where the trend is significantly negative (at more than 10% significance level). Increasing trends significant at 15% and 0.7% levels are observed over the NE and NW regions, respectively; but it is insignificant over the CI region. The increasing trend of CAPE over most parts of the Indian regions during the post-1980s was reported by Murugavel et al. (2012). They attributed it to the increase in moisture content in the lower troposphere and increasing temperature in the upper troposphere.

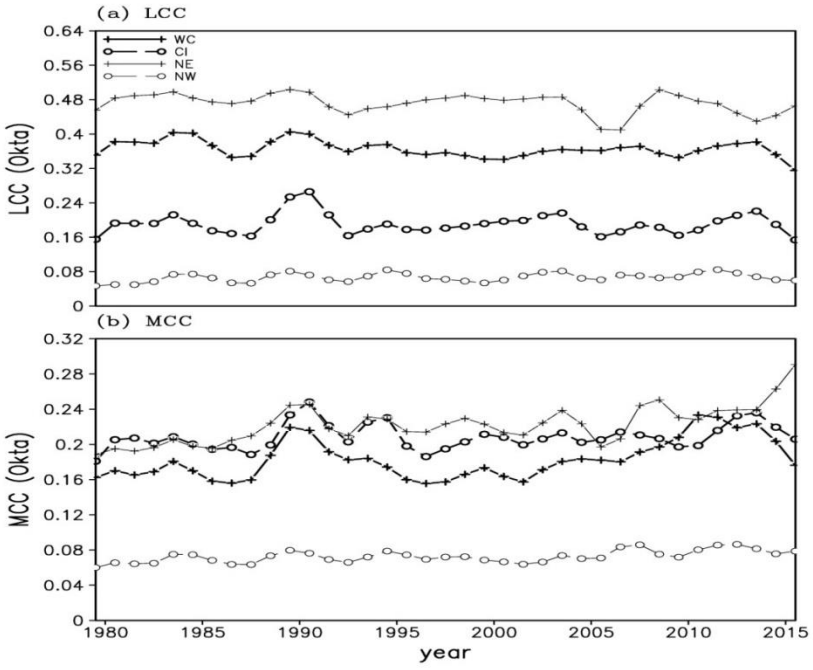

Figure 3.5: Interannual variability of (a) LCC (Okta) and (b) MCC (Okta) over WC, CI, NE, and NW regions during summer monsoon for the period 1979-2015.

Significant trends in LCC and MCC are observed over all the regions except over the CI region **(**Figure 3.5a and 3.5b**).** The trends of LCC are significant at 10%, 14%, and 15% levels over the WC, NE, and NW regions, respectively. However, in the case of MCC,

increasing trends are observed over the WC, NE, and NW regions at 1%, 0.1%, and 2.5% significant levels, respectively.

Variable	WC	CI	NE	NW
RF (mm)	-0.209	-2.27	-4.28*	-0.05
LTS (K)	-0.091*	0.01	0.02*	-0.04*
CAPE (J Kg^{-1})	-14.78*	6.11	16.10*	51.78*
LCC (Okta)	-0.007*	-0.001	-0.007*	0.003*
MCC (Okta)	0.01*	0.003	0.014*	0.004*

Table 3.1: The trend values (per decade) of rainfall, LTS, CAPE, LCC, and MCC over WC, CI, NE, and NW regions during the summer monsoon period.* represents the trend values with more than 15% significant level

3.5 Linkage between convective parameters and ISMR

To further explore the linkage between rainfall and convective parameters during the summer monsoon, the correlation coefficients between ISMR and convective parameters over the WC, CI, NE, and NW regions are analyzed (Table 3.2). LTS is positively (negatively) correlated with ISMR over the WC and CI regions (NE and NW). However, the correlation is significant only over the CI region (at 1% level). The increase in inversion strength in the lower troposphere during the summer monsoon causes an increase in moisture within the lower troposphere. It enhances the distribution of low-level clouds and thus the ISMR (Varikoden et al. 2011).

In the case of CAPE, its correlation with ISMR is significant over all the regions, except over the NE region. An in-phase (out-of-phase) relationship is observed over WC and NW (NE and CI) regions. The opposite nature of CAPE-ISMR correlation over the WC and CI may be due to the high and low orographic influences over the respective regions, as explained in Section 3.2. The variations in CAPE are driven by the low-level

moisture and inversion strength, which can favor an enhanced cloud cover and rainfall (Murugavel et al. 2012). This relationship is well observed in the case of WC and NW regions. Even though a high value of CAPE is associated with high convective activity, the regions of high CAPE need not always coincide with the regions of high precipitation since the convective inhibition energy (CINE) plays an important role (Jain et al. 2019). This may be the reason for the out-of-phase relationship between CAPE and ISMR observed over the NE and CI regions. It is also observed that the LCC is positively correlated with ISMR over all the four regions with more than 5% significant level. A similar in-phase-relationship is also observed for MCC, except over the NE region.

Variable	**WC**	**CI**	**NE**	**NW**
LTS (K)	0.051	0.334*	-0.118	-0.133
CAPE (JKg^{-1})	0.454*	-0.253*	-0.064	0.663*
LCC (Okta)	0.273*****	0.634*****	0.343*	0.804*
MCC (Okta)	0.370*	0.761*	0.192	0.803*

Table 3.2: Correlation coefficients between LTS, CAPE, LCC, and MCC with rainfall over the WC, CI, NE, and NW regions during the summer monsoon.* represents the correlations with more than 5% significant level.

3.6 Teleconnections with ENSO

To establish the linkage between ISMR and convective parameters with the tropical Pacific Ocean, the spatial correlation between ISMR, LTS, LCC, and CAPE with Niño 3.4 index during the summer monsoon season is analyzed (Figure 3.6). Since the relationship between LCC and ISMR is more robust than that with MCC, the analysis for MCC was excluded. From Figure 3.6, it is clear that ISMR is negatively significantly correlated with Niño 3.4 index over all the Indian regions except some areas in NE India (Figure 3.6a). This is in good agreement with the previous studies

(Mooley and Shukla 1987; Varikoden and Babu 2015; Varikoden and Revadekar 2019; Hrudya et al. 2020b).

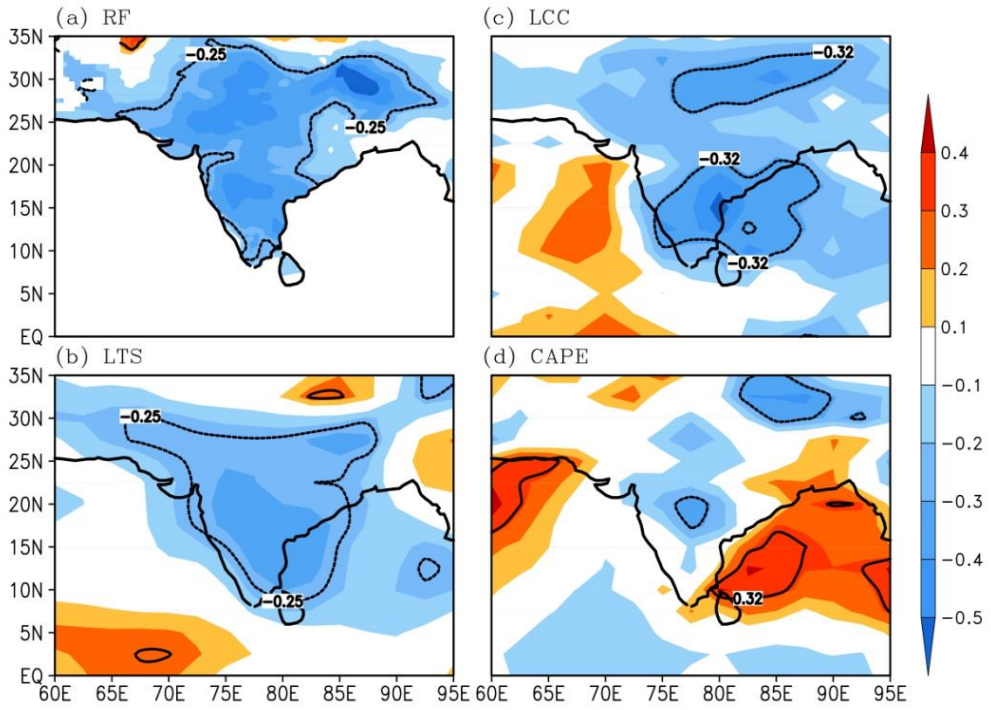

Figure 3.6: Spatial correlation between (a) rainfall, (b) LTS, (c) LCC, and (d) CAPE with Niño 3.4 index during the summer monsoon season. The contours represent 5% significant level.

A significant negative correlation between LTS and Niño 3.4 index is also observed over most of the Indian regions, whereas the NE region shows a positive insignificant correlation (Figure 3.6b). The out-of-phase relationship is dominated all over the Indian region for LCC also (Figure 3.6c), with significant correlations over the peninsular and northern regions. The correlation is relatively weak over the NE region as in the case of LTS. The correlation plot between Niño 3.4 index and CAPE is different from the other parameters (Figure 3.6d), where a negative correlation is observed only over the CI region. However, an in-phase relationship is observed over the NE and Bay of Bengal regions. Altogether, the analyses depict a negative significant correlation between ENSO with ISMR, LTS, and LCC during the summer monsoon season over most of the Indian regions, with weak or positive correlation over the NE region.

To check the consistency of these results, the 21-year sliding correlation between ISMR, LTS, LCC, and CAPE with Niño 3.4 index is analyzed (Figure 3.7)**.** The spatial correlations described in the earlier section between ISMR, LTS, LCC, and CAPE with Niño 3.4 index are well depicted in Figure 3.7.

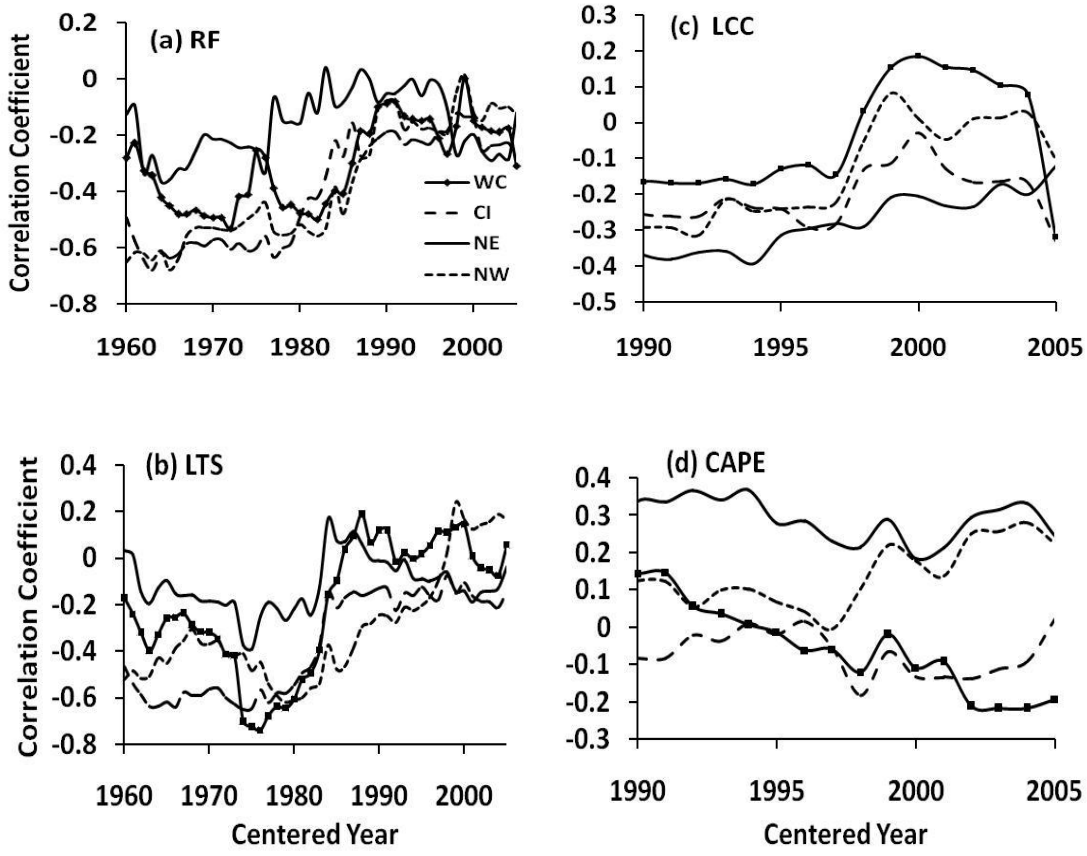

Figure 3.7: 21-year sliding correlation between (a) rainfall, (b) LTS, (c) LCC, and (d) CAPE with Niño 3.4 index over WC, CI, NE, and NW regions during the summer monsoon.

The negative correlation between ISMR and Niño 3.4 index over most of the Indian regions is clearly noticed in Figure 3.7a also, with some temporal fluctuations. Even though the out-of-phase relationship is dominated in all the four regions considered, it is relatively weak in the NE region as observed in Figure 3.6a. The out-of-phase relationship shows a decreasing trend from the 1980s up to 1990s in all the regions and thereafter it is almost consistent with less significance. This pattern of sliding correlation also holds good in the case of LTS (Figure 3.7b). The negative correlation between LCC and Niño 3.4 index is dominated over all four regions. It shows a

decreasing trend up to 1995 in all the regions, thereafter it turns to an in-phase relationship over the WC and NW regions (Figure 3.7c). However, it remains unchanged in the other two regions. In the case of CAPE (Figure 3.7d), the correlation patterns are different in which an out-of-phase relationship is dominated only in the CI region as observed in Figure 3.6d. An in-phase relationship is observed over the NE and NW regions, whereas it changes from in-phase to an out-of-phase relationship in the WC region after 2000. The different nature of CAPE-Niño 3.4 correlation may be due to the influence from other atmospheric and oceanic factors on CAPE, apart from ENSO.

3.7 Chapter summary

The regional variability of ISMR over the WC, CI, NE, and NW regions of India during the period 1950-2015 was explored by identifying its relationship with LTS, cloud cover, and CAPE. The summer monsoon rainfall over India exhibits high spatial and temporal variabilities over all four regions during the period of study. The annual cycle of LTS, LCC, and MCC is almost similar to that of rainfall during the summer monsoon season; whereas it is different for the other seasons. ISMR shows a decreasing trend in all the regions, with a significant decrease over the NE region. All the other parameters exhibit significant trends, except in the CI region, where the trends are insignificant.

Among all the regions considered, LTS is significantly correlated with summer monsoon rainfall only in central India, where the correlation is in-phase. The increase in inversion strength in the lower troposphere during the summer monsoon causes the distribution of more moisture within the lower troposphere. It enhances the low-level clouds and thus the rainfall. A contrasting nature of correlation between CAPE and ISMR is observed over the WC and CI regions, which may be due to the high and low orographic influences over the WC and CI regions, respectively. Both the LCC and MCC are positively correlated with ISMR over all four regions. However, more robust relationships are noticed in the case of LCC. All the convective parameters and ISMR exhibit significant association with the SST variations over the tropical Pacific Ocean during the study period. Niño 3.4 index is significantly negatively correlated with ISMR, LTS, and LCC over most of the Indian regions, but with an insignificant relationship over the NE region. The correlation patterns are different in the case of

CAPE and may be due to the influence from other atmospheric and oceanic factors apart from the ENSO.

CHAPTER 4

RECENT CHANGES IN THE ENSO-MONSOON RELATIONS DURING DIFFERENT PHASES OF INDIAN SUMMER MONSOON

CHAPTER 4

RECENT CHANGES IN THE ENSO-MONSOON RELATIONS DURING DIFFERENT PHASES OF INDIAN SUMMER MONSOON

4.1 Introduction

In the last chapter, the analysis of the relationship between ENSO and ISMR over different regions of India was initiated. The ENSO-ISMR relationship is further explored in this chapter by studying the changes in the relationship from early (1951-1980) to recent (1986-2015) decades during different phases (onset, peak, and withdrawal) of the Indian summer monsoon. The influence from SST, circulation features, low-level winds, etc. in the Pacific Ocean on the variability of ISMR is analyzed separately for El Niño and La Niña years.

4.2 ISMR climatology during onset, peak, and withdrawal phases

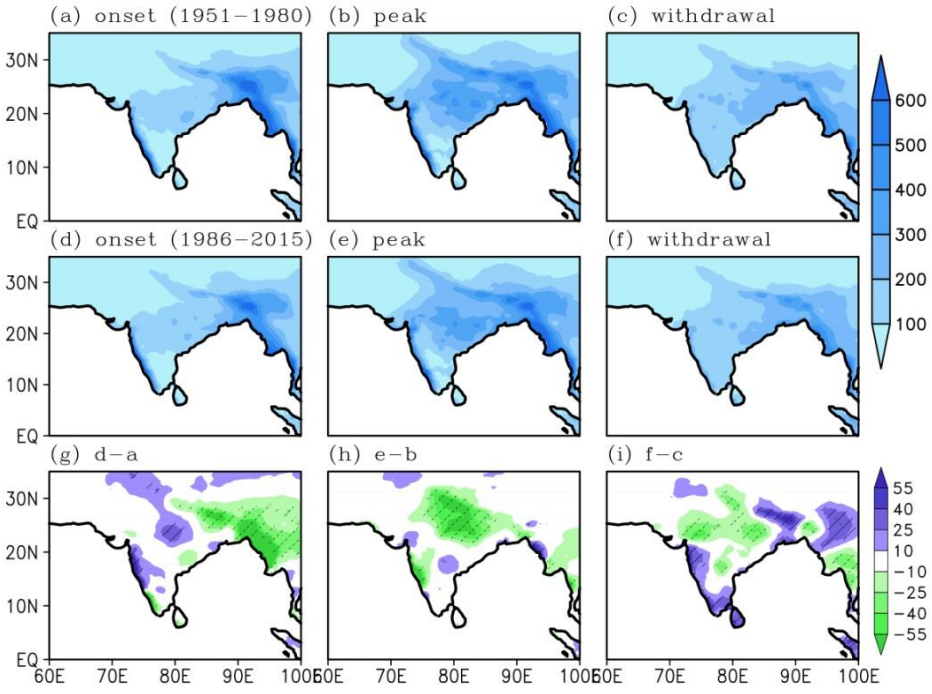

Figure 4.1: Climatology of ISMR (mm) during onset, peak, and withdrawal phases in early and recent decades. The hatches represent the regions with 5% significance.

Figure 4.1 shows the spatial variations of ISMR during onset, peak, and withdrawal phases in early and recent decades. According to previous studies, during the summer

monsoon, maximum rainfall is observed over the west coast and northeastern regions of India (>480 mm month^{-1}), moderate rainfall over central India (120 mm to 480 mm month^{-1}), and fewer amounts of rainfall over the northwest and southeast regions (<120 mm month^{-1}) (Rao 1976; Rajeevan et al. 2006; Kishore et al. 2015; Nair et al. 2018; Suthinkumar et al. 2019; Preethi et al. 2019). These threshold values for the different categories of rainfall in the respective regions are based on the studies of Suthinkumar et al. (2019) and Preethi et al. (2019). However, the ISMR climatology in relation to onset, peak, and withdrawal phases are slightly different from the seasonal pattern, particularly in terms of the amount of rainfall.

High regional variability in ISMR is observed during all three phases in the early decades. During the onset phase, precipitation is maximum over the west coast and northeast regions (Figure 4.1a). However, the regional distribution of ISMR is varied during the peak phase, particularly over the monsoon core zone (15°-25°N, 70°-90°E) and foothills of Himalaya. ISMR shows an increase of more than 250 mm from the onset phase over these two regions (Figure 4.1b). ISMR decreases to about 250 mm over the monsoon core zone, northeast regions, and foothills of Himalayas during the withdrawal phase (Figure 4.1c). During this phase, a noticeable decrease of more than 350 mm (~40 %) is observed over the west coast as compared to the other two phases. In the recent decades, ISMR distribution almost shows a similar climatology as that of the early decades during the onset phase (Figure 4.1d). However, significant changes are observed over the west coast, northeast, and central Indian regions (Figure 4.1g). ISMR shows a significant decrease over the foothills of Himalayas and northeast regions. A significant increase in ISMR is observed in the northern parts of the west coast, while it decreases in the southern parts. This result is consistent with Sandeep et al. (2018) and Varikoden et al. (2019).

Significant changes in ISMR spatial distributions are observed in recent decades during the peak phase also (Figure 4.1e and 4.1h). A significant decrease (less than 55 mm) in ISMR is observed mainly in the west coast and north-central Indian regions. A contrasting pattern is observed over the northern west coast, in which ISMR increases during the onset phase, but decreases during the peak phase. ISMR shows a significant increase in the northern parts of the west coast and northeast regions (Figure 4.1f and

4.1i) during the withdrawal phase. However, it shows a significant decrease in the north-central Indian region as in the case of the peak phase.

4.3 Changes in the ENSO-ISMR correlations from early to recent decades

To explore the changes in ENSO-ISMR relations from early to recent decades during different phases, the spatial correlation between the Niño 3.4 index and ISMR during onset, peak, and withdrawal phases in the early and recent decades is analyzed (Figure 4.2). A significant negative ENSO-ISMR correlation is observed over most parts of India during all the three phases in both the early and recent decades, consistent with the previous studies (Sikka 1980; Rasmussen and Carpenter 1983; Mooley and Parthasarathy 1983; Ihara et al. 2007).

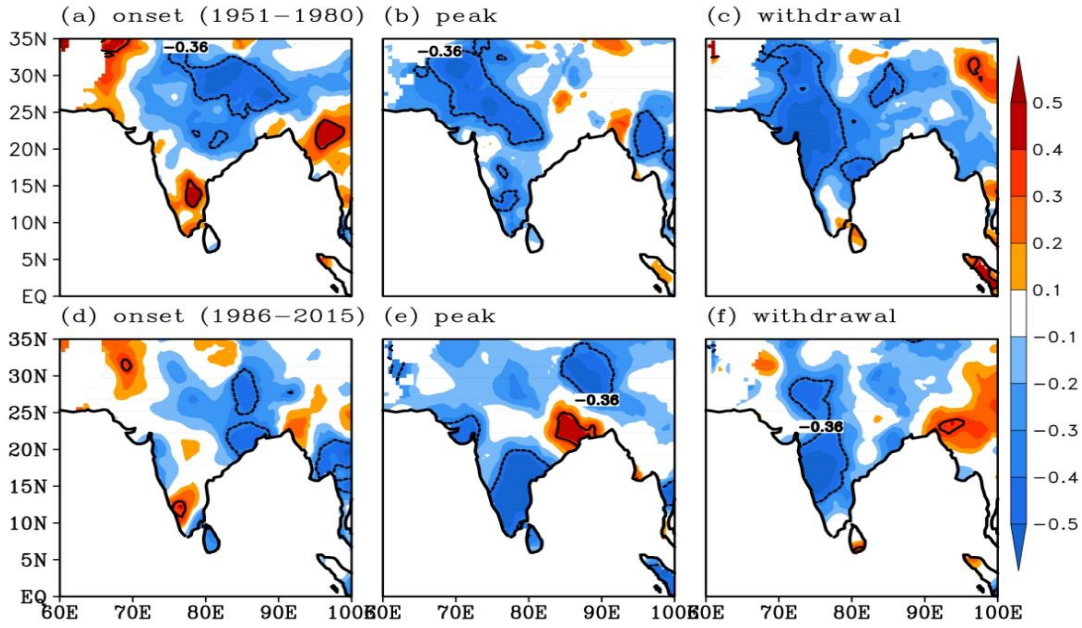

Figure 4.2: spatial correlation between Niño 3.4 index and ISMR during onset, peak, and withdrawal phases in the early and recent decades. The contours represent the regions with 5% significance.

ISMR shows an out-of-phase relationship (negative correlation) with the Niño 3.4 index over most of the Indian regions during the onset phase in the early decades. However, a significant relationship is observed mainly over the north-central regions and Gangetic plain (Figure 4.2a). In contrast, a positive correlation is observed over peninsular India, with a significant positive correlation in its southern parts. Significant negative

correlations are observed over the central and northwest regions (Figure 4.2b) during the peak phase. Here, a significant negative correlation is observed over the southern peninsular region also, which is entirely opposite from the onset phase. The ENSO-ISMR correlation is negative over most of the Indian regions, except the southeast and northern regions during the withdrawal phase, where the correlation is void or insignificantly positive. The central and entire western regions of India (Figure 4.2c) are associated with significant out-of-phase relationships during this phase. Unlike the other two phases, south peninsular India does not show any significant correlations during this phase. In general, the areas of significant out-of-phase relationships show a shift from the eastern region to the western region of India from the onset phase to the withdrawal phase in the early decades.

As compared to the early decades, the ENSO-ISMR correlation is weakening during all phases in the recent decades**.** During the onset phase, the areas with significant negative correlations decrease in the north-central region, and the areas with significant positive correlations decrease in the southern peninsular regions (Figure 4.2d). The significance of the ENSO-ISMR relationship loses over the northern regions, while the significance is gained over the southern regions during the peak phase (Figure 4.2e). During the withdrawal phase, significant negative correlation values are observed in some parts of central, northwest, and west coast regions. In general, there is a relative weakening of the ENSO-ISMR relationship in the recent decades with respect to the early decades during all phases. The weakening of the ENSO-monsoon relationship during the summer monsoon season was observed in the earlier studies (Kumar et al. 1999; Ashrit et al. 2001; Roy et al. 2019**)**. The weakening relationship (Based on reduced regions of insignificant correlation) is more prominent during the onset phase than that during the other two phases.

This observed ENSO-ISMR relationship is further explored by studying the impact of El Niño and La Niña phases on ISMR separately. The El Niño and La Niña years selected for the analysis along with the Niño 3.4 index values during all phases in early and recent decades are given in Table 4.1. The method of classification of El Niño and La Niña years has already been explained in Chapter 2.

Early Decades (1951-1980)						
	Onset		Peak		Withdrawal	
	Year	Niño 3.4 index	Year	Niño 3.4 index	Year	Niño 3.4 index
El Niño	1951	0.6	1951	0.8	1951	1
	1953	0.8	1953	0.7	1953	0.8
	1957	1.1	1957	1.3	1957	1.3
	1958	0.6	1958	0.5	1963	1.2
	1963	0.5	1963	1	1965	1.9
	1965	0.8	1965	1.35	1969	0.8
	1972	0.9	1968	0.55	1972	1.6
			1972	1.25	1976	0.6
					1977	0.6
La Niña	1954	-0.5	1954	-0.7	1954	-0.9
	1955	-0.7	1955	-0.7	1955	-1.1
	1956	-0.5	1956	-0.6	1956	-0.5
	1964	-0.6	1964	-0.65	1964	-0.8
	1971	-0.7	1970	-0.7	1970	-0.8
	1973	-0.9	1971	-0.8	1971	-0.8
	1974	-0.8	1973	-1.2	1973	-1.5
	1975	-1	1975	-1.15	1975	-1.4
Recent Decades (1986-2015)						
El Niño	1987	1.2	1987	1.6	1986	0.7
	1991	0.6	1991	0.65	1987	1.6
	1992	0.7	1997	1.75	1991	0.6
	1993	0.6	2002	0.85	1994	0.6
	1997	1.2	2004	0.55	1997	2.1
	2002	0.7	2009	0.5	2002	1
	2015	1.2	2015	1.65	2004	0.7
					2006	0.5
					2009	0.7
					2015	2.1
La Niña	1988	-1.3	1988	-1.2	1988	-1.2
	1999	-1	1998	-0.95	1995	-0.8
	2000	-0.6	1999	-1.1	1998	-1.3
	2008	-0.5	2000	-0.55	1999	-1.2
	2010	-0.6	2007	-0.65	2000	-0.5
			2010	-1.2	2007	-1.1
			2011	-0.6	2010	-1.6
					2011	-0.9

Table 4.1: El Niño and La Niña years and the corresponding Niño 3.4 index values during onset, peak, and withdrawal phases in the early and recent decades

Figure 4.3 and 4.4 illustrate the ISMR anomalies during El Niño and La Niña years, respectively, in the early and recent decades**.** During El Niño years, most of the Indian regions including central, northeast, northwest, north, and west coast show reduced rainfall conditions in the early decades during the onset phase (Figure 4.3a). It is consistent with the observations as shown in Figure 4.2a. ISMR decreases during the peak phase, mainly over the central and foothills of Himalayas. However, some parts of the northeast, west coast, and peninsular regions exhibit excess rainfall conditions (Figure 4.3b). During the withdrawal phase, the inverse relationship of El Niño with ISMR is clearly visible over most parts of India (Figure 4.3c), and this relationship is stronger during this phase than that during the other two phases.

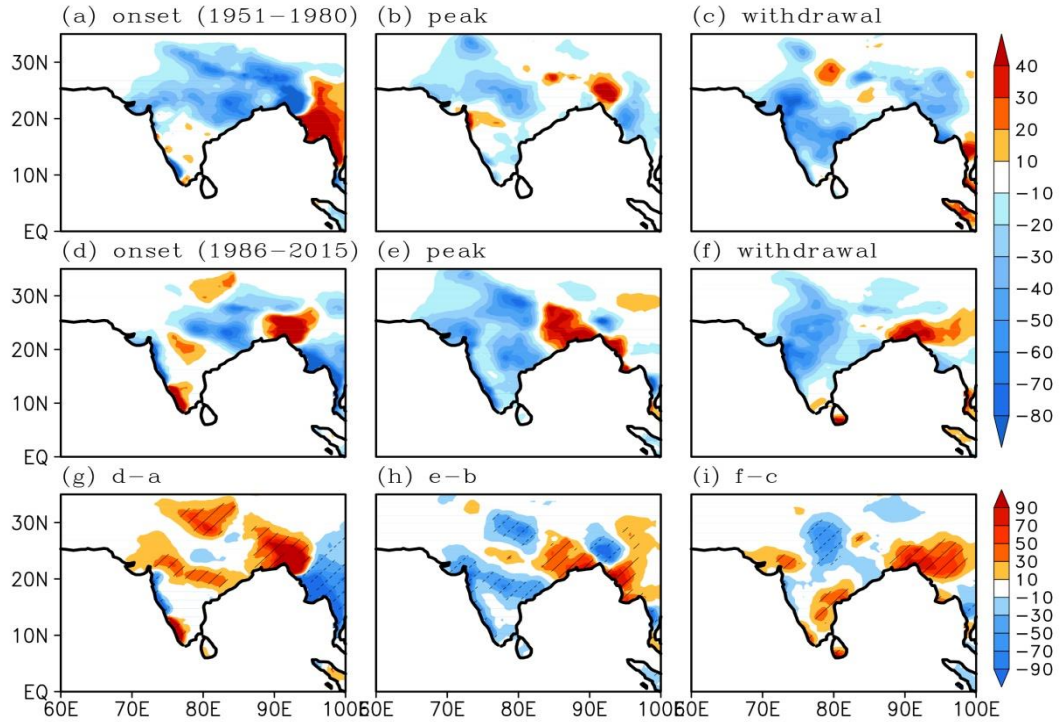

Figure 4.3: ISMR anomalies (mm) for El Niño years during onset, peak, and withdrawal phases in the early and recent decades. The hatches represent the regions with more than 5% significance.

In the case of recent decades, a significant increase in ISMR is observed over the southern west coast, northeast, and monsoon core zone during the onset phase (Figure 4.3d and 4.3g). A significant increase in ISMR is noticed over southern regions of the west coast. However, ISMR decreases significantly over the northern regions of the west coast. This contrasting pattern in ISMR over the west coast is comparable with the

results presented in Figure 4.2d, in which negative and positive correlations are found over the northern and southern west coast, respectively. During the peak phase, a significant decrease in ISMR (~ 50 mm below the normal) is observed almost all over India (Figure 4.3e and 4.3h). The areas of the northeast that are characterized by high precipitation show a strong ENSO-ISMR relationship as evidenced by Figure 4.2e. However, during the withdrawal phase, there is a significant decrease in ISMR over north-central India (~60 mm) and a significant increase over the peninsular and northeast regions (Figure 4.3f and 4.3i).

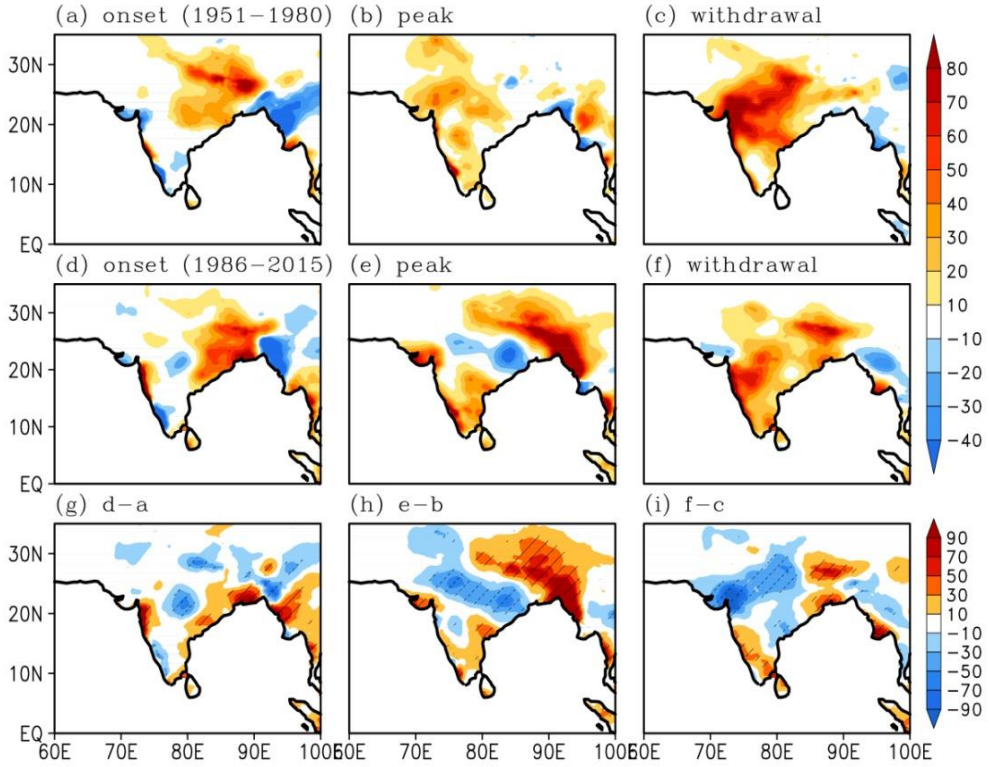

Figure 4.4: ISMR anomalies (mm) for La Niña years during onset, peak, and withdrawal phases in the early and recent decades. The hatches represent the regions with more than 5% significance.

As far as La Niña years are considered, the impact of La Niña is mainly observed over central India, foothills of Himalayas, and the northern west coast regions (Figure 4.4a) in the early decades during the onset phase. The regions of positive ISMR anomalies are observed mainly in the western regions during the peak phase (Figure 4.4b). These regions consist of major portions of the monsoon core zone, northwest, and west coast regions. Eastern regions are not much influenced by the La Niña events in the early

decades. In the case of the withdrawal phase, enhanced ISMR is observed over most parts of India, except in the southeast regions (Figure 4.4c). In recent decades, ISMR is significantly decreased (~60 mm) over the monsoon core zone during peak and withdrawal phases (Figure 4.4e, h, f, and i). However, a significant reduction is observed over some parts of central and northeast India during the onset phase (Figure 4.4d and 4.4g).

In general, the analysis of ISMR anomalies during El Niño years indicates a significant increase in ISMR during the onset phase and a significant decrease during peak and withdrawal phases over the monsoon core zone of India in recent decades. However, in the case of La Niña years, ISMR significantly decreases over the monsoon core zone during all phases. The reduction is more prominent during peak and withdrawal phases.

4.4 Indo-Pacific sea surface temperature

It is well known that the variability in the SST over the Indo-Pacific domain is related to the variability of ISMR (Cherchi and Navarra 2013). Hence, the impact of ENSO on different phases of ISMR is analyzed by connecting the SST anomalies over the Indo-Pacific domain to the ISMR during different phases separately.

4.4.1 SST-ISMR teleconnections during El Niño and La Niña years

Figure 4.5 and 4.6 show the SST anomalies over the Indo-Pacific domain during El Niño and La Niña years, respectively, for different phases of ISMR in the early and recent decades. SST over the Indo-Pacific domain shows considerable variability, particularly in the central and eastern Pacific during El Niño years. In the early decades, the SST anomalies have increased from onset to peak phase (about 0.4 °C) and again towards the withdrawal phase (Figure 4.5a-c**).** During the withdrawal phase, a westward shift of warm waters from the central equatorial Pacific is observed and the eastern region is replaced with relatively cooler SSTs**.** In recent decades, a significant increase in SST is observed over the central and eastern Pacific during the onset phase (Figure 4.5d and 4.5g)**.** The increase in SST over the central Pacific is higher than that over the eastern Pacific. Apart from the canonical El Niño, an El Niño 'Modoki-like' condition exists there, in which the central Pacific is warmer than the east. An increase of Indian Ocean SST is also observed, with significant increases in its eastern regions.

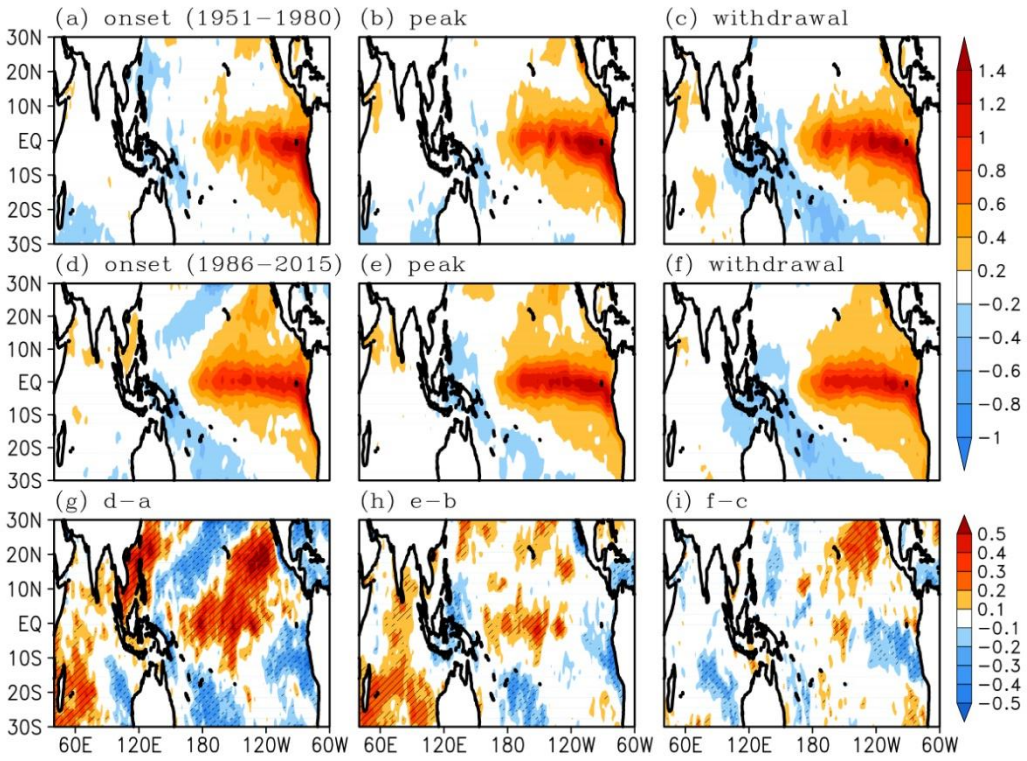

Figure 4.5: SST anomalies (°C) for El Niño years during onset, peak, and withdrawal phases in the early and recent decades. The hatches represent the regions with 5% significance.

The SST over the central Pacific and the Indian Ocean increases during the peak phase (Figure 4.5e and 4.5h) and withdrawal phase (Figure 4.5f and 4.5i) in recent decades. However, the areas with significant SST are reduced in both phases as compared to the onset phase. The increase in SST during El Niño years in the central Pacific and the Indian Ocean during the onset phase in recent decades can be associated with the decreased ENSO-ISMR correlation and thus the enhanced ISMR observed during the onset phase in recent decades (Figure 4.5g, 4.3g, and 4.2d)**.** However, this relationship is not much valid during peak and withdrawal phases, since the variations of SST during these phases are not significant as those during the onset phase. The changes in ISMR may also be influenced by the SST of other oceanic regions apart from the Pacific Ocean, such as the Indian Ocean (Francis and Gadgil 2013; Nair et al. 2018) and the Atlantic Ocean (Goswami et al. 2006b; Varikoden and Babu 2015).

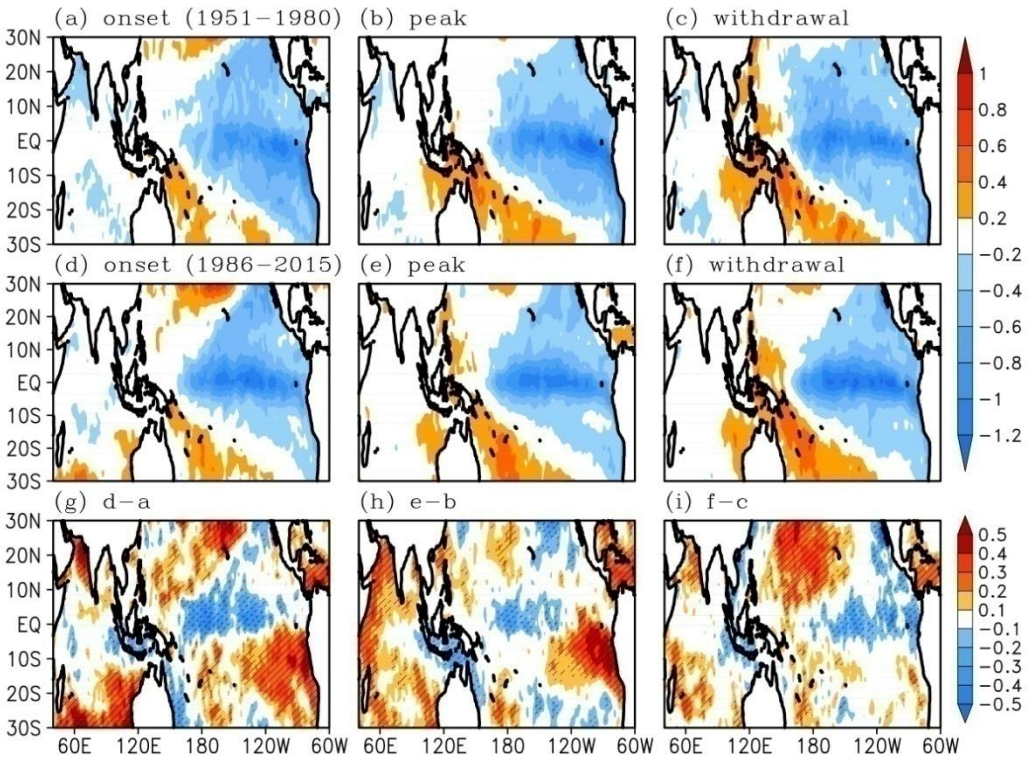

Figure 4.6: SST anomalies (°C) for La Niña years during onset, peak, and withdrawal phases in the early and recent decades. The hatches represent the regions with 5% significance.

In the case of La Niña years, the SST anomalies over the central and eastern Pacific have decreased from onset to peak and then to withdrawal phase in the early decades; indicating the strength of the La Niña phase (Figure 4.6a-c) from onset to withdrawal phase. In recent decades, SST significantly decreased in the central Pacific during all phases, particularly during the onset and withdrawal phases. However, in the eastern Pacific (Niño 1+2 regions), a significant increase in SST is observed during the onset and peak phases. During the peak phase, this increase is more than 0.4 °C from that of the early decades (Figure 4.6h). As far as the Indian Ocean is considered, a significant increase in the SST over its western parts is clearly observed during all phases in the recent decades, except in certain regions of the equatorial Indian Ocean. It indicates that the SST changes in the Pacific Ocean and the Indian Ocean together can influence the changing patterns of ISMR during La Niña years. As in the case of El Niño, the changes in SST pattern during La Niña years can also be connected to the observed changes in ISMR in the recent decades. These observed relationships can be further validated by

analyzing the circulation features over the Indo-Pacific domain since ISMR is influenced by other oceanic and atmospheric factors apart from SST.

4.5 Large scale circulation features

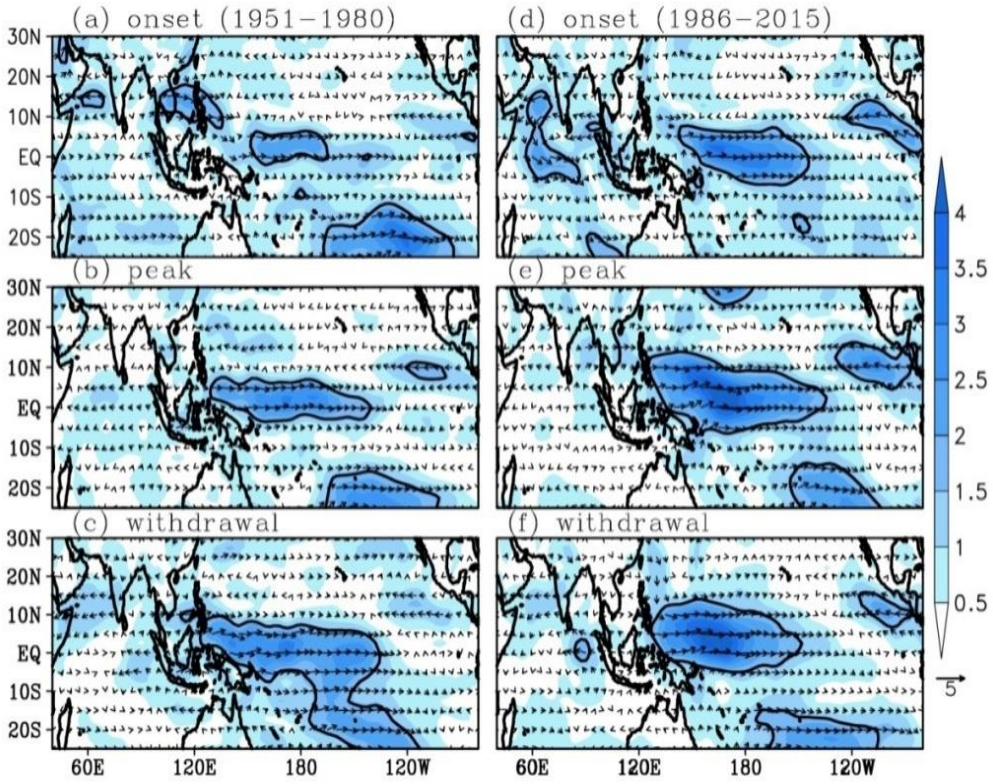

Figure 4.7: Low-level (850 h Pa) wind anomalies (vectors; in m s^{-1}) and magnitudes (shaded; in m s^{1}) for El Niño years during onset, peak, and withdrawal phases in the early and recent decades. The contours represent the regions with 5% significance.

The low-level circulation anomalies (850 h Pa) over the Indo-Pacific domain during El Niño and La Niña years are shown in Figure 4.7 and 4.8, respectively. The circulation patterns show noticeable differences from one phase to the other during El Niño and La Niña years. During El Niño years, the westerly component of easterly trade winds strengthens over the central Pacific in the recent decades during all phases (Figure 4.7d-f). This strengthening of the westerly component (weakening of easterly trade winds) modifies the ENSO-ISMR relationship, together with the warming of the equatorial Indian and central Pacific Oceans. A significant increase in the westerly component in recent decades is also observed over the western equatorial Indian Ocean during the onset phase and over the northeast Indian Ocean during the peak phase**.** This weakening

of easterly trade winds over the central Pacific and the Indian Ocean during the onset phase can be attributed to the enhanced warming of the same regions (Figure 4.5g), since, the high SST/low pressure in the central and eastern Pacific during El Niño years affects the ISMR (Ihara et al. 2007). It produces a weakened ENSO-ISMR relationship and thus enhanced ISMR over most of the Indian region during the onset phase (Figure 4.3g). Nevertheless, during peak and withdrawal phases, the weakening of trade winds is more confined to the western Pacific and SST over the central Pacific does not show large variations. Therefore, the ENSO-ISMR relationship does not vary significantly during these phases, although, a slight weakening is evident.

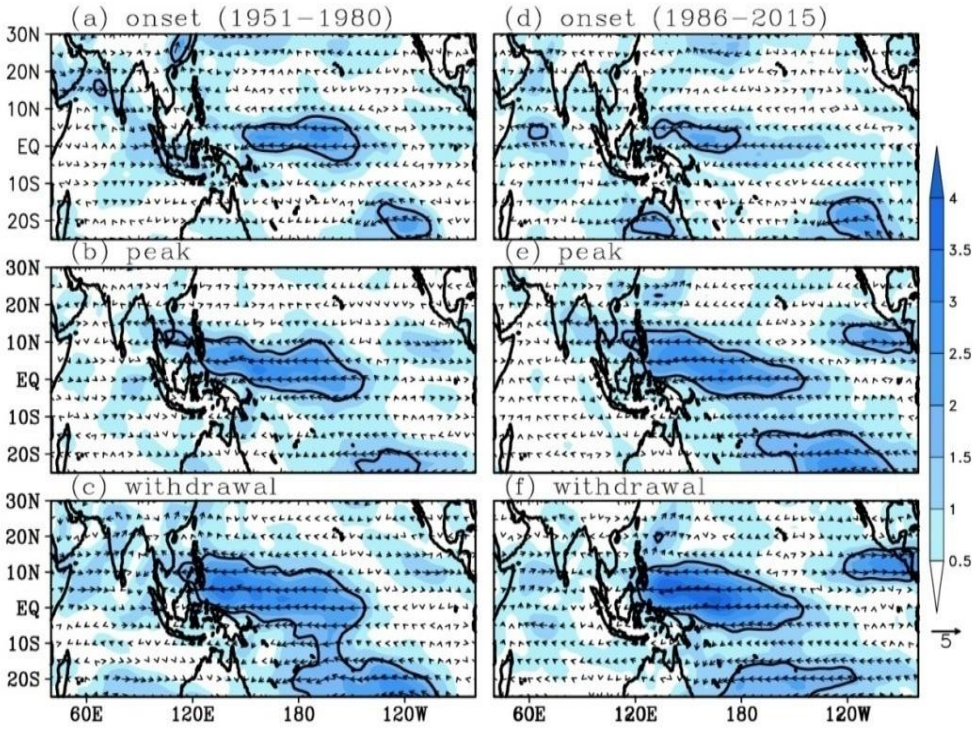

Figure 4.8: Low-level (850 h Pa) wind anomalies (vectors; in m s^{-1}) and magnitudes (shaded; in m s^{1}) for La Niña years during onset, peak, and withdrawal phases in the early and recent decades. The contours represent the regions with 5% significance.

During La Niña years (Figure 4.8), the equatorial easterly trade winds in the Pacific intensify, when compared to normal Pacific conditions. This intensification is seen more prominent in the central and western equatorial Pacific. Additionally, an intensification of low-level westerlies over the Arabian Sea is also observed, which enhances the moisture transport toward the Indian region. There are noticeable changes

in circulation patterns from early to recent decades during all three phases (Figure 4.8d-f). The intensification of easterly trade winds during the onset phase can be attributed to the decrease in SST over the central Pacific and hence the decrease in ISMR observed over the monsoon core zone of India in the recent decades (Figure 4.4d). Similarly, the intensification of easterlies during the other two phases can also be connected to the observed ISMR patterns. However, this relationship is not much evident during peak and withdrawal phases, since the SST over the equatorial Pacific does not show noticeable variations during these phases.

4.6 Changes in Walker circulation

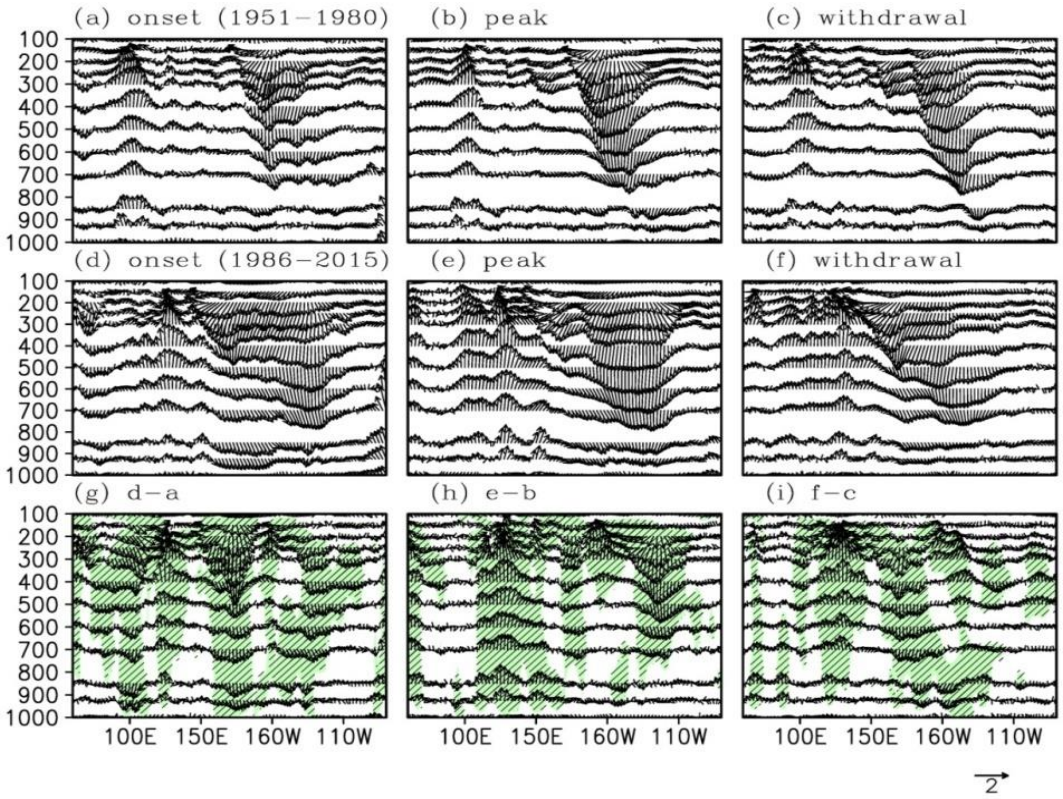

Figure 4.9: Walker circulation anomalies over the Indo-Pacific domain for El Niño years during onset, peak, and withdrawal phases in the early and recent decades. The shades represent the regions with 5% significance.

The changes in Walker circulation over the Indo-Pacific domain during onset, peak, and withdrawal phases in the early and recent decades for El Niño and La Niña years are shown in Figure 4.9 and 4.10, respectively. According to Kumar et al. (1999), the

weakening of the ENSO-ISMR relationship in recent decades is due to the eastward shift of the ascending branch of Walker circulation from the western equatorial Pacific to the central equatorial Pacific. As a result, there is a corresponding eastward shift of the subsidence zone. During El Niño years, the subsidence over the equatorial Indian Ocean has increased from onset to withdrawal phases in the early decades (Figure 4.9a-c). In recent decades, the subsidence over the same regions has significantly increased during the onset phase and decreased during the peak phase (Figure 4.9d, g, e, and h). The increase of subsidence over the equatorial Indian Ocean during the onset phase modifies the regional Hadley circulation by increasing the ascending motion over the Indian region. Hence, it produces enhanced rainfall over the Indian region during the summer monsoon. Similarly, the decrease in subsidence over the equatorial Indian Ocean during the withdrawal phase (Figure 4.9f and 4.9i) can be connected to the weakening of regional Hadley circulation and thus the reduction in ISMR during this phase. However, such a relationship is not observed during the peak phase since there are no noticeable changes in the subsidence from early to recent decades.

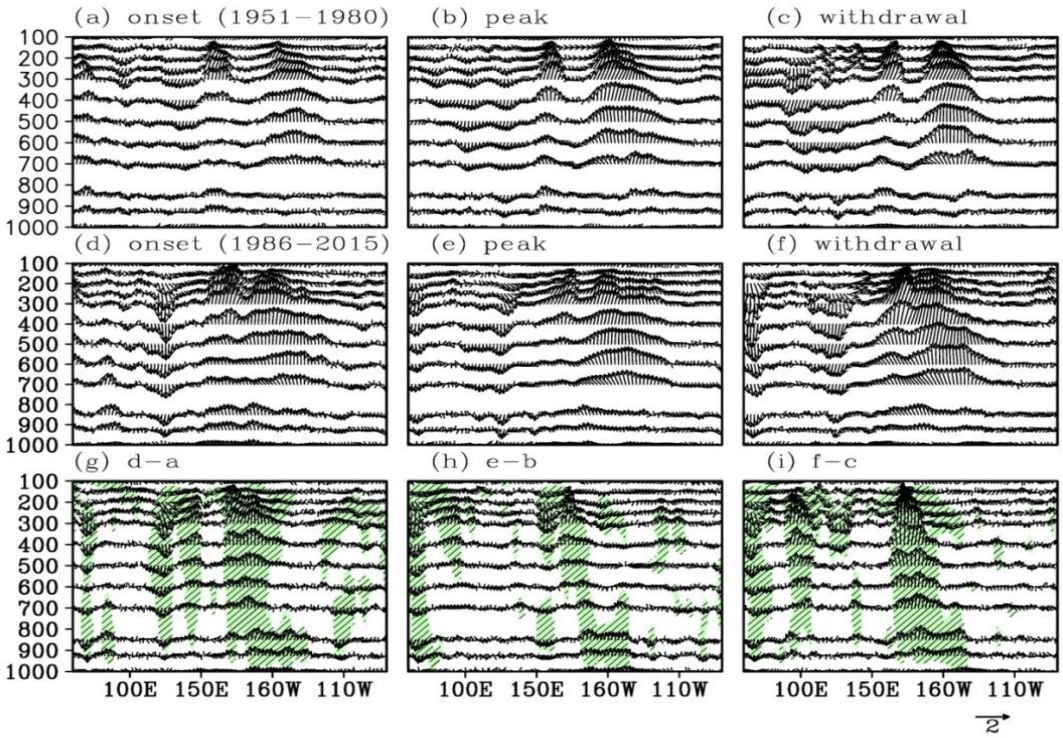

Figure 4.10: Walker circulation anomalies over the Indo-Pacific domain for La Niña years during onset, peak, and withdrawal phases in the early and recent decades. The shades represent the regions with 5% significance.

In the case of La Niña years (Figure 4.10), a significant change in the Walker circulation is observed in the recent decades during onset and withdrawal phases (Figure 4.10d, g, f, and i). The ascending motion over the equatorial Indian Ocean is increased during the onset phase in recent decades. This increase in ascending motion weakens the regional Hadley circulation to enhance its descending branch, which suppresses ISMR over most parts of India during this phase. Similar changes in Walker circulation anomalies are found during withdrawal phases also, but weak as compared to the onset phase. However, the changes are not noticeable during the peak phase (Figure 4.10 e and 4.10h).

Altogether, the analysis indicates a weakening of easterly trade winds over the equatorial Pacific and the Indian Ocean in recent decades during all phases during El Niño years and it may be related to the enhanced warming of the same regions. The subsidence over the equatorial Indian Ocean increases and it modifies the regional Hadley circulation by increasing the ascending motion over the Indian region and thus it enhances the ISMR. These changes are more evident during the onset phase. In the case of La Niña years, the reverse conditions are observed due to the strengthening of easterly trade winds over the equatorial Pacific in recent decades. It is also associated with the cooling of the central and eastern equatorial Pacific Ocean. The enhanced ascending motion over the equatorial Indian Ocean weakens the regional Hadley circulation, which reduces ISMR over most parts of the Indian region during all phases.

4.7 Chapter summary

The linkage between the tropical Pacific Ocean and ISMR variability was analyzed for the period 1951-2015, by studying the ENSO-ISMR relationship during onset, peak, and withdrawal phases of ISMR. The changes in the ENSO-ISMR relationship from early to recent decades were analyzed. The summer monsoon rainfall over India shows significant spatial variations during onset, peak, and withdrawal phases in both the early and recent decades. Significant changes in ISMR are mainly observed over the west coast, northeast, and the monsoon core zone of India in recent decades. ENSO shows significant negative correlation with ISMR during all three phases in both the epochs and, the correlation decreases in recent decades. During El Niño years, ISMR over most of the Indian regions significantly increases during the onset phase and decreases during

peak and withdrawal phases in the recent decades**.** In the case of La Niña, a significant decrease in ISMR is observed over the monsoon core zone during all phases in recent decades. The changes in SST, low-level circulation, and Walker circulation anomalies over the central and eastern Pacific and the Indian Ocean are linked to the changes in ISMR characteristics during all three phases. However, the changes are more significant during the onset phase than the other two phases.

CHAPTER 5

RECENT CHANGES IN THE ISMR-IOD RELATIONSHIP DURING ONSET, PEAK, AND WITHDRAWAL PHASES OF INDIAN SUMMER MONSOON

CHAPTER 5

RECENT CHANGES IN THE ISMR-IOD RELATIONSHIP DURING ONSET, PEAK, AND WITHDRAWAL PHASES OF INDIAN SUMMER MONSOON

5.1 Introduction

Apart from the tropical Pacific Ocean, coupled-ocean atmosphere interactions in the tropical Indian Ocean also make significant impacts on the variability of ISMR. The IOD phenomenon arises as a result of the mutual interactions between the ocean and atmosphere over the tropical Indian Ocean. The frequency and strength of IOD events have increased in recent decades (Abram et al. 2008), and also the IOD-ISMR relationship has strengthened (Ashok et al. 2001, 2004; Ummerhofer et al. 2011; Krishnaswami et al. 2015). However, within the summer monsoon season itself, the IOD-ISMR relationship highly varies for its onset, peak, and withdrawal phases. This chapter analyzes the IOD-ISMR relationship during the onset, peak, and withdrawal phases of the Indian summer monsoon by studying the changes in the relationship from early (1951-1980) to recent (1986-2015) decades. It also analyzes the impact of SST variations and circulation features over the tropical Indian Ocean on the ISMR patterns over different Indian regions for positive IOD (pIOD) and negative IOD (nIOD) events separately. Hence, it in turn illustrates the influence of Indian Ocean dynamics on the variability of ISMR.

5.2 Changes in the IOD-ISMR correlations from early to recent decades

Figure 5.1 shows the spatial correlation between ISMR and DMI during onset, peak, and withdrawal phases in the early and recent decades. ISMR shows an in-phase relationship with DMI over most parts of northern India and some parts of peninsular India during the onset phase in the early decades (Figure 5.1a). However, the correlation is negative over the monsoon core zone of India. Significant positive correlations are observed over northwest regions and central Konkan coast, and negative correlations over some areas of central India. During the peak phase, the correlation values are negative over most of the Indian regions and are prominent over the northern Indian

regions, where the relationship was in-phase during the onset phase (Figure 5.1b). Negative correlation values are dominant over most of the Indian regions during the withdrawal phase (Figure 5.1c). However, the areas of negative correlations are reduced as compared to the peak phase. It is noticed that the relationship is in-phase over the northern Konkan coast during the onset phase, but it is inverted during peak and withdrawal phases.

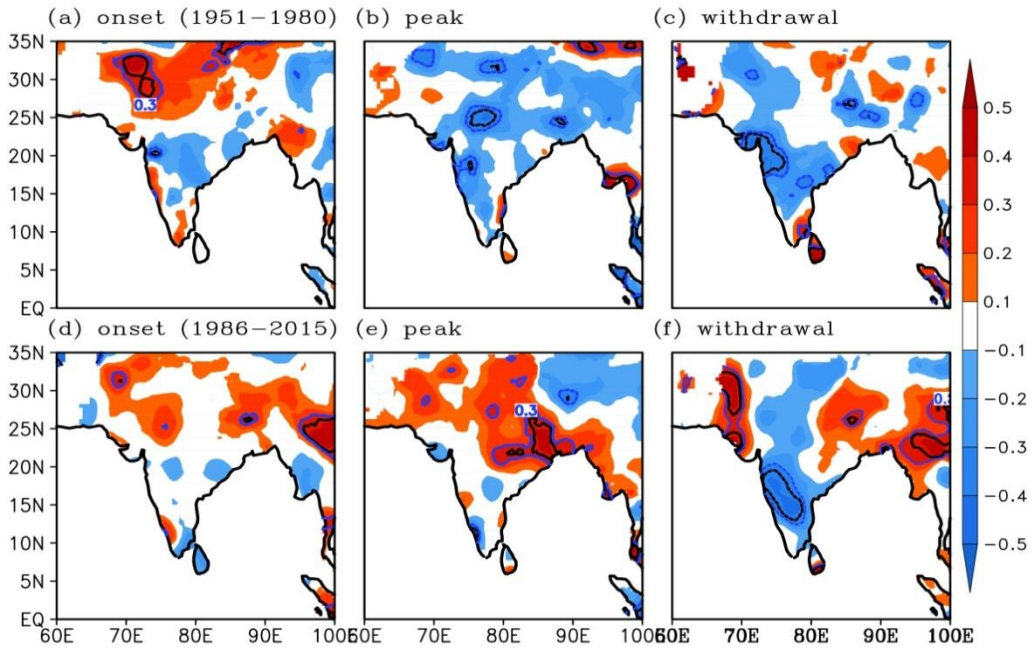

Figure 5.1: Spatial correlation between DMI and ISMR during onset, peak, and withdrawal phases in the early and recent decades. Contours represent the regions with 5% and 10% significance.

In recent decades, a weakening of the IOD-ISMR relationship is observed over the entire Indian subcontinent during the onset phase (Figure 5.1d). The weakened relationship is manifested by reduced negative (positive) correlation values over the southern peninsular (northern) Indian regions. However, a shift from an in-phase to an out-of-phase relationship is observed over the southeast regions, even though the values are insignificant. Considerable changes in correlations are observed during the peak phase, in which the out-of-phase relationship changes to in-phase relationship over the north, northeast, and central Indian regions (Figure 5.1e). Here, a significant increase in positive correlation is observed over the northeast region and a decrease in negative correlation over the peninsular region in the recent decades. During the withdrawal phase, a general increase in the correlations is observed over most of the Indian regions

with a significant increase over the northeast, northwest, and peninsular regions (Figure 5.1f).

As a whole, the correlation analysis indicates a general weakening of the IOD-ISMR relationship in recent decades during the onset phase and strengthening during the withdrawal phase. During the peak phase, the relationship changes from out-of-phase to in-phase relationship over most of the Indian regions. The strengthening of the IOD-ISMR relationship in recent decades during the summer monsoon has been previously studied (Askok and Saji 2007; Ummerhofer et al. 2011; Krishnaswami et al. 2015). However, the relationship significantly varies from one phase to another, which indicates the differences in the influencing mechanisms of the ISMR variability within each phase.

5.3 ISMR composites during positive and negative IOD years

Figure 5.2 and 5.3 show the ISMR composite anomalies during onset, peak, and withdrawal phases in the early and recent decades during pIOD and nIOD years, respectively. The pIOD and nIOD years selected for the analysis during all phases in the early and recent decades are given in Table 5.1. The method of classification of pIOD and nIOD years has already been explained in Chapter 2.

During pIOD years, the west coast, northeast, and northern regions of India are associated with enhanced rainfall during the onset phase (Figure 5.2a) in the early decades. However, ISMR decreases over central India and some parts of peninsular India. During the peak phase, ISMR shows an increase of about 50 mm in the eastern peninsular region with respect to the onset phase (Figure 5.2b). However, it decreases over all the other regions with a significant decrease of more than 150 mm over the northeast and northern west coast. An increase of 30-60 mm rainfall is observed over the south, north, central, and northeast regions of India, and a slight decrease over other regions during the withdrawal phase (Figure 5.2c). In recent decades, ISMR increases (about 50 mm) over most of the Indian regions during the onset phase (Figure 5.2d and 5.2g). However, a significant decrease (about 150 mm) is observed over the northeast and the northern west coast regions**.** The decrease in ISMR over the northeast region is consistent with the reduced IOD-ISMR correlation in Figure 5.1d.

	Onset	Peak	Withdrawal
Early decades (1951-1980)			
pIOD	**1968**	**1961**	1951
	1972	1963	**1961**
	1975	**1966**	1963
	1976	**1967**	**1966**
	1979	1972	**1967**
		1976	1972
nIOD	1954	1954	1954
	1956	1956	1955
	1957	1958	1956
	1958	**1959**	**1958**
	1959	**1960**	**1959**
	1960	1964	1964
	1965	**1980**	**1968**
	1969		1971
			1973
			1975
			1980
Recent decades (1986-2015)			
pIOD	1987	1987	1987
	1991	1991	1991
	1994	**1994**	1994
	1997	1997	1997
	1998	1999	1999
	2001	2000	2002
	2003	**2003**	2006
	2008	**2006**	2007
	2009	2007	**2008**
	2011	**2008**	2011
	2015	2011	**2012**
		2012	2015
		2015	
nIOD	**1989**	**1992**	**1992**
	1990	**1996**	**1996**
	1992		
	2013		

Table 5.1: pIOD and nIOD years during onset, peak, and withdrawal phases in the early and recent decades. The years with pure IOD events are marked as bold.

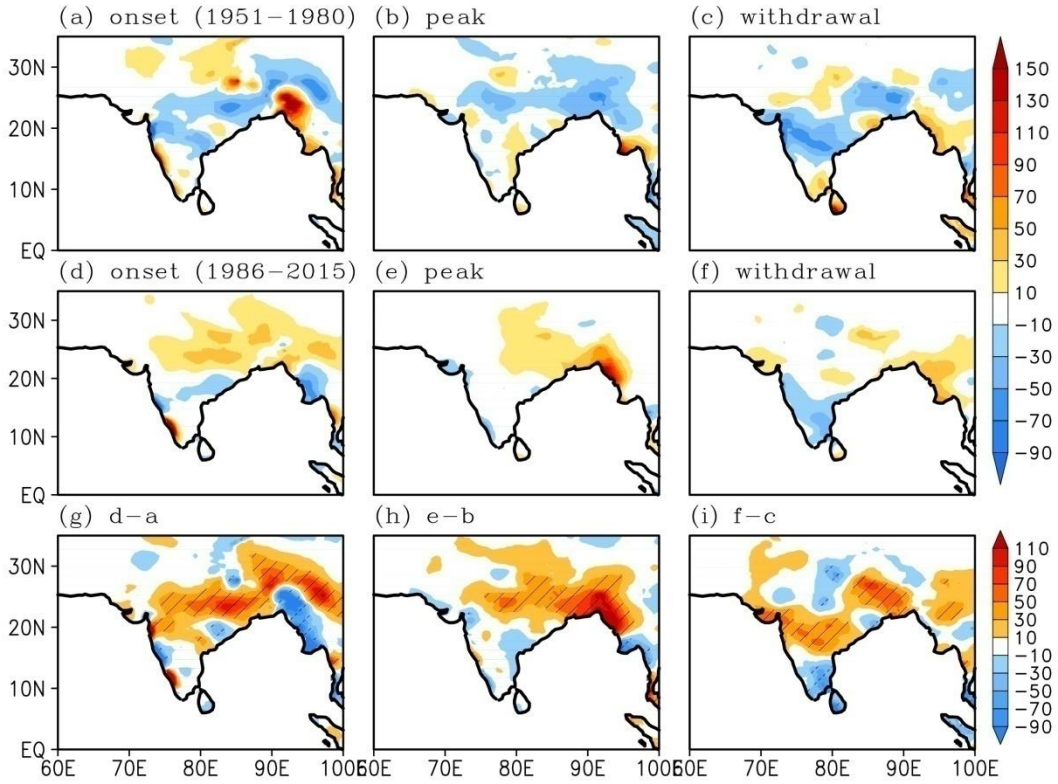

Figure 5.2: ISMR anomalies (mm) for positive IOD years during onset, peak, and withdrawal phases in the early and recent decades. The hatches represent the regions with more than 5% significance

During the peak phase, a general increase in ISMR over most of the Indian regions is observed with a significant increase of ~110 mm over the northeast region (Figure 5.2e and 5.2h). However, ISMR decreases over the southern west coast regions, which is in contrast to the early decades. During the withdrawal phase (Figure 5.2f and 5.2i), an increase in ISMR (60-90 mm) over the northeast, northwest, and monsoon core regions, and a decrease over the southern and northern regions of India (greater than 60 mm) is observed during the withdrawal phase.

In the case of nIOD years, below normal rainfall conditions are observed over most of the Indian regions except the southern peninsula during the onset phase in the early decades (Figure 5.3a). ISMR over all Indian regions shows an increase during the peak phase with respect to the onset phase. Here, a noticeable increase of about 150 mm is observed over the west coast and central Indian regions (Figure 5.3b). A general increase in ISMR with a significant increase of more than 100 mm over the northwest and central Indian regions is observed during the withdrawal phase also (Figure 5.3c).

In recent decades, ISMR significantly increases during the onset phase (Figure 5.3d and 5.3g), with an increase of 150 mm over the monsoon core zone. However, during peak (Figure 5.3e and 5.3h) and withdrawal (Figure 5.3f and 5.3i) phases, ISMR decreases over most of the Indian regions. During the peak phase, the reduction is more prominent over the west coast (more than 90 mm), and during the withdrawal phase, the reduction is prominent over the eastern and southern parts of the country.

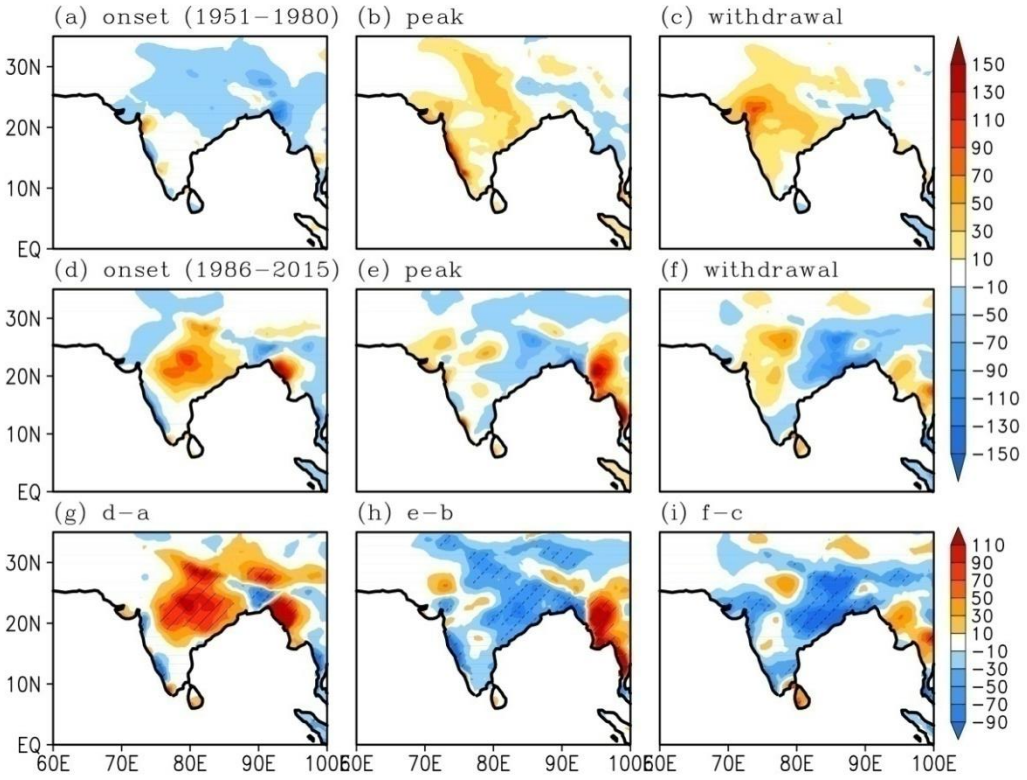

Figure 5.3: ISMR anomalies (mm) for negative IOD years during onset, peak, and withdrawal phases in the early and recent decades. The hatches represent the regions with more than 5% significance

Altogether, there is a significant increase in ISMR over most of the Indian regions during all three phases in the recent decades during pIOD years. This increase may be attributed to the enhanced occurrence of pIOD years in the recent decades. However, the analysis of ISMR anomalies during nIOD years indicates a significant increase in ISMR over the monsoon core zone of India during the onset phase and a decrease over most of the Indian regions during peak and withdrawal phases in the recent decades. These observed results are consistent with the correlation analysis given in Figure 5.1.

5.4 SST variations over the Indian Ocean

The linkage of ISMR with the events in the Indian Ocean is as important as the linkage of ISMR with the events in the Pacific Ocean (Gadgil et al. 2003). Hence, in addition to the analysis of ISMR patterns during pIOD and nIOD years, it is worth analyzing the relationship of these ISMR patterns with different oceanic and atmospheric components (SST, atmospheric circulations, etc.) over the Indian Ocean.

5.4.1 SST-ISMR teleconnections during different phases

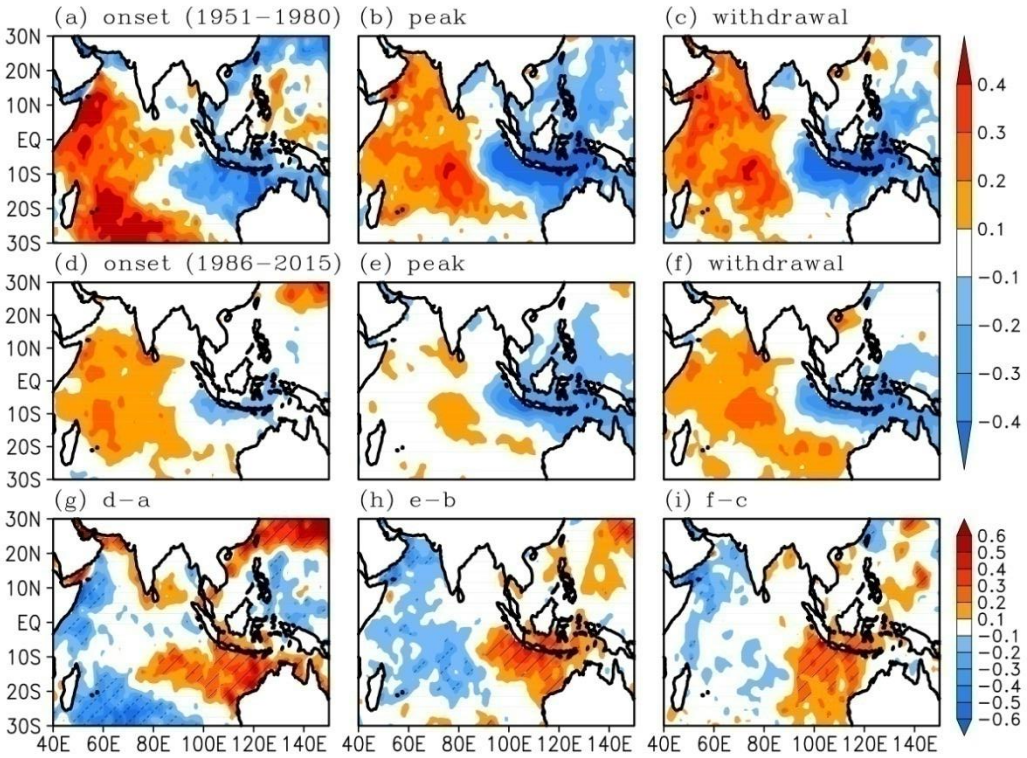

Figure 5.4: SST anomalies (°C) for positive IOD years during onset, peak, and withdrawal phases during early and recent decades. The hatches represent the regions with more than 5% significance.

SST anomalies over the Indian Ocean during pIOD and nIOD years during onset, peak, and withdrawal phases in the early and recent decades are shown in Figure 5.4 and Figure 5.5, respectively. It is known that a pIOD event is characterized by warm (cold) SST in the west (southeast) equatorial Indian Ocean (Saji et al. 1999; Vinayachandran et al. 2002; Rao et al. 2002). This pattern is clearly observed during all phases in the early decades (Figure 5.4a-c). High values of SST are observed over the western and

central equatorial Indian Ocean during the onset phase (Figure 5.4a) in the early decades. SST values slightly decrease during the peak phase (Figure 5.4b), and then slightly increase during the withdrawal phase (Figure 5.4c). A decrease in SST over the western and central equatorial Indian Ocean is observed during all phases in the recent decades. However, a considerable decrease is observed during the peak phase (Figure 5.4d-i**)**. The convection over the western equatorial Indian Ocean is considered more favorable for ISMR variability than the convection over the eastern part (Gadgil et al. 2004), although SST over the eastern equatorial Indian Ocean is significantly correlated with ISMR (Rajeevan et al. 2002). Following this result, the analysis of the changes in SST over the western Indian Ocean is more focused in the present analysis.

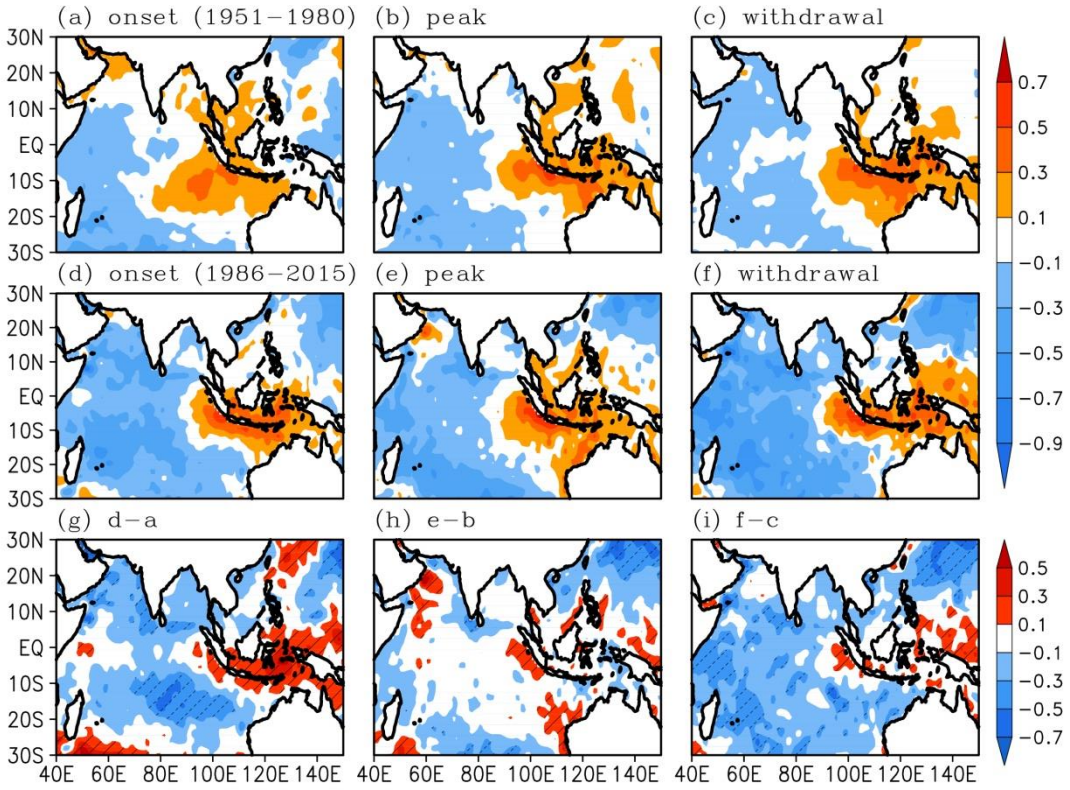

Figure 5.5: SST anomalies (°C) for negative IOD years during onset, peak, and withdrawal phases during early and recent decades. The hatches represent the regions with more than 5% significance.

In the early decades, cold (warm) SST anomalies are observed over the western (eastern) equatorial Indian Ocean during all phases in the case of nIOD years. The cooling over the western Indian Ocean slightly increases during the peak phase and decreases during the withdrawal phase as compared to the onset phase (Figure 5.5a-c).

The cooling significantly increases during the onset (Figure 5.5d and 5.5g) and withdrawal phases (Figure 5.5f and 5.5i), and it almost remains unchanged during the peak phase (Figure 5.5e and 5.5h) in recent decades. On the other hand, an increase in warming over the eastern equatorial Indian Ocean is observed during all phases in recent decades, which is prominent during the onset phase. According to Swapna et al. (2014), the increase in SST over the equatorial Indian Ocean is associated with the weakening of monsoon zonal winds over the region, which ultimately modulates the ISMR. A similar result was also reported by Roxy et al. (2015). Following these results, the changes in SST over the equatorial Indian Ocean during pIOD and nIOD years can be connected to the changes in ISMR patterns observed over the Indian region during all phases (Figure 5.2 and 5.3) and the IOD-ISMR correlation (Figure 5.1). These results are further explored by the analysis of the circulation features and moisture transports over the tropical Indian Ocean and the Indian region.

5.5 Circulation features and moisture transport

Figure 5.6 and 5.7 show the low-level wind anomalies (850 h Pa) over the Indian Ocean during pIOD and nIOD years, respectively. The high SST over the western Indian Ocean and the low SST over the eastern Indian Ocean are connected with the propagation of easterly winds over the Indian Ocean during pIOD years (Gadgil et al. 2007). In the early decades, a general weakening of the cross-equatorial low-level jets (LLJ) is observed over the equatorial Indian Ocean and the Arabian Sea during pIOD years in all phases. This weakening of LLJ is followed by a divergent pattern of low-level wind circulation (Figure 5.6a-c). This weakening of LLJ can be connected with the deficit ISMR observed over most of the Indian regions in the early decades (Figure 5.2a-c). However, the weakening is more prominent during the onset and withdrawal phases. Hence, they can be connected to the reduction in ISMR observed over the peninsular and central Indian regions during those phases in the early decades (Figure 5.2a and 5.2c).

However, as compared to the early decades, LLJ strengthens in the recent decades during all phases (Figure 5.6d-f). This relative strengthening causes a convergence zone of moisture over the northeast regions of India, which provides high summer monsoon rainfall in the monsoon trough zone. However, the low-level circulation anomalies are

feeble in the peninsular regions, and hence no significant changes in ISMR are observed there. A relative strengthening of LLJ over the Arabian Sea and a weakening over the eastern equatorial Indian Ocean is observed during the onset phase (Figure 5.6d). The strengthening of LLJ over the Arabian Sea can be associated with the decrease in SST over the western equatorial Indian Ocean (Figure 5.4d). Hence, it contributes to the enhancement of the moisture transport and the excess summer monsoon rainfall to the Indian region, especially over the northeast, west coast, and monsoon trough areas in the recent decades (Figure 5.2d). The strengthened LLJ is prominent over the central and eastern equatorial Indian Ocean (Figure 5.6e and 5.6f) during peak and withdrawal phases. Hence, it is conducive for the moisture supply towards the monsoon trough zone by transporting low-level westerlies through the western portion of the Bay of Bengal. This propagation of westerlies through the Bay of Bengal enhances ISMR (Figure 5.2e and 5.2f), as also observed by the earlier studies (Behera et al. 1999; Ashok et al. 2001; Ajayamohan and Rao 2008).

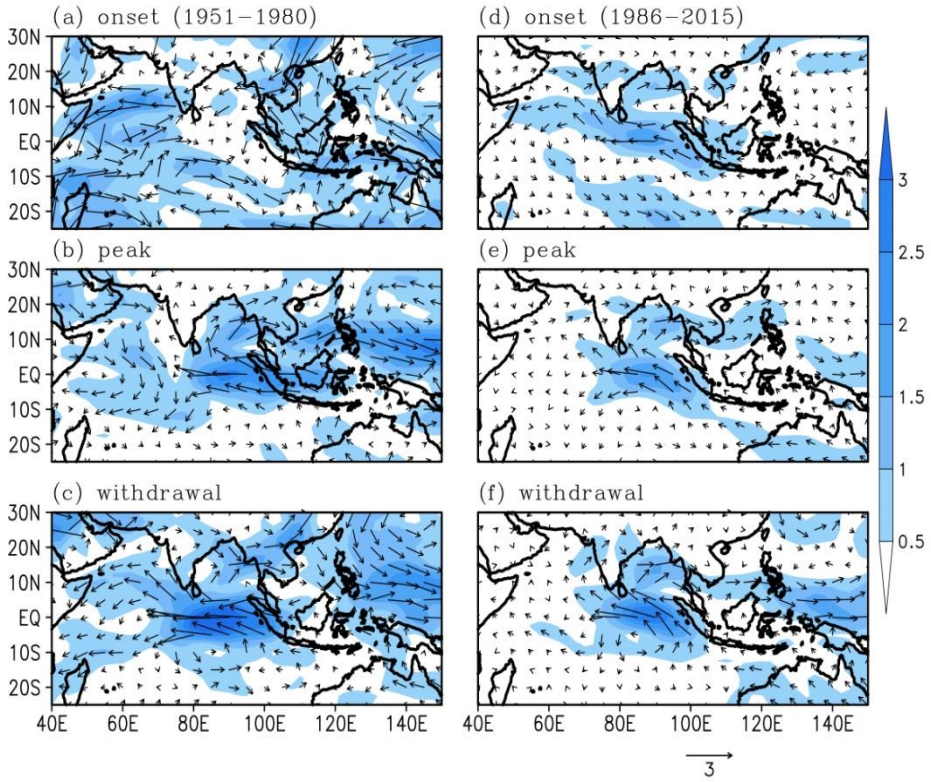

Figure 5.6: Low-level (850 h Pa) wind anomalies (vectors; in m s^{-1}) and magnitudes (shaded; in m s^{1}) for positive IOD years during onset, peak, and withdrawal phases in the early and recent decades

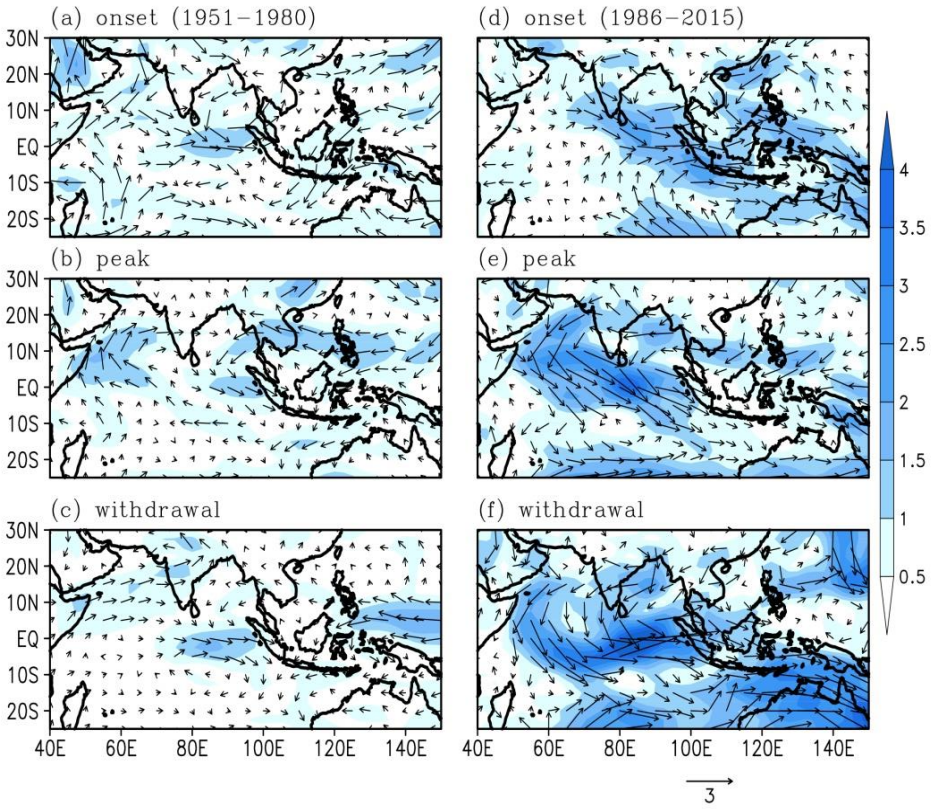

Figure 5.7: Low-level (850 h Pa) wind anomalies (vectors; in m s^{-1}) and magnitudes (shaded; in m s^{1}) for negative IOD years during onset, peak, and withdrawal phases in the early and recent decades

The low-level westerlies strengthen in the recent decades during all phases in the case of nIOD years, which is more prominent during peak and withdrawal phases (Figure 5.7d-f). This strengthening is followed by a divergent circulation of winds and a weakening of LLJ, which is associated with the ISMR patterns observed over the Indian region in recent decades**.** The strengthened westerlies over the western and central equatorial Indian Ocean (Figure 5.7e and 5.7f) can be attributed to the enhanced cooling of the same regions during peak and withdrawal phases (Figure 5.5e and 5.5f). This enhanced cooling suppresses the transport of moisture to the Indian region and thus provides a deficit ISMR in recent decades (Figure 5.3e and 5.3f). The divergent zone of moisture developed over the northeast region during peak and withdrawal phases caused a reduction in ISMR over the foothills of Himalayas and central-eastern regions**.** The westerlies are weakened over peninsular India and the central equatorial Indian Ocean during the onset phase as compared to the other two phases (Figure 5.7d), which

is associated with the enhanced ISMR observed over the Indian monsoon core zone (Figure 5.3d).

It is known that LLJ carries lots of moisture to the Indian subcontinent (Murukami et al. 1984), and the changes in LLJ can affect the rainfall characteristics of the Indian region (Aneesh and Sijikumar 2016). Hence, the vertically integrated moisture transport (VIMT) and moisture convergence (from the surface to 300 h Pa) during pIOD and nIOD years are analyzed. The difference in VIMT and moisture convergence between recent and early decades for pIOD and nIOD years is shown in Figure 5.8 and 5.9, respectively. During the onset phase, enhanced moisture transport and convergence are observed over the monsoon trough, northeast, and northwest regions in the recent decades during pIOD years (Figure 5.8a). A divergent zone of moisture is observed over the eastern peninsular region, and it is associated with the reduction in ISMR observed there in recent decades. The areas of moisture convergence (divergence) are related to excess (deficit) ISMR in recent decades (Figure 5.2d). The corresponding changes are also observed in the circulation features and SST patterns.

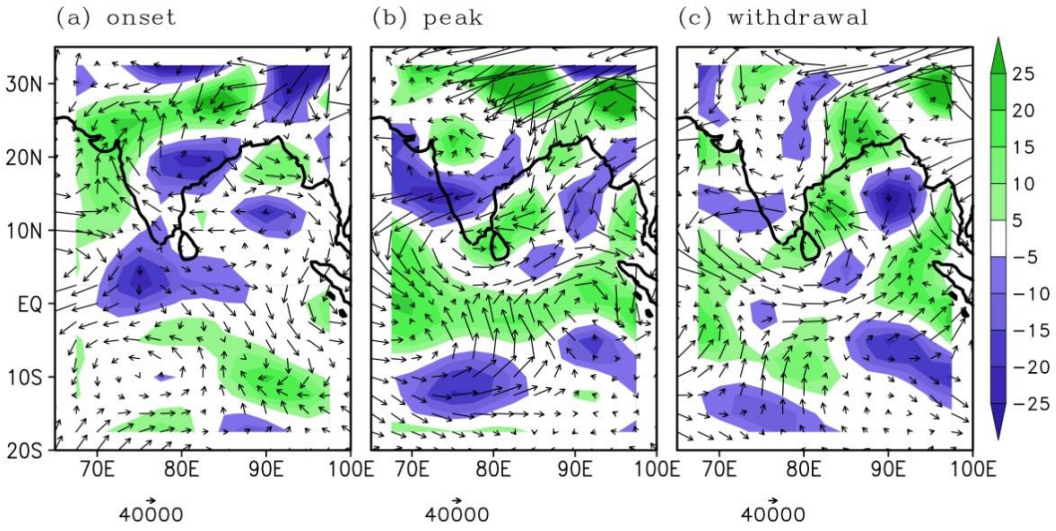

Figure 5.8: Difference in VIMT (Kg m^{-1} s^{-1}; vectors) and moisture convergence (× 10^2 in g Kg^{-1} s^{-1}; shaded) between the recent and early decades for positive IOD years during onset, peak, and withdrawal phases.

The convergent zone of moisture is shifted to the foothills of Himalayas and northeast regions in the recent decades during the peak phase. However, a divergent zone is observed over the southern peninsular region (Figure 5.8b). The areas of convergence

and divergence of moisture are associated with excess and deficit ISMR, respectively, as in the case of the onset phase. A similar type of relationship is noticed during the withdrawal phase (Figure 5.8c) also. Altogether, the observed changes in VIMT and moisture convergence from the early to recent decades are well related to the circulation features, SST, and ISMR characteristics observed over the Indian region during all phases during pIOD years.

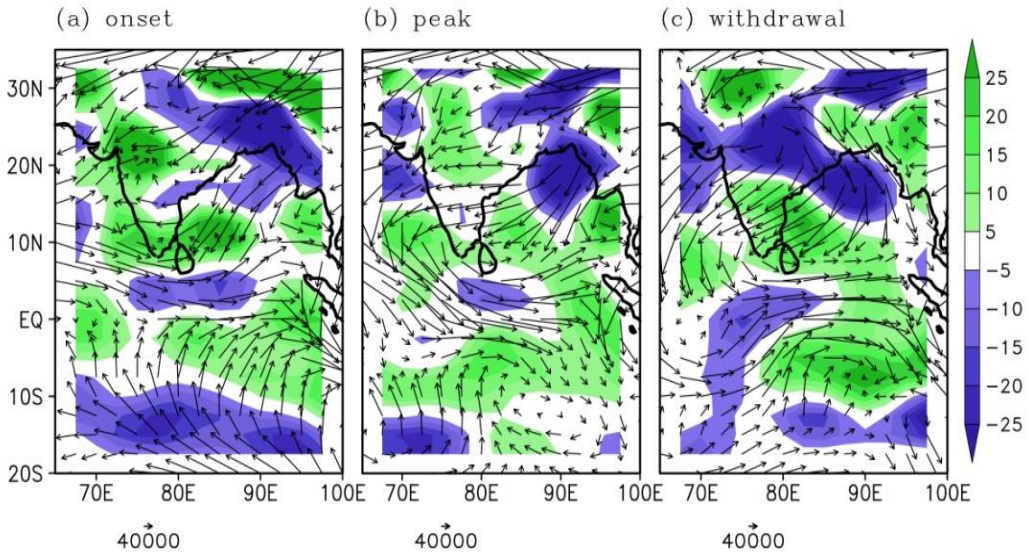

Figure 5.9: Difference in VIMT (in Kg m^{-1} s^{-1}; vectors) and moisture convergence ($\times 10^2$ in g Kg^{-1} s^{-1}; shaded) between the recent and early decades for negative IOD years during onset, peak, and withdrawal phases

On the other hand, during nIOD years, enhanced moisture convergence is observed over the monsoon core zone in the recent decades during the onset phase (Figure 5.9a). Hence, it can be associated with the increase in ISMR over the monsoon core zone (Figure 5.3a). A divergent zone of moisture is observed over the eastern and central portions of the Indian region during peak and withdrawal phases (Figure 5.9b and 5.9c). Hence, they are also connected with the observed ISMR characteristics (Figure 5.3e and 5.3f). As in the case of pIOD, the changes in VIMT and moisture convergence are strongly related to the circulation features, SST patterns, and thus the ISMR patterns during nIOD years. However, the changes are more noticeable during peak and withdrawal phases.

Figure 5.10 and 5.11 show the velocity potential anomalies at 200 h Pa during pIOD and nIOD years, respectively. The analysis of velocity potential was carried out to validate the results obtained in the earlier sections. The velocity potential is a commonly used scalar function in meteorology to analyze irrotational flows and calculated based on zonal and meridional wind velocities at 200 h Pa. During both the pIOD and nIOD years, the obtained results are in good agreement with those in the earlier sections.

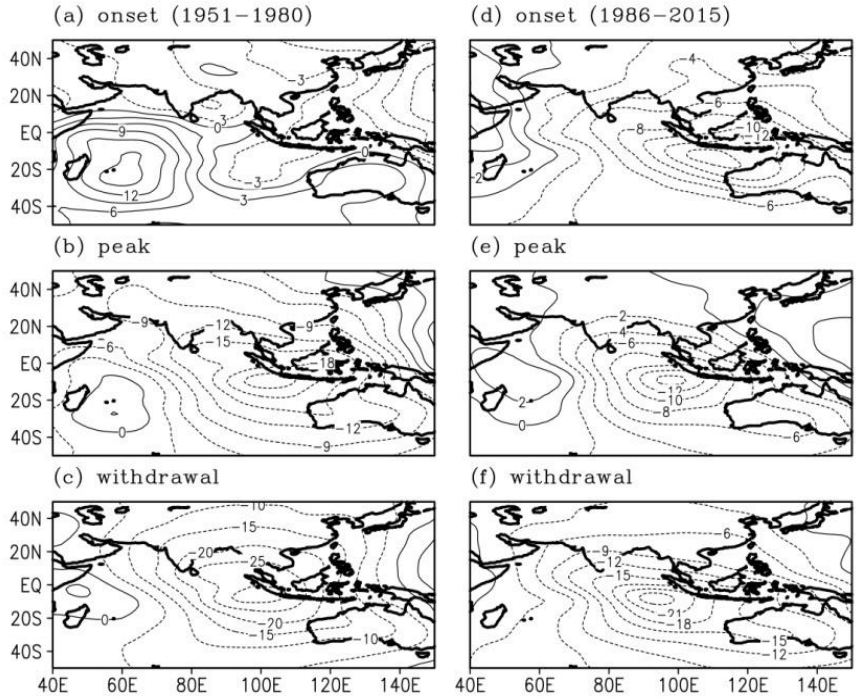

Figure 5.10: Velocity potential anomalies ($\times 10^{-6}$ in $m^2 s^{-1}$) at 200 h Pa for positive IOD years during onset, peak, and withdrawal phases in the early and recent decades

An increase in ascending motion over the eastern equatorial Indian Ocean and the Indian region is observed in recent decades during pIOD years (Figure 5.10d-f). It is corroborated with the divergence at 200 h Pa (negative contours in velocity potential at upper levels). The divergence observed over the Indian subcontinent in the recent decades is more evident during peak and withdrawal phases. The increase in ascending motion over the Indian region during peak and withdrawal phases is well related to the circulation features, SST patterns, and thus the ISMR anomalies in the recent decades. During nIOD years, an increase in descending motion over the eastern equatorial Indian Ocean and the Indian region is observed mainly during peak phase in the recent decades (Figure 5.11e). It can be connected to the reduction in ISMR observed over the Indian

region during the peak phase. However, an ascending motion at lower levels over the northern Indian regions and descending motion over the southern Indian regions are observed during the onset and withdrawal phases (Figure 5.11d and 5.11f). These are also concurrent with the ISMR patterns observed during these phases in the recent decades.

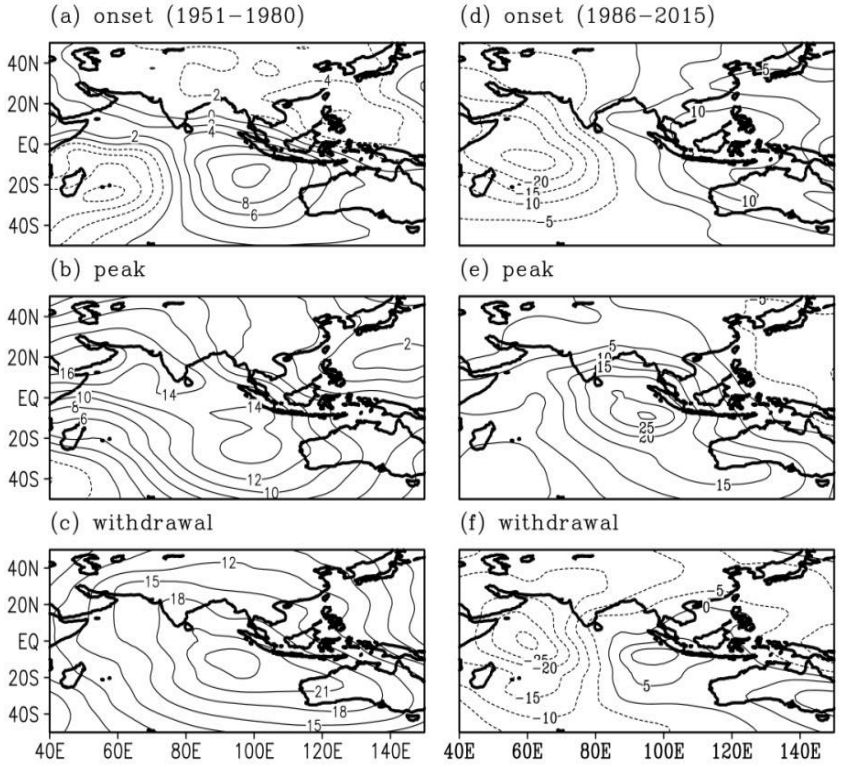

-

Figure 5.11: Velocity potential anomalies ($\times 10^{-6}$ in $m^2 s^{-1}$) at 200 h Pa for negative IOD years during onset, peak, and withdrawal phases in the early and recent decades

5.6 Pure IOD events

The IOD events that take place independent of ENSO events are called pure IOD events. The analysis of pure IOD events determines how the SST variations over the tropical Indian Ocean can make impacts on ISMR without the influence from ENSO. The analyses described in sections 5.2 to 5.5 were carried out for pure IOD events and similar results were obtained, but with slight differences in magnitudes. A similar pattern of ISMR, SST, circulation features, moisture transport, and velocity potential was observed but with a slight increase in their magnitudes for all three phases. Even

though these changes were clearly observed in recent decades during all three phases, they significantly vary from one phase to another.

5.7 Chapter summary

The impact of Indian Ocean dynamics on ISMR variability was studied by identifying the changes in the IOD-ISMR relationship from the early to recent decades. A weakening of the IOD-ISMR relationship is observed in the recent decades during the onset phase and a strengthened relationship during the withdrawal phase. During the peak phase, the relationship changes from out-of-phase to in-phase relationship in most parts of the Indian regions. A general increase in ISMR over most parts of the Indian regions is observed during all phases during pIOD years in the recent decades. However, in the case of nIOD years, ISMR decreases during peak and withdrawal phases, but increases during the onset phase. Significant changes in the SST anomalies over the western and central equatorial Indian Ocean are observed in the recent decades during both the pIOD and nIOD years. These changes are well connected to the corresponding ISMR characteristics.

During pIOD years, a relatively strengthened LLJ is observed over the equatorial Indian Ocean and the Arabian Sea during all phases in the recent decades. It causes a convergence zone over the northeast regions of India, which causes relatively more rainfall in the monsoon trough zone by transporting excess moisture to the region. However, in the case of nIOD years, strengthened westerlies are dominated during peak and withdrawal phases in the recent decades. This strengthening is followed by a weakening of LLJ, which suppresses the transport of moisture causing reduced ISMR. Even though the observed changes in circulation features and moisture convergence are well related to the SST anomalies and ISMR characteristics during all the three phases during both the pIOD and nIOD years, changes are more noticeable during peak and withdrawal phases. The analysis of velocity potential anomalies also has provided the changes in the zones of ascending and descending motions over the Indian region during pIOD and nIOD years, which is consistent with the observed ISMR characteristics.

CHAPTER 6

HISTORICAL AND FUTURE PROJECTIONS OF ISMR VARIABILITY AND ENSO-ISMR RELATIONSHIPS USING CMIP5 MODELS

CHAPTER 6

HISTORICAL AND FUTURE PROJECTIONS OF ISMR VARIABILITY AND ENSO-ISMR RELATIONSHIPS USING CMIP5 MODELS

6.1 Introduction

In the previous chapters, the influence of different internal and external climate factors on the ISMR variability was identified. This chapter analyzes the historical and projected changes of ISMR variability and ENSO-ISMR relationships using CMIP5 models. Under the present climate scenario, where there is a large increase in greenhouse gas emissions and global temperature, it is highly relevant to analyze how these changes will affect the ocean-atmosphere interactions and the related climate phenomena in future decades. Hence, the changes in ISMR variability and the ENSO-ISMR relationship in a historical (1951-2005) period and their changes in a future (2050-2099) period in different RCP scenarios (RCP 4.5 and 8.5) are analyzed using multiple CMIP5 models. The historical and future projections of ISMR variability over different regions of India are carried out to find out the changes in the regional variations of ISMR in the future decades. Further, the influence of SST changes and circulation features over the tropical Indo-Pacific domain on the ISMR variability in future decades is analyzed separately for El Niño and La Niña events.

6.2 Selection of models

The details of CMIP5 models selected for the study have already been given in Chapter 2. Out of 25 CMIP5 models considered, the models that well simulate the ISMR variability were screened out using the annual cycle of ISMR and Taylor diagram.

6.2.1 Annual variations of precipitation in CMIP5 models

To ensure the reliability of each model with respect to the observations, the annual cycle of rainfall over the central Indian region during the historical period is analyzed for all 25 models (Figure 6.1a). All models follow a similar pattern of the annual cycle as that of the observation (CRU data). The precipitation values are maximum during the

summer monsoon season (June-September), decreases during the post-monsoon season (October-December), and the least precipitation is observed during the winter (January-February) and pre-monsoon (March-May) seasons. Even though this trend is followed by all the models, the precipitation values in each model differ from one another, as observed by Jayasankar et al. (2015).

6.2.2 Taylor diagram analysis

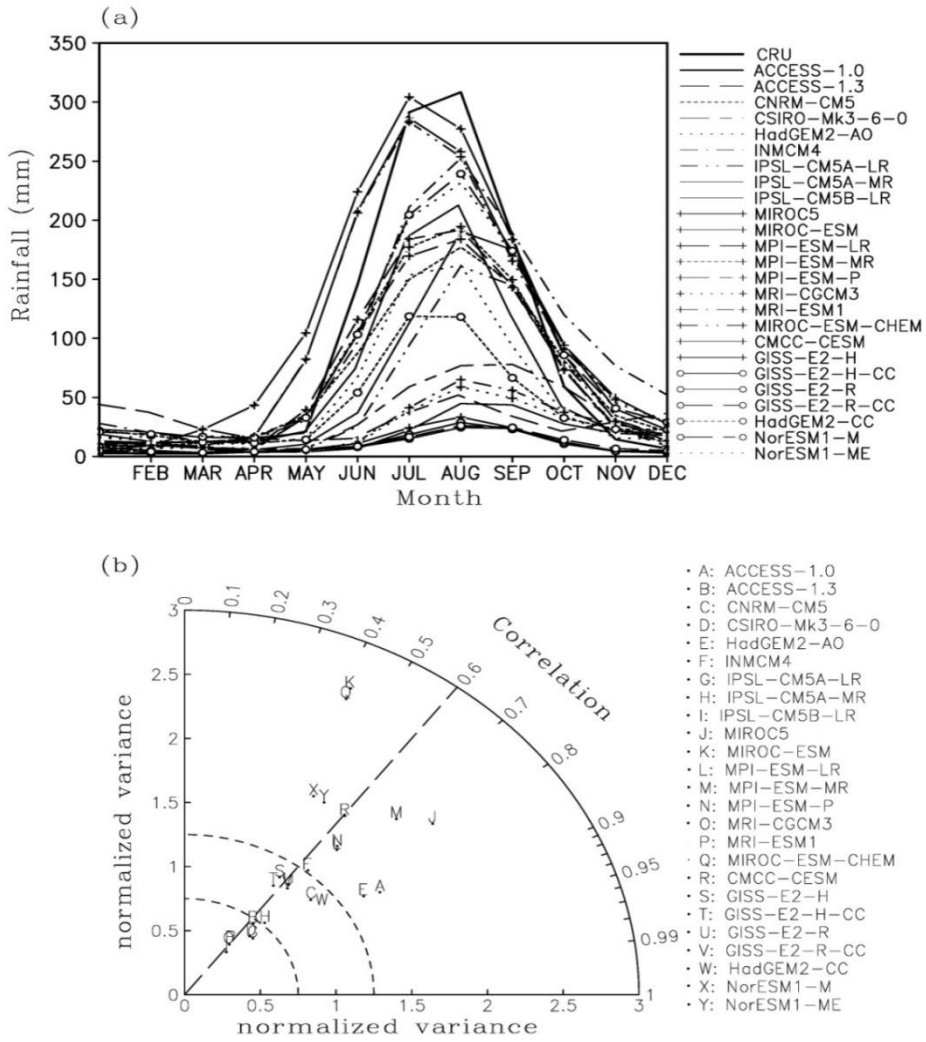

Figure 6.1: (a) Annual cycle of rainfall over central India (15°-25°N, 70°-90°E) from observation (CRU) and models for the historical period (1951-2005) (b) Taylor diagram of summer monsoon rainfall over the Indian region (5°-35°N, 60°-100°E) for the same period.

Using the Taylor diagram, the models with correlation coefficients greater than 0.6 and normalized variance between 0.75 and 1.25 were filtered out (Figure 6.1b). Based on

this criterion, five models were selected out of 25 models considered. Further analyses are carried out using the selected models and they are CNRM-CM5, GISS-E2-R, GISS-E2-R-CC, HadGEM2-CC, and IPSL-CM5A-MR as explained in Chapter 2.

6.3 Historical and projected changes of ISMR

The climatology of ISMR along with the standard deviation for the observation and models during the historical period is given in Figure 6.2. The observation data (CRU) shows high regional variability during the historical period, as observed in the previous chapters.

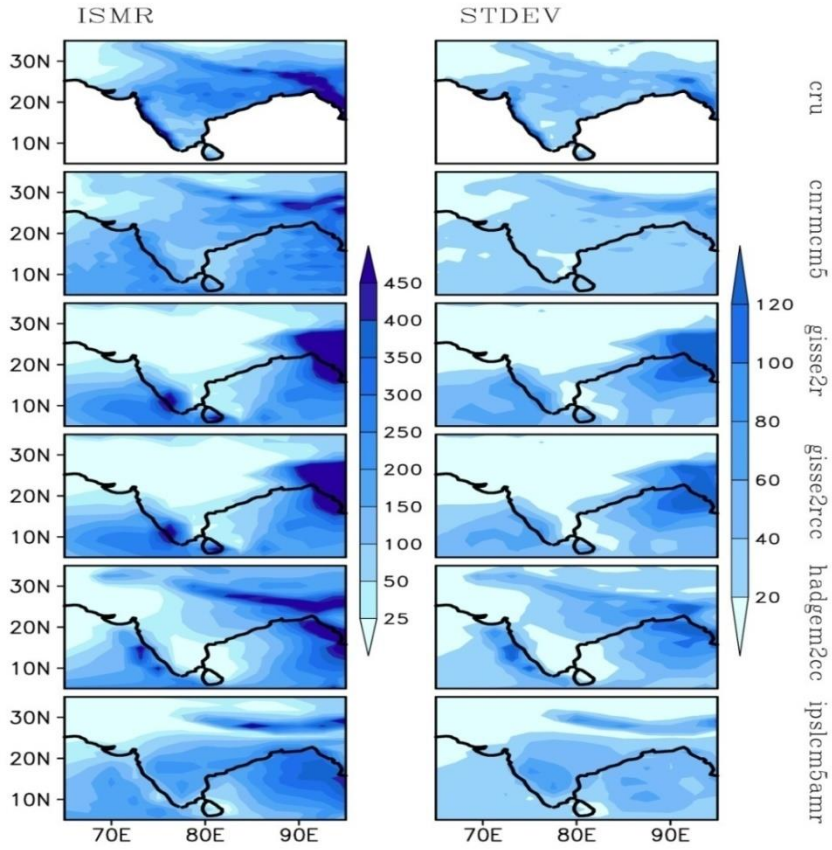

Figure 6.2: ISMR climatology (mm) and standard deviation from observation and models for the historical period (1951-2005).

However, the spatial distributions of ISMR simulated by all five models are more or less the same as that of the observation. The CNRM-CM5, HadGEM2-CC, and IPSL-CM5A-MR models show high spatial variability in ISMR as in the case of CRU. In all these three models, above normal rainfall (~600-700 mm) is observed over the northeast

and foothills of Himalayas, and a relatively small amount over central India and west coastal regions (~150-300 mm), consistent with the results of Menon et al. (2013). The other models; GISS-E2-R and GISS-E2-R-CC do not capture the ISMR spatial variability as in CRU and other models, although they are capable of reproducing the main rainfall zones such as the southern west coast and northeast regions.

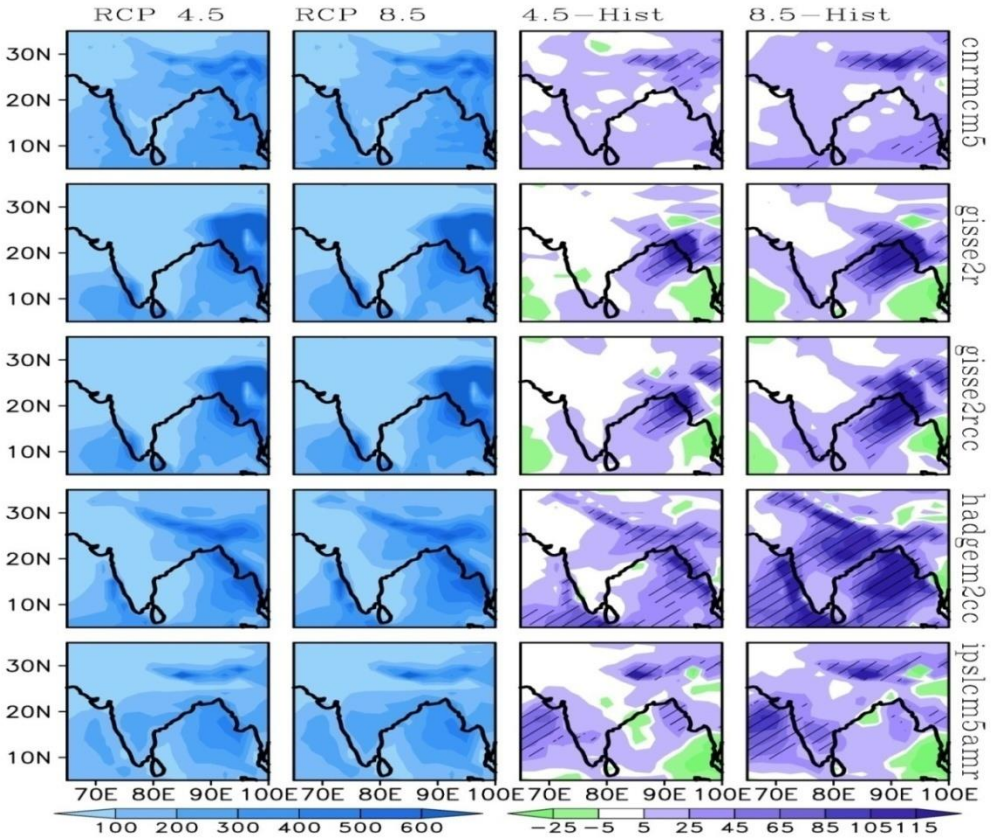

Figure 6.3: ISMR climatology (mm) in RCP 4.5 and RCP 8.5 scenarios for the period 2050-2099 along with their differences from the historical period. Hatches represent the regions with 5% significance.

The regional variability of ISMR in the historical period is almost well captured in the future scenarios by all models (Figure 6.3). As in the case of the historical period, the ISMR in the CNRM-CM5 model shows high spatial variations in RCP 4.5 and 8.5 scenarios. The model HadGEM2-CC simulates high values of precipitation over the northeast and foothills of Himalayas, while IPSL-CM5A-MR simulates high values of precipitation over the northeast, foothills of Himalayas, and peninsular Indian regions in both the RCPs. However, the models GISS-E2-R and GISS-E2-R-CC show small

variabilities with high rainfall over the northeast and west coast regions, and low rainfall over the other regions as in the case of the historical period.

In future decades, all models simulate a significant increase in ISMR in both RCPs while comparing with the historical period. Similar results were also reported by other studies (Kitoh et al. 2013; Menon et al. 2013; Wang et al. 2014; Jayasankar et al. 2015; Sharmila et al. 2015; Sudeepkumar et al. 2018), but with different CMIP5 models. The increase in ISMR is more prominent in CNRM-CM5, HadGEM2-CC, and IPSL-CM5A-MR models. The models CNRM-CM5 and HadGEM2-CC simulate an overall increase in ISMR over most of the Indian regions in both RCPs, with a significant increase of more than 80 mm over central India, foothills of Himalayas, and northeast regions. However, the increase in ISMR is larger in RCP 8.5 than that in the RCP 4.5 scenario. In the case of IPSL-CM5A-MR, a significant increase in ISMR is observed over the west coast, northeast, foothills of Himalayas, and peninsular Indian regions in both RCPs. However, the increase in ISMR is small in the case of GISS-E2-R and GISS-E2-R-CC models as compared to other models. Both models simulate an increase in ISMR over the northeast, west coast, and peninsular regions, with a noticeable increase in the RCP 8.5 scenario. In brief, all models simulate an increase in ISMR in both RCPs over the northeast, west coast, foothills of Himalayas, central India, and the peninsular Indian regions. It is also found that the representation of the regional variability of ISMR is more robust in RCP 8.5 than in RCP 4.5, as observed by Kitoh et al. (2013).

6.4 Future projections of ENSO-ISMR relationships

Figure 6.4 shows the spatial correlation between Niño 3.4 index and ISMR using the observational data for the historical period. ISMR is significantly negatively correlated with Niño 3.4 index over most of the Indian regions during the historical period, as also noted in the previous studies (Mooley and Shukla 1987; Varikoden and Babu 2015; Varikoden and Revadekar 2019; Hrudya et al. 2020b). However, a relatively weak correlation is observed over the northeast region. To find out the changes in the observed ENSO-ISMR correlation in different CMIP5 models, the spatial correlation between Niño 3.4 index and ISMR for each model is analyzed in both the historical and RCP scenarios (Figure 6.5).

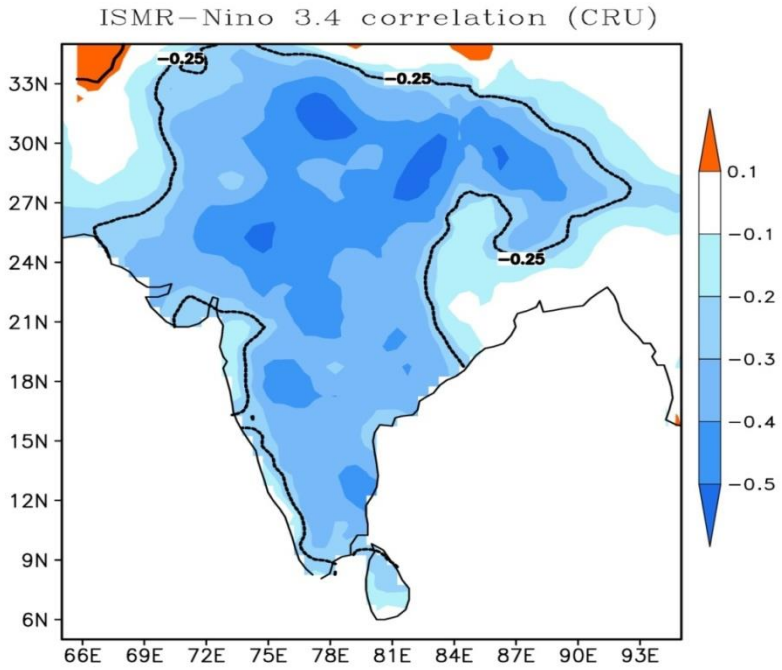

Figure 6.4: Spatial correlation between Niño 3.4 index and ISMR during the historical period (1951-2005) from observation. Contours represent the regions with 5% significance.

The correlation between Niño 3.4 index and ISMR highly varies from one model to another in both the historical and RCP scenarios. Moreover, the ENSO-ISMR relationship noticeably changes from one region to another over the Indian region. In the historical period, ISMR over most of the Indian regions shows an in-phase relationship with Niño 3.4 index in CNRM-CM5, and GISS-E2-R models (mainly over the central and northwest Indian regions), which is slightly different from the observation as shown in Figure 6.4.

However, a different pattern of correlation is observed in GISS-E2-R-CC, in which most of the Indian regions, particularly the southern and eastern parts of the country show an out-of-phase ENSO-ISMR relationship as found in the observation. Here, significant negative correlations are observed over some parts of the west coast and northeast regions. In HadGEM2-CC, some isolated areas of the central and peninsular Indian regions show negative ENSO-ISMR correlations. In IPSL-CM5A-MR, some areas of the central, northwest, and north Indian regions exhibit an out-of-phase ENSO-ISMR relationship with insignificant correlation coefficients.

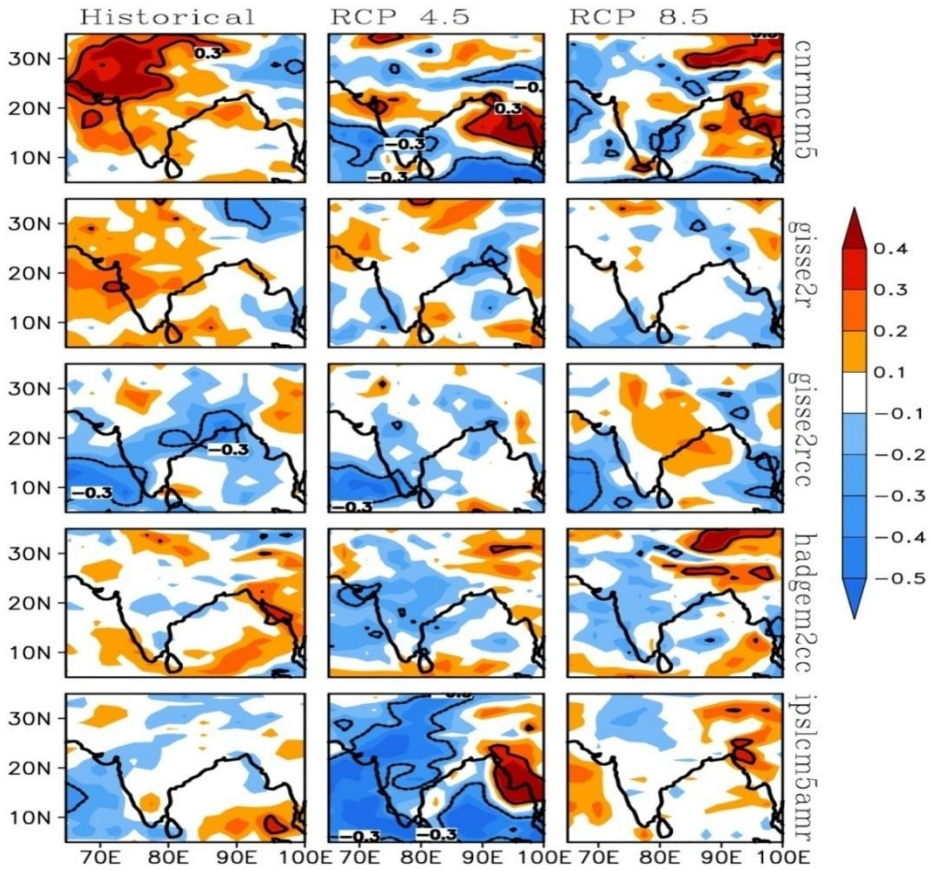

Figure 6.5: Spatial correlation between Niño 3.4 index and ISMR in historical (1951-2005) and RCP 4.5 and 8.5 scenarios (2050-2099) using models. Contours represent the correlations with 5% significance.

The patterns of ENSO-ISMR correlations are different from the historical simulations in both RCP scenarios. In CNRM-CM5 and GISS-E2-R models, the areas of positive correlations observed in the historical period decreases, and some portions of the central, northeast, and southern peninsular regions are dominated with significant negative ENSO-ISMR correlations in both the RCPs. The model GISS-E2-R-CC simulates an out-of-phase ENSO-ISMR relationship over the west coast, northeast, and peninsular regions in RCP 4.5. However, an in-phase relationship is observed over central India in RCP 8.5. In HadGEM2-CC, an out-of-phase ENSO-ISMR relationship is observed over most of the Indian regions, except in the northeast regions in RCP 4.5. However, the areas of negative correlation reduce in RCP 8.5. The model IPSL-CM5A-MR also simulates a significant negative correlation over most of the Indian regions except the northeast in RCP 4.5. Here, the areas of significant negative correlations

shrink in RCP 8.5. The negative correlation between Niño 3.4 index and ISMR in HadGEM2-CC and IPSL-CM5A-MR models in future decades was reported also by Roy (2017).

As a whole, the correlation analysis indicates noticeable changes in the ENSO-ISMR relationship from one model to the other in both the historical and RCP scenarios; mainly over the central, northeast, west coast, and southern Indian regions. The correlations observed in GISS-E2-R-CC, HadGEM2-CC, and IPSL-CM5A-MR models are mostly consistent with the observation, and they well simulate a negative relationship between ENSO and ISMR in RCP 4.5. However, the other two models do not capture the observed ENSO-ISMR relationship, which suggests the lack of reliability of these models in simulating the ENSO-ISMR relationships.

To diagnose the consistency of models and to find the spread of the ENSO-ISMR relationship across the models, the 31-year sliding correlation between Niño 3.4 index and ISMR for all five models in the historical and RCP scenarios is analyzed. The Niño 3.4 index-ISMR sliding correlation values together with the standard deviations for each model are given in Table 6.1. The values of correlation show the nature of the ENSO-ISMR relationship in each model and the standard deviation shows the discernible spread of the ENSO-ISMR relationship across models. It is clear that there are noticeable changes in the ENSO-ISMR relationship from one model to another in both the historical and RCP scenarios as observed in Figure 6.5. In the historical period, the model GISS-E2-R-CC shows the highest ENSO-ISMR negative correlation (-0.45) among all the other models. In RCP 4.5, GISS-E2-R-CC and IPSL-CM5A-MR models exhibit relatively high values of correlations (-0.37 and -0.68, respectively). However, the correlation is weak in RCP 8.5 as compared to the historical and RCP 4.5 scenarios. Therefore, it indicates the weakening of the ENSO-ISMR out-of-phase relationship in the RCP 8.5 scenario in the future decades.

Considering the standard deviations, it varies from 0.08 to 0.12 among the models in the historical period, from 0.03 to 0.09 in RCP 4.5, and from 0.03 to 0.2 in RCP 8.5. I. e, the spread of ENSO-ISMR relationship across models is higher in RCP 8.5 (spread=0.17) as compared to the RCP 4.5 and the historical period. Altogether, the analysis presented in Table 6.1 indicates that the ENSO-ISMR inverse relationship is

stronger and consistent in the GISS-E2-R-CC model in the historical period. In RCP 4.5, both the GISS-E2-R-CC and IPSL-CM5A-MR models show good ENSO-ISMR relationships. However, in the RCP 8.5 scenario, the ENSO-ISMR relationship is relatively weak and the spread of relationships among models is also high. Table 6.1 also indicates the limitation of CNRM-CM5 and GISS-E2-R models in reproducing the ENSO-ISMR relationships in the historical and future scenarios. These results are consistent with the correlations observed in Figure 6.5.

	Historical period		**RCP 4.5**		**RCP 8.5**	
Model name	Correlation	Std. dev	Correlation	Std. dev	Correlation	Std. dev
CNRM-CM5	-0.147	0.093	-0.194	0.056	-0.116	0.075
GISS-E2-R	0.157	0.081	-0.294	0.052	-0.195	0.065
GISS-E2-R-CC	-0.451	0.122	-0.372	0.034	-0.194	0.035
HadGEM2-CC	0.084	0.117	-0.140	0.098	-0.021	0.204
IPSL-CM5A-MR	-0.069	0.113	-0.687	0.041	-0.045	0.07

Table 6.1: Correlation coefficients between ISMR and Niño 3.4 index along with the standard deviations (from 31-year sliding correlation) for all the selected models in the historical and RCP scenarios.

6.5 Projected changes in ISMR during El Niño and La Niña years

To explore the ENSO-ISMR relationship further, the influences of El Niño and La Niña events on ISMR variability are analyzed for both the historical and RCP scenarios. The El Niño and La Niña years selected for the analysis in the historical and RCP scenarios are given in Table 6.2. ISMR anomalies over the Indian region during El Niño events in the historical and RCP scenarios during the summer monsoon season are shown in Figure 6.6. Usually, an El Niño event is associated with deficit rainfall over the Indian region and La Niña event with excess rainfall (Sikka 1980; Rassmussen and Carpenter 1983**;** Varikoden and Preethi 2013; Nair et al. 2018; Hrudya et al. 2020a, b). However, the ISMR patterns over the Indian region during El Niño events vary highly among the models with significant spatial variations.

Historical period (1951-2005)		
	El Niño	**La Niña**
CNRM-CM5	1955, 1959, 1961, 1963, 1972, 1977, 1984, 1986, 1991, 1993, 1994, 2003, 2005	1952, 1953, 1956, 1957, 1960, 1964, 1965, 1967, 1968, 1970, 1973, 1976, 1978, 1980, 1985, 1992, 1996, 2004
GISS-E2-R	1954, 1963, 1966, 1981,1983,1993, 1995, 1997, 1999, 2001	1952, 1953, 1955, 1958, 1961, 1962, 1968, 1969, 1984
GISS-E2-R-CC	1960, 1989, 1992, 1997,1999,2002, 2004	1953, 1955, 1958, 1964, 1969, 1971, 1979, 1984, 1990, 1993
HadGEM2-CC	1951, 1953, 1954, 1959, 1962,1963, 1970, 1975, 1986, 1989, 1990,1992, 1993, 1998, 1999, 2003	1955, 1956, 1957, 1960, 1961, 1964, 1965, 1966, 1968, 1971, 1976, 1983, 1984, 1987, 1995, 1996
IPSL-CM5A-MR	1958, 1964, 1971, 1976, 1979, 1980, 1983, 1986, 1987, 1989, 1992, 1995, 1996, 1998, 2001, 2005	1951, 1952, 1955, 1961, 1962, 1963, 1974, 1975, 1978, 1984, 1988, 1991, 2000
Observation	1957, 1963, 1965, 1972, 1982, 1987, 1991, 1994, 1997, 2002, 2004	1954, 1955, 1956, 1964, 1970, 1971, 1973, 1974, 1975, 1988, 1998, 1999
RCP 4.5 (2050-2099)		
CNRM-CM5	2050, 2054, 2064, 2070, 2072, 2074, 2076, 2080, 2082, 2084, 2086, 2088, 2093, 2095, 2097, 2099	2051, 2053, 2055, 2056, 2058, 2060, 2065, 2067, 2073, 2075, 2077, 2079, 2081, 2085, 2089, 2094, 2096, 2098
GISS-E2-R	2055, 2087, 2091, 2092	2059, 2061, 2077, 2081, 2084, 2086
GISS-E2-R-CC	2063, 2072, 2078, 2081, 2090, 2092, 2094	2052, 2057, 2068, 2077, 2080, 2082, 2093
HadGEM2-CC	2050, 2058, 2060, 2064, 2066, 2067, 2079, 2083, 2087, 2089, 2097	2052, 2053, 2055, 2056, 2062, 2069, 2074, 2082, 2085, 2094, 2095
IPSL-CM5A-MR	2052, 2061, 2065, 2071, 2075, 2076, 2080, 2085, 2087, 2088, 2092, 2095, 2099	2051, 2055, 2056, 2059, 2062, 2063, 2066, 2068, 2069, 2074, 2093, 2094 2096
RCP 8.5 (2050-2099)		
CNRM-CM5	2058, 2064, 2066, 2074, 2079, 2081, 2083, 2086, 2088, 2090, 2092, 2094, 2096, 2097, 2099	2050, 2051, 2053, 2055, 2057, 2059, 2060, 2061, 2063, 2065, 2067, 2069, 2070, 2073, 2075, 2077, 2084, 2089

GISS-E2-R	2078, 2080, 2082, 2084, 2087, 2089, 2090, 2092, 2093, 2094, 2097, 2098	2050, 2051, 2053, 2055, 2058, 2059, 2061, 2066, 2068, 2072, 2095
GISS-E2-R-CC	2071, 2076, 2079, 2081, 2084, 2086, 2089, 2092, 2095, 2096, 2097, 2098, 2099	2050, 2052, 2055, 2057, 2061, 2063, 2064, 2066, 2067, 2072, 2082
HadGEM2-CC	2063, 2071, 2072, 2076, 2079, 2081, 2083, 2087, 2088, 2090, 2091, 2092, 2093, 2094, 2095, 2097, 2099	2050, 2051, 2053, 2054, 2055, 2056, 2057, 2059, 2064, 2067, 2068, 2069, 2077, 2082
IPSL-CM5A-MR	2072, 2075, 2078, 2079, 2081, 2083, 2086, 2088, 2089, 2090, 2091, 2092, 2095, 2096, 2097, 2098, 2099	2050, 2051, 2052, 2053, 2054, 2055, 2057, 2058, 2060, 2061, 2064, 2065, 2066, 2071, 2082

Table 6.2: El Niño and La Niña years selected for the study in the historical and RCP scenarios using observation and model datasets.

In the historical period, CNRM-CM5 shows an increase in ISMR over the central and northwest Indian regions, whereas GISS-E2-R shows an increase over the northeast and peninsular regions during El Niño events. These patterns of rainfall anomalies are consistent with the correlations observed in Figure 6.5. An increase in ISMR over the northeast, west coast, and foothills of Himalayas is observed in the simulations of HadGEM2-CC. However, the models GISS-E2-R-CC and IPSL-CM5A-MR show a decrease in ISMR over the peninsular and some areas of the central Indian regions, respectively. These results are also in agreement with the inverse El Niño-ISMR relationship found in the correlation analysis.

The models CNRM-CM5 and GISS-E2-R do not fully able to reproduce the observed El Niño-ISMR inverse relationship in both RCPs. However, this relationship is well represented in the other three models in RCP 4.5. The model GISS-E2-R-CC simulates a decrease in ISMR over the west coast and northeast regions in RCP 4.5. Similarly, a small amount of ISMR over the central and northern Indian regions is simulated by HadGEM2-CC, but for most of the Indian regions by IPSL-CM5A-MR in RCP 4.5, except for northeast India. However, Most of the models simulate a general increase in ISMR over different regions of India during El Niño events in RCP 8.5. The ISMR anomalies observed in both RCPs are also in good agreement with the ENSO-ISMR

correlation patterns (Figure 6.5). In comparison with the historical period, there is a general decrease in ISMR over most of the Indian regions during El Niño events in RCP 4.5. This decrease is clearly found in all models except GISS-E2-R-CC. The other four models simulate a decrease in ISMR, particularly HadGEM2-CC and IPSL-CM5A-MR models, in which ISMR shows a significant decrease over most of the Indian regions. In the RCP 8.5 scenario, CNRM-CM5, GISS-E2-R, and HadGEM2-CC models simulate a significant reduction in ISMR over different regions of India (e.g. the northwest, central India, and peninsular regions) whereas the other two models simulate an increase, mainly over the peninsular and central Indian regions.

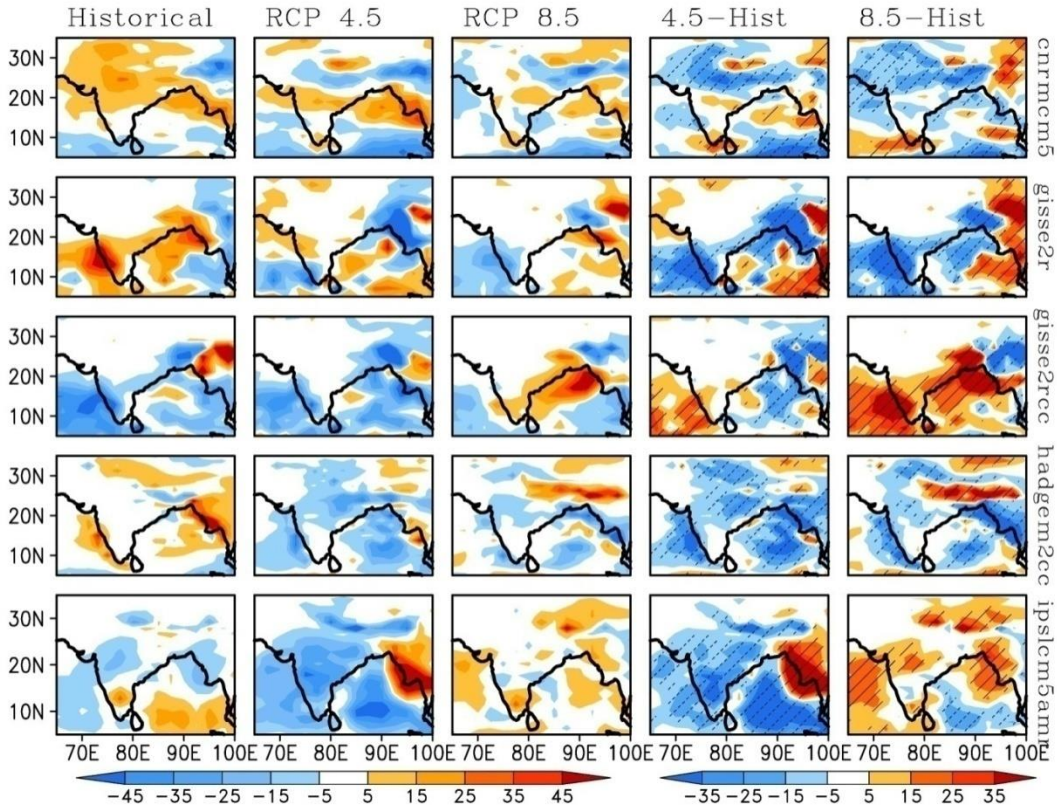

Figure 6.6: ISMR anomalies during El Niño years in historical (1951-2005) and RCP (2050-2099) scenarios along with their differences from the historical period. The hatches represent the regions with 5% significance.

In the case of La Niña events (Figure 6.7), all the models except CNRM-CM5 and GISS-E2-R exhibit a general increase in ISMR over different regions of India (e.g. west coast, northeast, and central India) in the historical period. As in the case of El Niño, CNRM-CM5 and GISS-E2-R models are not able to fully capture the observed La

Niña-ISMR in-phase relationship as shown earlier. However, in RCP 4.5, all models except CNRM-CM5 simulate an increase in ISMR over different regions of India. The increase is clearly observed in HadGEM2-CC and IPSL-CM5A-MR models, in which ISMR over most of the Indian regions shows an increase during La Niña events. A general increase in ISMR is observed in RCP 8.5 also, but the areas of positive rainfall anomalies decrease. The ISMR patterns observed during La Niña events in the historical and RCP scenarios are consistent with the results of the correlation analysis presented in Figure 6.5.

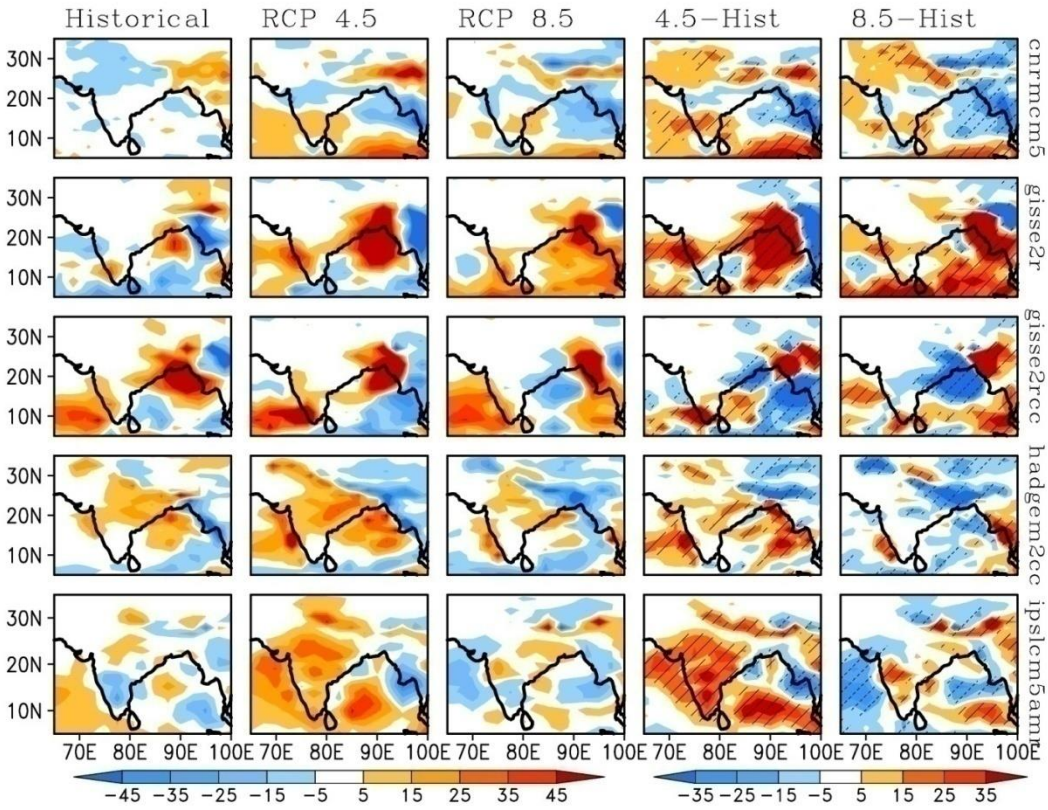

Figure 6.7: ISMR anomalies during La Niña years in historical (1951-2005) and RCP (2050-2099) scenarios along with their differences from the historical period. The hatches represent the regions with 5% significance.

As compared to the historical period, there is a significant enhancement in ISMR over most of the Indian regions in RCP 4.5, particularly in HadGEM2-CC and IPSL-CM5A-MR models. The other three models also simulate an increase in ISMR, mainly over the peninsular and northeast regions. While the models, CNRM-CM5, GISS-E2-R, and IPSL-CM5A-MR simulate an increase in ISMR in RCP 8.5 over the northwest and

peninsular regions, the other two models simulate a general decrease in ISMR over the eastern peninsular and central Indian regions during La Niña events. So, as a whole, the analysis of ISMR anomalies during El Niño events shows a general decrease in ISMR over most of the Indian regions in RCP 4.5, and the decrease is well simulated by HadGEM2-CC and IPSL-CM5A-MR models. In the case of La Niña events, a general increase in ISMR over most of the Indian regions is observed in RCP 4.5 and the increase is well simulated by HadGEM2-CC and IPSL-CM5A-MR models. The projected changes in ISMR patterns are mainly observed over the peninsular, northeast, and central Indian regions during El Niño and La Niña events. However, this pattern is not well followed in the RCP 8.5 scenario, in which the anomalies show different spatial distributions.

6.6 Projected changes in Indo-Pacific SSTs.

The changes in SST anomalies over the Indo-Pacific domain from historical to future decades during El Niño (Figure 6.8) and La Niña (Figure 6.9) years are analyzed. Generally, an El Niño event is characterized by high SST over the central and eastern Pacific and relatively low SST over the western Pacific (Rasmusson and Carpenter 1982, 1983). This pattern is clearly reproduced by all models in the historical period (Figure 6.8). This study mainly focused on the SST variations over the eastern Pacific than that over the western Pacific, as the SST over the eastern Pacific shows a significant inverse correlation with the ISMR (Mooley and Parthasarathy 1983). It is also noted that the warming over the eastern Pacific is stronger in HadGEM2-CC and IPSL-CM5A-MR models.

Significant changes in SST patterns (especially over the eastern Pacific) during the historical period are also found in RCP 4.5, albeit with slight changes in the magnitudes. However, the entire Indo-Pacific domain undergoes general warming in RCP 8.5, together with the warming of the eastern Pacific. The warming of the Indo-Pacific domain is stronger in HadGEM2-CC and IPSL-CM5A-MR models, as compared to the other models. A significant decrease in SST over the central and eastern Pacific is observed in RCP 4.5 in CNRM-CM5, GISS-E2-R, and GISS-E2-R-CC models as compared to the historical simulations. However, an increase in SST is dominated over the central and eastern Pacific Ocean in the other two models. These

changes in SST in RCP 4.5 can be associated with the ISMR patterns observed over the Indian region in RCP 4.5 (Figure 6.6) and the ENSO-ISMR correlation (Figure 6.5).

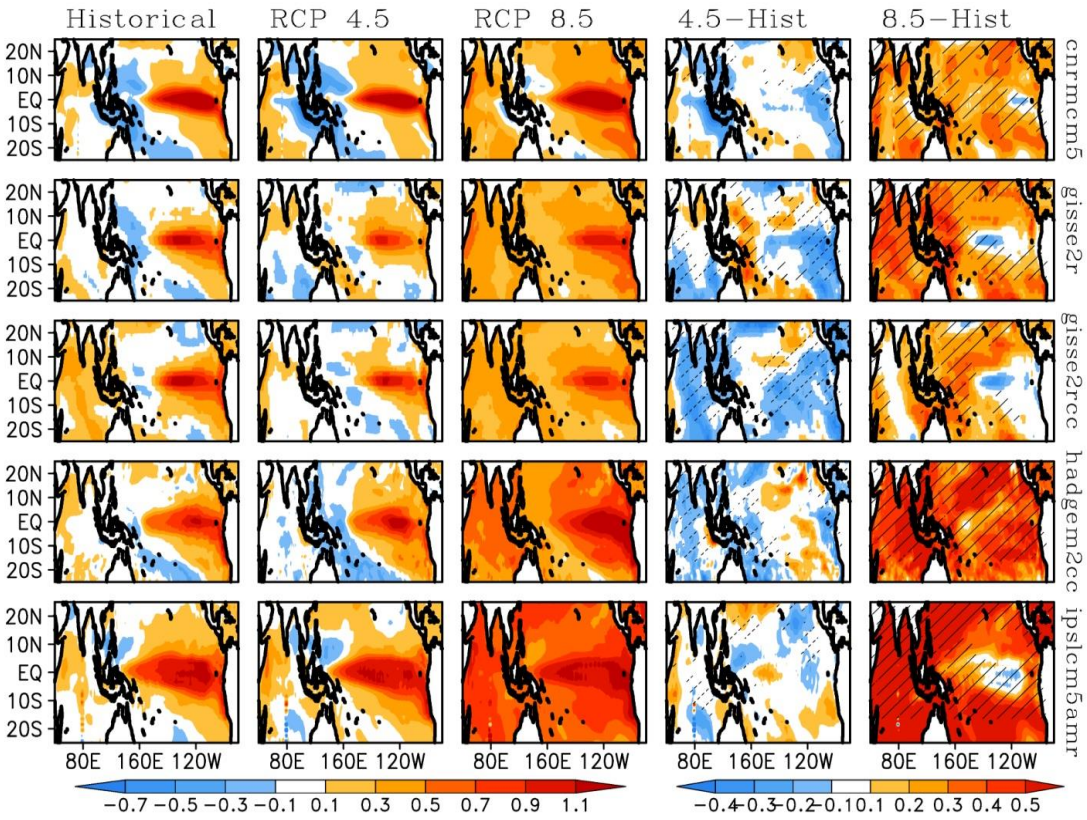

Figure 6.8: SST anomalies (°C) over the Indo-Pacific domain during El Niño years in historical (1951-2005) and RCP (2050-2099) scenarios along with their differences from the historical period. The hatches represent the regions with 5% significance.

Since HadGEM2-CC and IPSL-CM5A-MR models simulate an increase in SST over the eastern Pacific in RCP 4.5, it can be well related to the reduced ISMR observed over most of the Indian regions during El Niño events in these models. However, when compared to the historical period, the Indo-Pacific domain undergoes general warming in RCP 8.5. All models simulate a significant increase in SST over the Indo-Pacific domain, except in some areas of the eastern Pacific. However, HadGEM2-CC simulates an increase in SST over the eastern Pacific. Since the projected changes of SST in RCP 8.5 do not completely reproduce the El Niño features, they can't be well correlated with the observed ISMR patterns in that scenario.

During the La Niña events (Figure 6.9), the observed SST anomalies are well followed in all models in the historical period, with cold SST over the central and eastern Pacific and relatively higher SST over the western Pacific. In RCP 4.5 also, all models simulate a decrease in SST over the eastern Pacific. However, the SST variations over the western Pacific and the Indian Ocean are different in each model simulation. The enhanced cooling over the eastern Pacific is also well simulated in the RCP 8.5 scenario. However, the models HadGEM2-CC and IPSL-CM5A-MR simulate a general cooling of the Indo-Pacific domain during La Niña events, together with the enhanced cooling of the eastern Pacific.

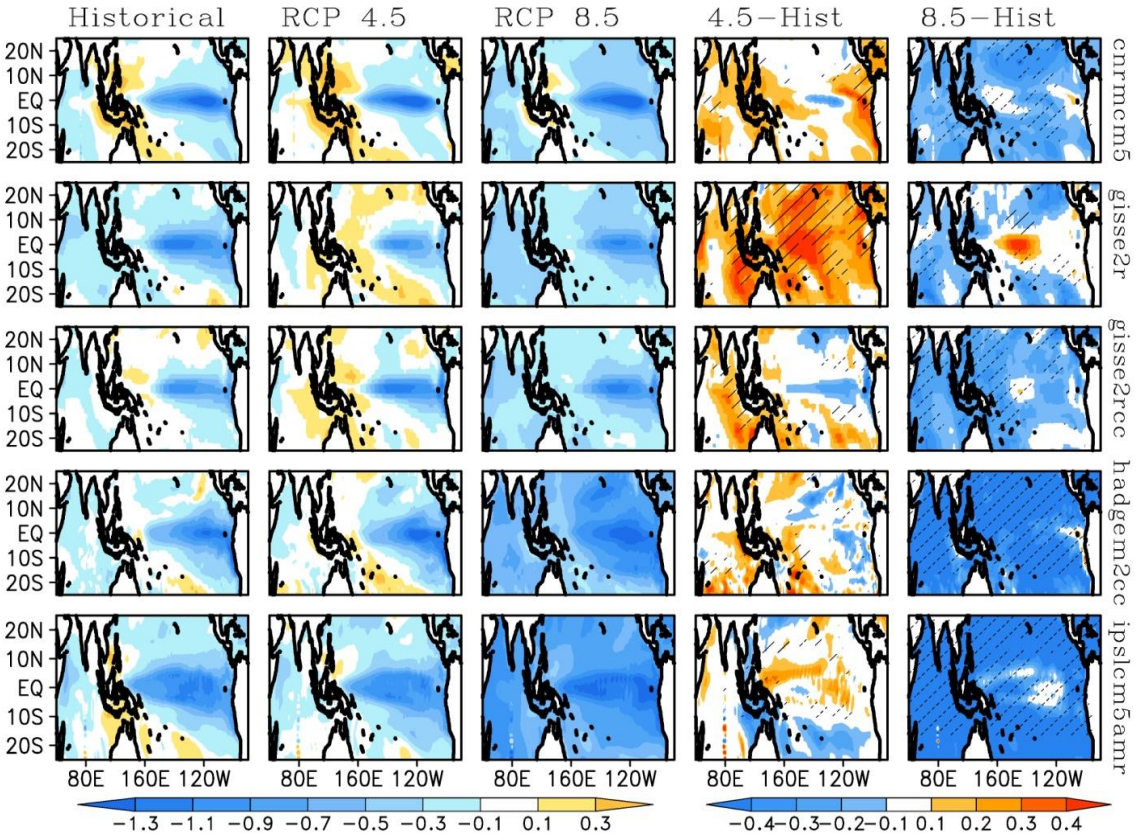

Figure 6.9: SST anomalies (°C) over the Indo-Pacific domain during La Niña years in historical (1951-2005) and RCP (2050-2099) scenarios along with their differences from the historical period. The hatches represent the regions with 5% significance.

There is a significant increase in SST over the Indo-Pacific domain in RCP 4.5 during La Niña events as compared to the historical period. However, the increase is more prominent in GISS-E2-R than in the other models. While CNRM-CM5 and GISS-E2-R simulate an increase in SST over the entire eastern Pacific, GISS-E2-R-CC simulates a

decrease in SST over some areas of the eastern Pacific. The increase in SST is more confined to the central Pacific than the eastern Pacific in HadGEM2-CC and IPSL-CM5A-MR models. A significant decrease in SST or is observed over the Indo-Pacific domain in RCP 8.5. Only the model GISS-E2-R shows a different pattern, where there is an increase in SST over the central Pacific. The observed changes in SST over the Indo-Pacific domain in RCP 4.5 can be associated with the ISMR patterns observed over the Indian region (Figure 6.7) and therefore, the ENSO-ISMR correlation (Figure 6.5) in the same scenario during La Niña events. As in the case of El Niño, the association does not hold well in the case of the RCP 8.5 scenario.

So, the analysis of SST anomalies has provided the projected changes in the SST over the Indo-Pacific domain in future decades during El Niño and La Niña events and their association with the ISMR patterns over the Indian region. It is also found that the simulations of ISMR and SST variabilities during El Niño and La Niña events are more robust in RCP 4.5 than in RCP 8.5. Since the connection between the SST patterns over the Indo-Pacific domain and the ISMR does not hold well in RCP 8.5 during both the El Niño and La Niña events, it may indicate the substantial changes in the ENSO-ISMR teleconnections in future decades in the RCP 8.5 scenario.

6.7 Evaluation of the consistency of models using multiple observational datasets

To identify how models in the historical period perform compared to the observation, and also to check the consistency of models, the SST and ISMR anomalies during El Niño and La Niña events are analyzed using multiple observational datasets (Figure 6.10). Here, the ISMR anomalies are analyzed by using CRU and APHRODITE observational datasets, and the SST anomalies using HadISST and ERSST observational datasets.

Considering the ISMR anomalies, both CRU and APHRODITE datasets show similar spatial patterns of ISMR during both El Niño and La Niña events. ISMR over most of the Indian regions shows a decrease (increase) during El Niño (La Niña) events during the historical period. Furthermore, these variations in ISMR during the historical period are almost consistent with the ISMR patterns found in the model results (Figure 6.6 and 6.7). However, the spatial patterns in CNRM-CM5 and GISS-E2-R models are not

consistent with the observation during the El Niño and La Niña events. Regarding SST, both the HadISST and ERSST datasets well capture the SST changes over the Indo-Pacific domain during El Niño and La Niña events. An increase (decrease) in SST is observed over the central and eastern equatorial Pacific during El Niño (La Niña) events in both datasets. However, the patterns of SST are not in agreement with those observed in CNRM-CM5 and GISS-E2-R models (Figure 6.8 and 6.9).

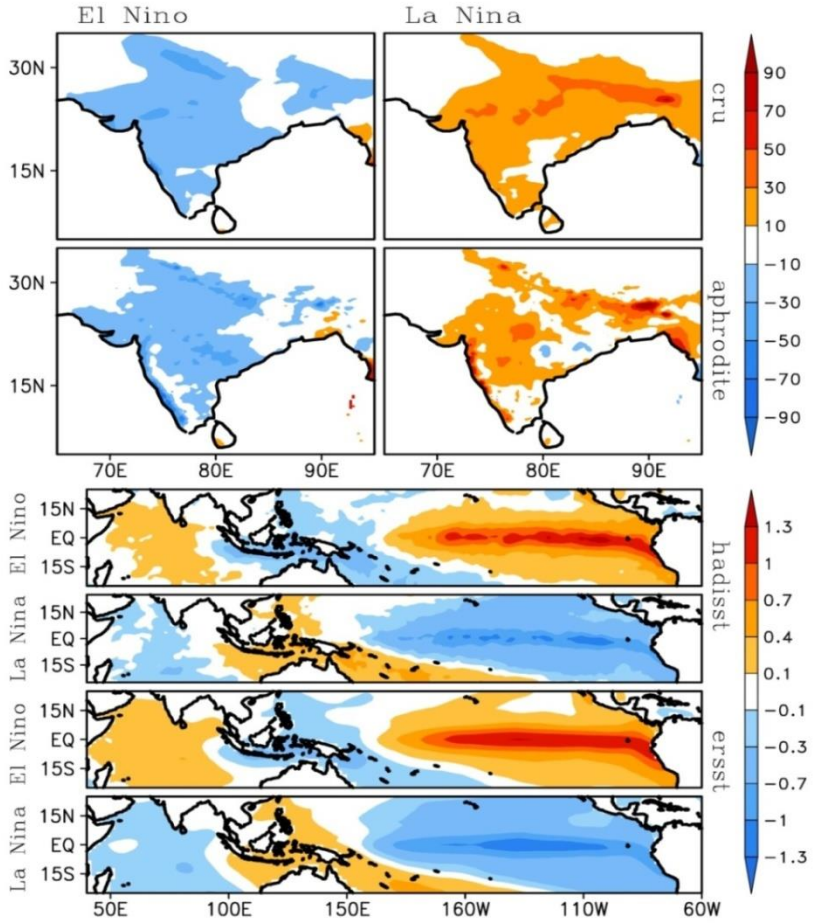

Figure 6.10: ISMR and SST anomalies (in mm and °C, respectively) during the historical period (1951-2005) using multiple observational datasets (CRU and APHRODITE for ISMR and HadISST and ERSST for SST) for El Niño and La Niña events.

6.8 Changes in Walker circulation

It was already noticed that the SST changes over the Indo-Pacific domain during El Niño and La Niña phases can make significant impacts on the regional variations of

ISMR in the future decades. To further explore the observed relationships, the changes in Walker circulation over the tropical Indo-Pacific domain during both El Niño and La Niña phases (Figure 6.11 and 6.12, respectively) in the historical and RCP scenarios are analyzed. Here the analysis of the HadGEM2-CC model was excluded due to the non-availability of vertical wind data for that model in the future period.

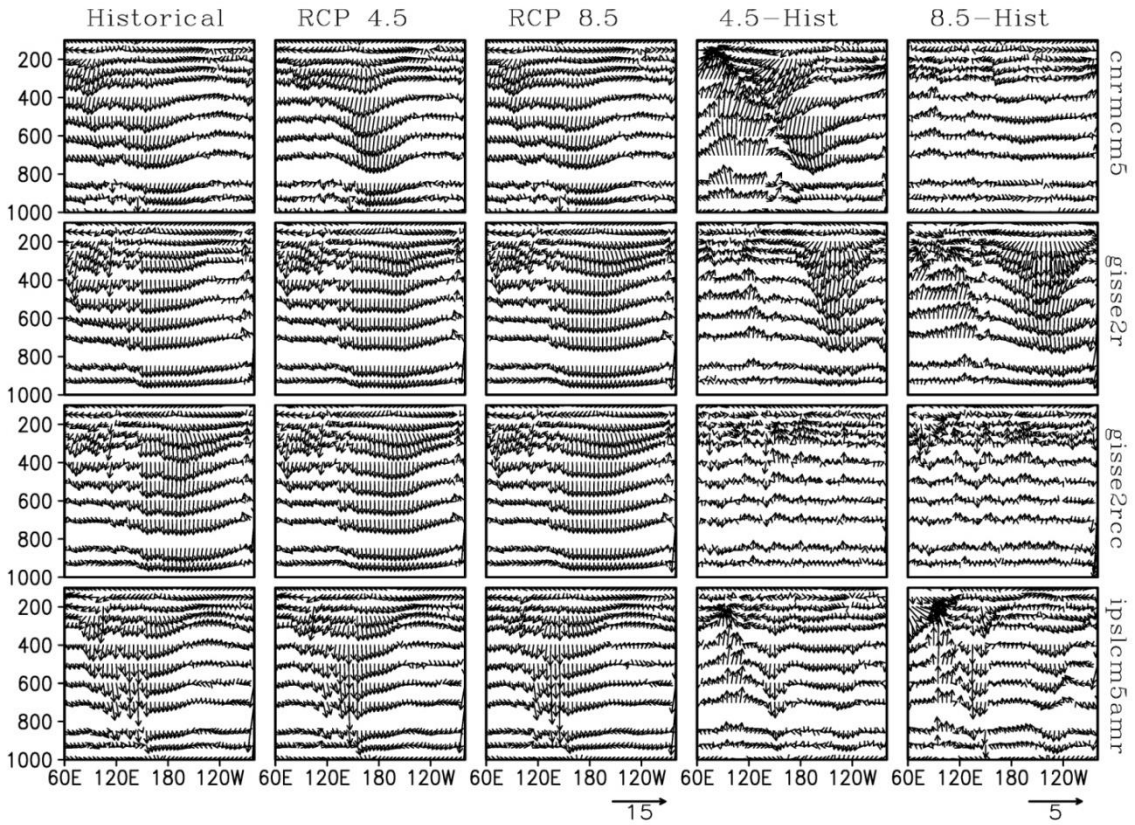

Figure 6.11: Walker circulation over the Indo-Pacific domain during El Niño years in historical (1951-2005) and RCP (2050-2099) scenarios along with their differences from the historical period.

Considerable changes in the Walker circulation are observed over the Indo-Pacific domain from historical to future decades during both El Niño and La Niña events. An eastward shift in Walker circulation is observed in both historical and RCP scenarios during El Niño events and an associated weakening of ISMR. Kumar et al. (1999) has also proposed that there is an eastward shift of the ascending branch of Walker circulation from the western equatorial Pacific to the central equatorial Pacific during El Niño events in recent decades. The study of Bayr et al. (2014) has also reported such a shift in Walker circulation, but in future decades using CMIP5 models. In comparison

with the historical period, an enhanced ascending motion over the equatorial Indian Ocean is observed in the RCP 4.5 scenario during El Niño events (Figure 6.11). The enhanced ascending motion over the equatorial Indian Ocean modifies the regional Hadley circulation by increasing the subsidence over the Indian region and thus, suppresses ISMR over the region (Hrudya et al. 2020b). Henceforth, the patterns of Walker circulations can be related to the SST changes over the Indo-Pacific domain (Figure 6.8) and the decrease in ISMR (Figure 6.6) observed over most of the Indian regions in RCP 4.5 during El Niño years.

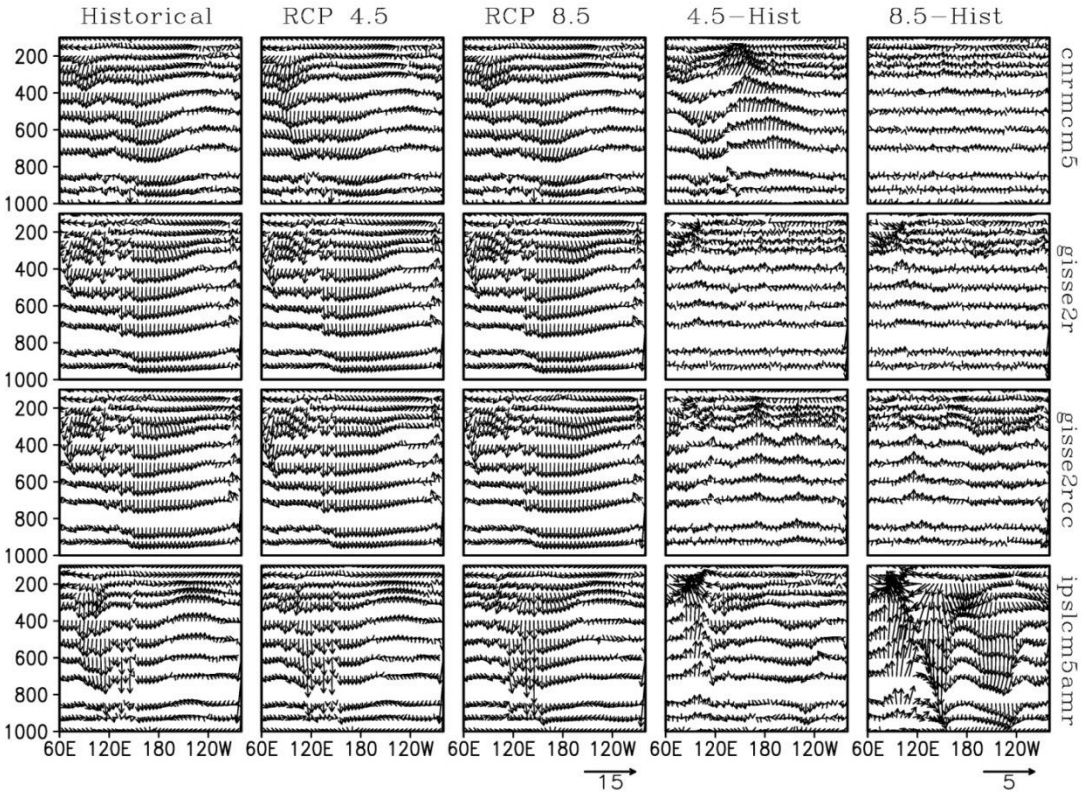

Figure 6.12: Walker circulation over the Indo-Pacific domain during La Niña years in historical (1951-2005) and RCP (2050-2099) scenarios along with their differences from the historical period.

For La Niña years also (Figure 6.12), the patterns of Walker circulations can be related to the SST patterns over the Indo-Pacific domain (Figure 6.9) and the general increase in ISMR over most of the Indian regions in RCP 4.5 (Figure 6.7). Although such a relationship exists in all the models, they highly differ from one another which indicates the inconsistency among the models in representing the Walker circulation. For both the

El Niño and La Niña events, a significant relationship between the Walker circulation and ISMR is not observed in the RCP 8.5 scenario, and therefore, it cannot be connected to the observed SST patterns over the Indo-Pacific domain and thus the ISMR in that scenario.

6.9 Chapter summary

The historical and projected changes of ISMR and the ENSO-ISMR relationship by the end of the 21st century (2050-2099) were analyzed using 25 CMIP5 models. Out of 25 CMIP5 models, five models (CNRM-CM5, GISS-E2-R, GISS-E2-R-CC, HadGEM2-CC, and IPSL-CM5A-MR) were selected for the future projection analysis by using the annual cycle of ISMR and Taylor diagram. As compared to the historical period, all models simulate an increase in ISMR in both the RCPs, mainly over the northeast, west coast, foothills of Himalayas, central India, and the peninsular Indian region in future decades. The models GISS-E2-R-CC, HadGEM2-CC, and IPSL-CM5A-MR simulate an out-of-phase relationship between Niño 3.4 index and ISMR in RCP 4.5. However, the relationship is not fully captured by the other two models, indicating the lack of reliability of these models in simulating the ENSO-ISMR relationships**.** The ISMR over most of the Indian regions is decreased (increased) during El Niño (La Niña) events in the RCP 4.5 scenario. In both cases, the changes in ISMR are well simulated by HadGEM2-CC and IPSL-CM5A-MR models, mainly over the peninsular, northeast, and central Indian regions. Significant changes in the SST are observed over the Indo-Pacific domain in RCP 4.5 during both the El Niño and La Niña events. These changes can be associated with the observed ISMR patterns over the Indian region during the El Niño and La Niña events. However, the relationship is not well held in RCP 8.5, as the Indo-Pacific domain undergoes total warming (cooling) during El Niño (La Niña) events in the RCP 8.5 scenario. The Walker circulation over the Indo-Pacific domain is also related to the SST changes over the same domain, and thus the observed ISMR patterns over the Indian region during El Niño and La Niña events, particularly in RCP 4.5. Even though noticeable variations in Walker circulation are observed in the RCP 8.5 scenario, they are not found to impact the ISMR patterns over the Indian region in that scenario.

CHAPTER 7

SUMMARY AND CONCLUSIONS

CHAPTER 7

SUMMARY AND CONCLUSIONS

The present thesis is an attempt to understand the spatio-temporal variabilities of ISMR by identifying its relationship with different oceanic and atmospheric parameters. The variability and trends of ISMR over different regions of India (west coast, northeast, northwest, and central India) were analyzed and their relationship with different convective parameters of the atmosphere (LTS, cloud cover, and CAPE) was established. The thesis also analyzed the impact of different coupled ocean-atmosphere interactions in the tropical Indian Ocean and the Pacific Ocean on ISMR variability, especially in regional scale. Since ENSO and IOD are considered as two important coupled ocean-atmosphere phenomena in the tropical Pacific Ocean and the tropical Indian Ocean, respectively, their relationship with ISMR variability was analyzed. The changes in the ENSO-ISMR and IOD-ISMR relationships from early to recent decades were analyzed separately for the onset, peak, and withdrawal phases of ISMR. Moreover, the thesis put forward a future projection of ISMR variability along with the ENSO-ISMR relationship using different CMIP5 models.

From the analyses, it is found that ISMR exhibits significant variability in spatial and temporal scales over different regions of India during the study period (1950-2015). High values of precipitation are observed over the west coast and northeast regions, moderate values over the foothills of Himalayas and central Indian regions, and the least amount over the northwest and southeast regions during the period. All convective parameters considered significantly influence the summer monsoon rainfall over different regions of India. ISMR and other convective parameters exhibit significant interannual variations and trends during the study period. ISMR shows a decreasing trend in the northeast, northwest, west coast, and central Indian regions. However, a significant trend is observed only over the northeast region. All the convective parameters exhibit significant trends, except in the central Indian region**.** To find out the nature of relationships between ISMR and convective parameters, correlation analysis was carried out. A significant positive correlation is observed between LTS and ISMR over the central Indian region. Since LTS is a measure of inversion strength in the lower

troposphere, an increase in LTS causes more moisture to be trapped within the lower troposphere. It enhances the low cloud cover and thus the ISMR. It can be attributed as the reason for the in-phase relationship between LTS and summer monsoon rainfall over the central Indian region.

CAPE shows a positive correlation with summer monsoon rainfall over the west coast and northwest regions, whereas, the correlation is negative over the northeast and central Indian regions. The increase in CAPE can produce high inversion strength, and thus enhances the cloud cover and rainfall. On the other hand, the regions of high CAPE need not always coincide with the regions of high rainfall, due to the influence of convective inhibition energy. It can be attributed as the reason for the out-of-phase relationship between CAPE and ISMR observed over the northeast and central Indian regions. The CAPE-ISMR relationship is almost opposite over the west coast and central Indian regions, which may be due to the high and low orographic influences over the respective regions. Both the LCC and MCC show an in-phase relationship with ISMR over most of the Indian regions, with more robust relationships in the case of LCC. All the convective parameters and ISMR are significantly linked to the ocean-atmospheric interactions in the tropical Pacific Ocean. A significant negative correlation between Niño 3.4 index with ISMR, LTS, and LCC is observed over most of the Indian regions, however, an insignificant negative correlation is observed over the NE region. The correlation patterns are different in the case of CAPE, where, a negative correlation is observed only over the central Indian region. The different spatial patterns of CAPE may due to the influence from other atmospheric and oceanic factors apart from the ENSO.

To establish the linkage between the tropical Pacific Ocean and ISMR variability, the ENSO-ISMR teleconnections and their changes from early (1951-1980) to recent (1986-2015) decades were analyzed. The SST variations and circulation features over the tropical Pacific and their impacts on ISMR variability were analyzed for the onset, peak, and withdrawal phases of ISMR. Significant changes in the spatial distribution of ISMR are observed from early to recent decades over the west coast, northeast, and the monsoon core zones. It is found that ENSO shows a significant negative correlation with ISMR during all three phases in both the early and recent decades, and the

correlation decreases in recent decades. ISMR over most of the Indian regions significantly increases during the onset phase and decreases during peak and withdrawal phases in the recent decades during El Niño years. On the other hand, ISMR decreases over the monsoon core zone during all phases in the recent decades during La Niña events. These changes in ISMR patterns are closely related to the SST changes and circulation features over the tropical Pacific Ocean.

There is a significant increase (decrease) in SST over the central equatorial Pacific and the Indian Ocean in recent decades during the onset phase during El Niño (La Niña) years. Noticeable changes in SST are observed during the other two phases also, but with less significance. These changes in SST make significant impacts on ISMR during all phases in recent decades. During El Niño events, the westward component of easterly trade winds is strengthened (easterly trade winds are weakened) over the central equatorial Pacific and western equatorial Indian Ocean during the onset phase in recent decades. The weakening of easterly trade winds over these regions can be related to the high SST over the same regions and thus the increase in ISMR during the onset phase. On the other hand, there is a relative strengthening of easterly trade winds during the onset phase during La Niña events, which is also related to the decrease in ISMR during the same phase. Such kind of relationship is observed during peak and withdrawal phases also, but weak as compared to the onset phase. The analysis of Walker circulation anomalies has provided the zones of ascending and descending motions over the Indian region, which coincide with the enhanced and deficit ISMR regions, respectively. During El Niño years, the subsidence over the equatorial Indian Ocean is increased during the onset phase in the recent decades. It strengthens the regional Hadley circulation by increasing the ascending motion over the Indian region and enhances ISMR. On the other hand, the enhanced ascending motion over the equatorial Indian Ocean weakens the regional Hadley circulation, which suppresses ISMR over most parts of India during the onset phase during La Niña years. A similar type of association is observed during peak and withdrawal phases, but with less significance as compared to the onset phase.

Apart from the tropical Pacific Ocean, the tropical Indian Ocean also makes significant impacts on the ISMR variability, which is supported by the analysis of IOD-ISMR

teleconnections and their changes from early to recent decades. Significant changes in the IOD-ISMR relationship are observed from the early to recent decades during the onset, peak, and withdrawal phases of ISMR. The IOD-ISMR relationship is weakening (strengthening) during the onset (withdrawal) phase in recent decades. During the peak phase, the relationship changes from out-of-phase to in-phase relationship over most of the Indian regions. The changes in the ISMR patterns during pIOD and nIOD events were separately analyzed in connection with the changes in SST, moisture transport, and low-level winds over the tropical Indian Ocean and the Indian region. ISMR noticeably increases over most parts of the Indian regions during all phases during pIOD events in the recent decades. On the other hand, ISMR decreases during peak and withdrawal phases and increases during the onset phase during nIOD events. Significant changes in SST are observed over the western and central equatorial Indian Ocean during all phases, but with slight variations from one phase to another.

The LLJ over the equatorial Indian Ocean and the Arabian Sea is strengthened (low-level westerlies weaken) during pIOD events during all phases in recent decades. This relative strengthening (with respect to early decades) creates a moisture convergence zone over the northeast regions of India, which causes relatively high summer monsoon rainfall in the monsoon trough zone by transporting excess moisture to the region. However, the LLJ is feeble in the peninsular regions and hence there are no significant changes in ISMR. Almost opposite conditions are observed during nIOD events, where there is a weakening of LLJ (strengthening of low-level westerlies) during peak and withdrawal phases. It suppresses the transport of moisture to the Indian region and thus reduces the summer monsoon rainfall over the region. A divergent zone of moisture is developed over the northeast region, which reduces ISMR over the foothills of Himalayas and central-eastern regions. But, the westerlies are relatively weak over peninsular India and the central equatorial Indian Ocean during the onset phase and are associated with the enhanced ISMR over the monsoon core zone of India. These changes in circulation features and moisture convergence are well related to the SST anomalies and ISMR characteristics in all three phases during both the pIOD and nIOD events in recent decades. However, the most significant changes are observed during peak and withdrawal phases. The analysis of velocity potential anomalies also has provided the zone of ascending and descending motions, which coincide with the

enhanced and deficit ISMR regions, respectively. The analysis of IOD-ISMR teleconnections with pure IOD events also revealed the same patterns of ISMR, SST, circulation, moisture transport, and velocity potentials, however, with a slight increase in their magnitudes. It indicates the weakening of the ENSO-ISMR relationship when IOD events co-occur with the ENSO events.

The present thesis also attempted to torchlight the projected changes in ISMR variability and ENSO-ISMR relationship by the end of the 21st century using CMIP5 models. Total 25 models were considered for the study, out of which, five models (CNRM-CM5, GISS-E2-R, GISS-E2-R-CC, HadGEM2-CC, and IPSL-CM5A-MR) were selected by using the seasonal cycle of ISMR and Taylor diagram. The models, CNRM-CM5, HadGEM2-CC, and IPSL-CM5A-MR show high spatial variability in ISMR in the historical period (1951-2005) and are consistent with the observational datasets. However, the models; GISS-E2-R, and GISS-E2-R-CC do not well reproduce the ISMR spatial variability. As compared to the historical period, all models simulate an increase in ISMR in future decades (2050-2099) in both RCP 4.5 and RCP 8.5 scenarios and the increase is higher in RCP 8.5. A significant increase in ISMR is observed over the northeast, west coast, foothills of Himalayas, central India, and the peninsular Indian region, particularly in CNRM-CM5, HadGEM2-CC, and IPSL-CM5A-MR models. It is also found that the representation of regional variations of ISMR is more robust in RCP 8.5 than in RCP 4.5.

The ENSO-ISMR teleconnections show significant changes in both the RCPs. The SST changes and circulation features over the tropical Indo-Pacific domain are significantly related to the ISMR characteristics during El Niño and La Niña events in future decades, particularly in RCP 4.5. A negative association between ENSO and ISMR is simulated by GISS-E2-R-CC, HadGEM2-CC, and IPSL-CM5A-MR models in RCP 4.5. ISMR over most of the Indian regions decreases (increases) during El Niño (La Niña) events in the RCP 4.5 scenario. In both cases, the changes in ISMR are well simulated by HadGEM2-CC and IPSL-CM5A-MR models. The changes are mainly observed over the peninsular, northeast, and central Indian regions. However, different spatial patterns of ISMR are observed for the RCP 8.5 scenario, which highly differs from one model to another.

The changes in the SST and Walker circulation over the Indo-Pacific domain significantly influence the ISMR during both the El Niño and La Niña events in RCP 4.5. The changes in Walker circulation affect the observed ISMR patterns over the Indian region through the modulation of regional Hadley circulation. These teleconnections are better represented in HadGEM2-CC and IPSL-CM5A-MR models. However, the Indo-Pacific domain undergoes total warming (cooling) during El Niño (La Niña) events in the RCP 8.5 scenario. Hence, they are not much capable of influencing the ISMR patterns over the Indian region. The Walker circulation over the Indo-Pacific domain is connected with the SST changes there, and thus the observed ISMR patterns during the El Niño and La Niña events, particularly in RCP 4.5. Even though noticeable variations in Walker circulation are observed in the RCP 8.5 scenario, they are not found to make an impact on the ISMR patterns during El Niño and La Niña events. From the analysis, it is also identified that the representation of the ENSO-ISMR relationship is more robust in RCP 4.5 than in RCP 8.5 and the relationship is well represented in HadGEM2-CC and IPSL-CM5A-MR models. The other two models are not fully able to capture the teleconnections which indicates the lack of reliability of these models in simulating the ENSO-ISMR relationships.

7.1 Scope for future studies

- The convective parameters have significant impacts on the global monsoon, weather prediction systems, and hydrological balance across the world. Thus, their analysis can be extended to global monsoon domains apart from the Indian region.
- The present thesis analyzes the changes in ISMR variability and ENSO-ISMR relationship in future decades under different RCP scenarios. The analysis can be further explored for different phases (onset, peak, and withdrawal) of ISMR separately since the rainfall characteristics during different phases and their influencing mechanisms highly differ from one another.
- The analysis of the ENSO-ISMR relationship can be extended by using the recently developed Coupled Model Inter Comparison Project Phase 6 (CMIP6).

The analysis can be separately done for the onset, peak, and withdrawal phases of ISMR.

- The analysis of the influence of El Niño and La Niña events on ISMR variability in future decades can be further explored by giving additional focus to sub-divisional analysis. It will provide the impacts of SST changes over the Indo-Pacific domain during El Niño and La Niña events on the ISMR variability over different sub-divisions of India in the upcoming decades.
- The entire analysis in this thesis was carried out by considering the Indian Ocean and Pacific Ocean variabilities as interlinked. The influence from the tropical Pacific Ocean on the ISMR regional variability can be analyzed by masking the influences from the tropical Indian Ocean, and vice versa. This method of analysis can be done separately for the onset, peak, and withdrawal phases.

Bibliography

Abram NJ, Gagan MK, Cole JE, Hantoro WS, Mudelsee M (2008) Recent intensification of tropical climate variability in the Indian Ocean. Nat Geo Sci 1:849–853

Achuthavarier D, Krishnamurthy V (2011) Role of Indian and Pacific SST in Indian summer monsoon intraseasonal variability. J Clim 24:2915-2930

Ajayamohan RS, Rao SA (2008) Indian Ocean Dipole modulates the number of extreme rainfall events over India in a warming environment. J Meteorol Soc Jpn 86:245-252

Aneesh S, Sijikumar S (2016) Changes in the south Asian monsoon low level jet during recent decades and its role in the monsoon water cycle. J Atmos Sol-Terr Phys 138:47-53

Annamalai H, Liu P (2005) Response of the Asian summer monsoon to changes in El Niño properties. Q J R Meteorol Soc131:805-831

Annamalai H, Slingo JM (2001) Active/break cycles: diagnosis of the intraseasonal variability of the Asian Summer Monsoon. Clim Dyn 18:85-102

Ashok K, Feba F, Tejavath CT (2019) The Indian summer monsoon rainfall and ENSO. Mausam 70:443-452

Ashok K, Guan Z, Saji NH, Yamagata T (2001) Impact of the Indian Ocean Dipole on the relationship between Indian monsoon rainfall and ENSO. Geophys Res Lett 28:4499-4502

Ashok K, Guan Z, Saji NH, Yamagata T (2003) A look at the relationship between ENSO and the Indian Ocean Dipole. J Meteorol Soc Jpn 81:41-56

Ashok K, Guan Z, Saji NH, Yamagata T (2004) Individual and combined influences of ENSO and the Indian Ocean Dipole on the Indian summer monsoon. J Clim 17:3141-3155

Ashok K, Saji NH (2007) On impacts of ENSO and Indian Ocean Dipole events on the sub regional Indian summer monsoon rainfall. Nat Hazards 42:273-285

Ashrit RG, Kumar R, Krishna Kumar K (2001) ENSO-monsoon relationship in a greenhouse warming scenario. Geophys Res Lett 28:1727-1730

Azad S, Rajeevan M (2016) Possible shift in the ENSO-Indian monsoon rainfall relationship under future global warming. Sci Rep 6:20145

Bayr T, Dommenget D, Martin T, Power SB (2014) The eastward shift of the Walker Circulation in response to global warming and its relationship to ENSO variability. Clim Dyn 43:2747-2763

Behera SK, Krishnan K, Yamagata T (1999) Unusual ocean-atmosphere conditions in the tropical Indian Ocean during 1994. Geophys Res Lett 26:3001-3004

Behera SK, Luo JJ, Masson S, Delecluse P, Gualdi S, Navarra A, Yamagata T (2005) Paramount impact of the Indian Ocean dipole on the East African short rains: A CGCM study. J Clim 18:4514-4530

Behera SK, Luo JJ, Masson S, Rao SA, Sakuma H (2006) A GCM study on the interaction between IOD and ENSO. J Clim 19:1688-1705

Behera SK, Ratnam JV (2018) Quasi-asymmetric response of the Indian summer monsoon rainfall to opposite phases of the IOD. Sci Rep 8:1-8

Behera SK, Yamagata T (2003) Influence of Indian Ocean Dipole on Southern Oscillation. J Meteorol Soc Jpn 81:169-177

Bjerknes J (1969) Atmospheric teleconnections from the equatorial Pacific. Mon Weather Rev 97:163-172

Cash BA, Kinter JL, Adams J, Altshuler E, Haung B, Jin EK, Manganello J, Marx L, Jung T (2015) Regional structure of Indian summer monsoon in observations, reanalysis and simulation. J Clim 28:1824-1841

Ceppi P, Gregory JM (2017) Relationship of tropospheric stability to climate sensitivity and Earth's observed radiation budget. Proc Natl Acad Sci 114:13126-13131

Chandrasekar A (2010) Basics of Atmospheric Science. PHI Learning Pvt. Ltd, New Delhi, India

Chatterjee P, Goswami BN (2004) Structure, genesis and scale selection of the tropical quasi-biweekly mode. Q J R Meteorol Soc 130:1171-1194

Chaturvedi RK, Joshi J, Jayaraman M, Bala G, Ravindranath NH (2012) Multi-model climate change projections for India under representative concentration pathways. Curr Sci 103:791-802

Cherchi A, Alessandri A, Masina S, Navarra A (2011) Effects of increased CO2 levels on monsoons. Clim Dyn 37:83-101

Cherchi A, Navarra A (2013) Influence of ENSO and of the Indian Ocean Dipole on the Indian summer monsoon variability. Clim Dyn 41:81-103

Chowdary JS, Bandgar AB, Gnanaseelan C, Luo JJ (2015) Role of tropical Indian Ocean air-sea interactions in modulating Indian summer monsoon in a coupled model. Atmos Sci Lett 16:170-176

Das PK, Chakraborty A, Seshasai MVR (2014) Spatial analysis of temporal trend of rainfall and rainy days during the Indian Summer Monsoon season using daily gridded (0.5°×0.5°) rainfall data for the period of 1971–2005. Meteorol Appl 21:481-493

Dash SK**,** Kulkarni MA, Mohanty UC, Prasad K (2009) Changes in the characteristics of rain events in India. J Geophys Res. http://doi.org/10.1029/2008JD010572

Dee DP, Uppala SM, Simmons AJ, Berrisford P, Poli P, Kobayashi S, Andrae U, Balmaseda MA, Balsamo G, Bauer DP, Bechtold P (2011) The ERA-Interim reanalysis: configuration and performance of the data assimilation system. Q J R Meteorol Soc 137:553-597

DelSole T, Shukla J (2012) Climate models produce skillful predictions of Indian summer monsoon rainfall. Geophys Res Lett 39:1-8

Emanuel KA (1994) Atmospheric Convection. Oxford University Press: Oxford, UK.

Feba F, Ashok K, Ravichandran M (2018) Role of changed Indo-Pacific atmospheric circulation in the recent disconnect between Indian summer monsoon and ENSO. Clim Dyn 52:1461-1470

Feng S, Hu Q (2008) How the North Atlantic Multidecadal Oscillation may have influenced the Indian summer monsoon during the past two millennia. Geophys Res Lett. http://doi.org/10.1029/2007G L0324 84

Francis PA, Gadgil S (2013) A note on new indices for the equatorial Indian Ocean oscillation. J Earth Syst Sci 122:1005–1011

Gadgil S (1988) Recent advances in monsoon research with particular reference to the Indian monsoon. Aust Meteorol Mag 36:193-204

Gadgil S (2003) Indian monsoon and its variability. Annu Rev Earth Planet Sci 31:429-467

Gadgil S, Rajeevan M, Francis PA (2007) Monsoon variability: Links to major oscillations over the equatorial Pacific and Indian Oceans. Curr Sci 93:182-195

Gadgil S, Vinayachandran PN, Francis PA (2003) Droughts of Indian summer monsoon: Role of clouds over the Indian Ocean. Curr Sci 85:1713-1719

Gadgil S, Vinayachandran PN, Francis PA (2004) Extremes of the Indian summer monsoon rainfall, ENSO and equatorial Indian Ocean Oscillation. Geophys Res Lett. http://doi.org/10.1029/2004GL019733

Ghosh S, Luniya V, Gupta A (2009) Trend analysis of Indian summer monsoon rainfall at different spatial scale. Atmos Sci Lett 10:285–290

Ghosh S, Vittal H, Sharma T, Karmalar S, Kasiviswanathan KS, Dhanesh Y, Sudheer KP, Gunthe SS (2016) Indian summer monsoon rainfall: Implications of contrasting trends in the spatial variability of means and extremes. PLoS One. http://doi.org/10.1371/journal.pone.0158670

Goswami BN (2005a) South Asian summer monsoon: An overview. In: CP Chang, B Wang, and G Lau (eds) The global monsoon system: Research and forecast. World Meteorology Organization Tech. Doc. WMO/TD-1266, pp 47-71

Goswami BN (2005b) South Asian monsoon. In: WKM Lau and DE Waliser (eds) Intraseasonal Variability of the Atmosphere–Ocean Climate System. Springer, New York, pp 19–61

Goswami BN, Ajayamohan RS (2001a) Intraseasonal oscillations and interannual variability of the Indian summer monsoon. J Clim 14:1180-1198

Goswami BN, Ajayamohan RS (2001b) Intraseasonal oscillations and predictability of the Indian summer monsoon. Proc Indian Natl Sci Acad A 67:369-383

Goswami BN, Madhusoodanan MS, Neema CP, Sengupta D (2006b) A physical mechanism for North Atlantic SST influence on the Indian summer monsoon. Geophys Res Lett. http://doi.org/10.1029/2005G L024803

Goswami BN, Wu G, Yasunari T (2006a) The Annual Cycle, Intraseasonal Oscillations, and Roadblock to Seasonal Predictability of the Asian Summer Monsoon. J Clim 19:5078-5099

Goswami BN, Xavier PK (2005) Dynamics of "internal" interannual variability of the Indian summer monsoon in a GCM. J Geophys Res. http://doi.org/1029/2005JD006042

Guhathakurta P, Rajeevan M (2008) Trends in the rainfall pattern over India. Int J Climatol 28:1453-1469

Guhathakurta P, Rajeevan M, Sikka DR, Tyagi A (2014) Observed changes in southwest monsoon rainfall over India during 1901-2011. Int J Climatol 35:1881-1898

Guilyardi E (2006) El Niño-mean state-seasonal cycle interactions in a multi model ensemble. Clim Dyn 26:329-348

Guilyardi E, Wittenberg A, Fedorov A, Collins M, Wang C, Capotondi A, Stockdale T (2009) Understanding El Niño in ocean–atmosphere general circulation models: Progress and challenges. Bull Amer Meteorol Soc 90:325-340

Guo F, Liu Q, Sun S, Yang J (2015) Three types of Indian Ocean dipoles. J Clim 28:3073–3092

Han W, Vialard J, McPhaden MJ, Lee T, Masumoto Y, Feng M, De Ruijter W (2014) Indian Ocean decadal variability: A review. Bull Amer Meteorol Soc. http://doi.org/10.1175/BAMS-D-13-00028.1

Harris I, Jones PD, Osbornaand TJ, Listera DH (2014) Updated high-resolution grids of monthly climatic observations – the CRU TS3.10 dataset. Int J Climatol 34:623-642

Hernandez M, Ummenhofer CC, Anchukaitis KJ (2015) Multi-scale drought and ocean–atmosphere variability in monsoon Asia. Environ Res Lett. http://doi.org/10.1088/1748-9326/10/7/074010

Hrudya PH, Varikoden H, Vishnu R (2020a) A review on the Indian summer monsoon rainfall, variability and its association with ENSO and IOD. Meteorol Atmos Phys 133:1-14

Hrudya PH, Varikoden H, Vishnu R (2021) Changes in the relationship between Indian Ocean dipole and Indian summer monsoon rainfall in early and recent multidecadal epochs during different phases of monsoon. Int J Climatol 41:305-318

Hrudya PH, Varikoden H, Vishnu R, Kuttippurath J (2020b). Changes in ENSO-monsoon relations from early to recent decades during onset, peak and withdrawal phases of Indian summer monsoon. Clim Dyn 55:1457-1471

Hu ZH, Latif M, Roecknera E, Bengtsson L (2000) Intensified Asian summer monsoon and its variability in a coupled model forced by increasing greenhouse gas concentrations. Geophys Res Lett 27:2681–2684

Huang B, Thorne PW, Banzon VF, Boyer T, Chepurin G, Lawrimore JH, Zhang HM (2017) Extended reconstructed sea surface temperature, version 5 (ERSSTv5): upgrades, validations, and intercomparisons. J Clim 30:8179-8205

Ihara C, Kushnir Y, Cane MA (2008) Warming trend of the Indian Ocean SST and Indian Ocean dipole from 1880 to 2004. J Clim 21:2035-2046

Ihara C, Kushnir Y, Cane MA, De La Pena VH (2007) Indian summer monsoon and its link with ENSO and Indian Ocean climate indices. Int J Climatol 27:179-187

Jain D, Chakraborty A, Nanjundiah RS (2019) Convective available potential energy and precipitation in a cloud-resolving model simulation of Indian summer monsoon. Current Trends in the Representation of Physical Processes in Weather and Climate Models. Springer, Singapore. 113-137

Jain DK, Chakraborty A, Nanjundiah RS (2013) Role of the cloud adjustment time scale in simulation of the interannual variability of Indian summer monsoon. Meteorol Atmos Phys 122:159-173

Jayakumar A, Sethunadh J, Arulalan RT, Mohandas S, Iyengar GR (2017) Behaviour of predicted convective clouds and precipitation in the high resolution unified model over the Indian summer monsoon region. Earth Space Sci 4:303-313

Jayasankar CB, Surendran S, Rajendran K (2015) Robust signals of future projections of Indian summer monsoon rainfall by IPCC AR5 climate models: Role of seasonal cycle and interannual variability. Geophys Res Lett 42:3513-3520

Jena P, Azad S, Rajeevan MN (2016) CMIP5 projected changes in the annual cycle of Indian monsoon rainfall. Climate. https://doi.org/10.3390/cli4010014

Jourdain NC, Gupta AS, Taschetto AS, Ummenhofer CC, Moise AF, Ashok K (2013) The Indo-Australian monsoon and its relationship to ENSO and IOD in reanalysis data and the CMIP3/CMIP5 simulations. Clim Dyn 41:3073-3102

Kalnay E, Kanamitsu M, Kistler R, Collins W, Deaven D, Gandin L, Iredell M, Saha S, Walt G, Woollen J, Zhu Y, Chelliah M, Ebisuzaki W, Higgins W, Janowiak J, Mo KC, Ropelewski C, Wang J, Leetmaa A, Reynolds R, Jenne R, Joseph D (1996) The NCEP/NCAR 40-year reanalysis project. Bull Amer Meteorol Soc 77:437-471

Kerr RA (2000) A North Atlantic climate pacemaker for the centuries. Science 288:1984–1985

Kishore P, Jyothi S, Bhasha G, Rao SVB, Rajeevan M, Velicogna I, Sutterley TC (2015) Precipitation climatology over India: validation with observational and reanalysis datasets and spatial trends. Clim Dyn 46:541-556

Kitoh A, Endo H, Krishna Kumar K, Cavalcanti IF, Goswami P, Zhou T (2013) Monsoons in a changing world: a regional perspective in a global context. J Geophys Res 118:3053-3065

Klien SA, Hartmann DL (1993) The seasonal cycle of low stratiform clouds. J Clim 6:1588-1606

Konwar M, Parekh A, Goswami BN (2012) Dynamics of east-west asymmetry of Indian summer rainfall trends in recent decades. Geophys Res Lett. http://doi.org/10.1029/2012GL052018

Kripalani RH, Oh JH, Kulkarni A, Sabade SS, Chaudhari HS (2007) South Asian summer monsoon precipitation variability: coupled climate model simulations and projections under IPCC AR4. Theor Appl Climatol 90:133-159

Krishnamurthy V, Kinter JL (2003) Indian monsoon and its relation to global climate variability. Global climate. Springer, Berlin, Heidelberg. 186-236

Krishnamurthy V, Shukla J (2000) Intraseasonal and interannual variability of rainfall over India. J Clim 13:4366-4377

Krishnamurthy V, Shukla J (2007) Intraseasonal and seasonally persisting patterns of Indian monsoon rainfall. J Clim 20:3-20

Krishnan R, Sugi M (2003) Pacific decadal oscillation and variability of Indian summer monsoon rainfall. Clim Dyn 21:233–242

Krishnaswami J, Vaidyanathan S, Rajagopalan B, Bonnel M, Sankaran M, Bhalla RS, Badiger S (2015) Non-stationary and non-linear influence of ENSO and Indian Ocean Dipole on Indian summer monsoon rainfall and extreme rain events. Clim Dyn. http://doi/org/10.1007/s00382-014-2288-0

Kucharski F, Bracco A, Yoo H, Molteni F (2008) Atlantic forced component of the Indian monsoon interannual variability. Geophys Res Lett. http://doi.org/10.1029/2007G L0330 37

Kumar KK, Kamala K, Rajagopalan B, Hoerling MP, Eischeid JK, Patwardhan SK, Nemani R (2010) The once and future pulse of Indian monsoonal climate. Clim Dyn 36:2159-2170

Kumar KK, Patwardhan SK, Kulkarni A, Kamala K, Rao KK, Jones R (2011) Simulated projections for summer monsoon climate over India by a high-resolution regional climate model (PRECIS). Curr Sci 101:312-326

Kumar KK, Rajagopalan B, Cane MA (1999) On the weakening relationship between the Indian monsoon and ENSO. Science 284:2156-2159

Kumar KK, Rajagopalan B, Hoerling M, Bates G, Cane M (2006) Unraveling the mystery of Indian monsoon failure during El Nino. Science 314:115-119

Lau NC, Nath MJ (2000) Impact of ENSO on the variability of the Asian-Australian Monsoons as simulated in GCM experiments. J Clim 13:4287-4309

Li S, Perlwitz J, Quan X, Hoerling MP (2008) Modelling the influence of North Atlantic multidecadal warmth on the Indian summer rainfall. Gephys Res Lett. http://doi.org/1029/2007G L0329 01

Li T, Wang B, Chang CP, Zhang Y (2003) A theory for the Indian Ocean dipole–zonal mode. J Atmos Sci 60:2119-2135

Liu Z, Alexander M (2007) Atmospheric bridge, oceanic tunnel, and global climatic teleconnections. Rev Geophys 45:1-34

Lu R, Dong B, Ding H (2006) Impact of the Atlantic Multidecadal Oscillation on the Asian summer monsoon. Geophys Res Lett. http://doi.org/10.1029/2006G L027655

Luo JJ, Zhang R, Behera SK, Masumoto Y (2010) Interaction between El Niño and Extreme Indian Ocean Dipole. J Clim 23:726-742

Maharana P, Dimri AP (2015) Study of intraseasonal variability of Indian summer monsoon using a regional climate model. Clim Dyn. http://doi.org/10.1007/s00382-015-2631-0

Mani NJ, Suhas E, Goswami BN (2009) Can global warming make Indian monsoon weather less predictable? Geophys Res Lett. http://doi.org/1029/2009GL037989

Meehl GA (1994) Couple land-ocean-atmosphere processes and south Asian monsoon variability. Science 266:262–266

Meehl GA, Washington WM (1993) South Asian summer monsoon variability in a model with doubled atmospheric carbon dioxide concentration. Science 260:1101-1104

Menon A, Levermann A, Schewe J, Lehmann J, Frieler K (2013) Consistent increase in Indian monsoon rainfall and its variability across CMIP-5 models. Earth Syst Dyn 4:287-300

Miller AJ, Cayan DR, Barnett TP, Graham NE, Oberhuber JM (1994) The 1976-77 climate shift of the Pacific Ocean. Oceanography 7:21-26

Mishra V, Smoliak BV, Lettenmaier DP, Wallace JM (2012) A prominent pattern of year-to-year variability in Indian Summer Monsoon Rainfall. Proc Natl Acad Sci 109:7213-7217

Mooley DA, Parthasarathy B (1983) Variability of Indian summer monsoon and tropical circulation features. Bull Amer Meteorol Soc 111:967-978

Mooley DA, Shukla J (1987) Characteristics of the westward-moving summer monsoon low pressure systems over the Indian region and their relationship with the monsoon rainfall. University of Maryland Center for Ocean-Land-Atmosphere Interactions Rep, 47 pp

Murugavel P, Pawar SD, Gopalakrishnan V (2012) Trends of convective available potential energy over the Indian region and its effect on rainfall. Int J Climatol 32:1362-1372

Murukami T, Nakazawa T, He J (1984) On the 40-50 days oscillations during the 1979 Northern Hemisphere Summer. J Meteorol Soc Jpn 62:440-467

Nair PJ, Chakraborty A, Varikoden H, Francis PA, Kuttipurath J (2018) The local and global climate forcings induced inhomogeneity of Indian rainfall. Sci Rep. http://doi.org/10.1038/s41598-018-24021-x

Pillai PA, Chowdary JS (2016) Indian summer monsoon intra-seasonal oscillation associated with the developing and decaying phase of El Nino. Int J Climatol 36:1846-1862

Pokhrel S, Sikka DR (2013) Variability of the TRMM-PR total and convective and stratiform rain fractions over the Indian region during the summer monsoon. Clim Dyn 41:21-44

Power SB, Smith IN (2007) Weakening of the Walker Circulation and apparent dominance of El Nino both reach record levels, but has ENSO really changed? Geophys Res Lett. http://doi.org/10.1029/2007GL03085

Preethi B, Kripalani RH, Kumar KK (2010) Indian summer monsoon rainfall variability in global coupled ocean-atmospheric models. Clim Dyn 35:1521-1539

Preethi B, Ramya R, Patwardhan SK, Mujumdar M, Kripalani RH (2019) Variability of Indian summer monsoon droughts in CMIP5 climate models. Clim Dyn 53:1937-1962

Rajeevan M, Bhate J, Kale JD, Lal B (2006) High resolution daily gridded rainfall data for the Indian region: Analysis of break and active monsoon spells. Curr Sci 91:296-306

Rajeevan M, Pai DS, Thapliyal V (2002) Predictive relationships between Indian Ocean sea surface temperatures and Indian summer monsoon rainfall. Mausam 53:337-348

Ramesh KV, Goswami P (2007) Reduction in temporal and spatial extend of the Indian summer monsoon. Geophys Res Lett. http://doi.org/10.1029/2007GL031613

Ramu DA, Sabeerali CT, Chattopadhyay R, Rao DN, George G, Dhakate AR, Rao SA (2016) Indian summer monsoon rainfall simulation and prediction skill in the CFSv2 coupled model: Impact of atmospheric horizontal resolution. J Geophys Res Atmos 121:2205-2221

Rao SA, Behera SK, Masumoto Y, Yamagata T (2002) Interannual subsurface variability in the Tropical Indian Ocean with a special emphasis on the Indian Ocean Dipole. Deep Sea Res part II 49:1549–1572

Rao SA, Chaudhari HS, Pokhrel S, Goswami BN (2010) Unusual central Indian drought of summer monsoon 2008: Role of southern tropical Indian Ocean warming. J Clim. http://doi.org/10.1175/2010JCLI3257.1

Rao SA, Masson S, Luo JJ, Behera SK,Yamagata T (2007) Termination of Indian Ocean dipole events in a coupled general circulation model. J Clim 20:3018-3035.

Rao YP (1976) Southwest Monsoon. Meteorological Monograph No. 1, India Meteorological Department, New Delhi

Rasmusson EM, Carpenter TH (1982) Variations in tropical sea surface temperature and surface wind fields associated with the Southern Oscillation/El Niño. Mon Weather Rev 110:354-384

Rasmusson EM, Carpenter TH (1983) The relationship between eastern equatorial Pacific sea surface temperatures and rainfall over India and Sri Lanka. Mon Weather Rev111:517-528

Ratnam JV, Behera SK, Masumoto Y, Takahashi K, Yamagata T (2010) Pacific Ocean origin for the 2009 Indian summer monsoon failure. Geophys Res Lett. http://doi.org/10.1029/2010GL042798

Rayner NA, Parker DE, Horton EB, Folland CK, Alexander LV, Rowell DP, Kent E, Kaplan, A (2003) Global analyzes of sea surface temperature, sea ice, and night marine air temperature since the late nineteenth century. J Geophys Res. http://doi.org/10.1029/2002JD002670

Revadekar JV, Varikoden H, Preethi B, Mujumdar M (2016) Precipitation extremes during Indian summer monsoon: role of cyclonic disturbances. Nat Hazards 81:1611-1625

Roxy MK, Ritika K, Terray P, Murtugudde R, Ashok K, Goswami BN (2015) Drying of Indian subcontinent by rapid Indian Ocean warming and a weakening land-sea thermal gradient. Nat Commun 6:1-10

Roy I **(**2017) Indian summer monsoon and El Niño southern oscillation in CMIP5 models: a few areas of agreement and disagreement. Atmosphere. https://doi.org/10.3390/atmos8080154

Roy I, Tedeschi RG**,** Collins M (2019) ENSO teleconnections to the Indian summer monsoon under changing climate. Int J Climatol 39:3031-3042

Roy SS, Goodrich GB, Balling RC (2003) Influence of El Niño/southern oscillation, Pacific decadal oscillation, and local sea-surface temperature anomalies on peak season monsoon precipitation in India. Clim Res 25:171–178

Sabeerali CT, Ajayamohan RS, Bangalath HK, Chen N (2019) Atlantic Zonal Mode: an emerging source of Indian summer monsoon variability in a warming world. Geophys Res Lett 46:4460–4464

Sabeerali CT, Rao SA, Ajayamohan RS, Murtugudde R (2012) On the relationship between Indian summer monsoon withdrawal and Indo-Pacific SST anomalies before and after 1976/1977 climate shift. Clim Dyn 39:841-859.

Sabeerali CT, Rao SA, Dhakate AR, Salunke K, Goswami BN (2015) Why ensemble mean projection of south Asian monsoon rainfall by CMIP5 models is not reliable?. Clim Dyn 45:161-174

Sahana AS, Ghosh S, Ganguly A, Murtugudde R (2015) Shift in Indian summer monsoon onset during 1976/1977. Environ Res Lett 10 054006

Saji NH, Goswami BN, Vinayachandran PN, Yamagata T (1999) A dipole mode in the tropical Indian Ocean. Nature 401:360-363

Saji NH, Yamagata T (2003) Possible impacts of Indian Ocean Dipole mode events on global climate. Clim Res 25:151-169

Sandeep S, Ajayamohan RS, Boos WR, Sabin TP, Praveen V (2018). Decline and poleward shift in Indian summer monsoon synoptic activity in a warming climate. Proc Natl Acad Sci 115:2681–2686

Sarthi PP, Ghosh S, Kumar P (2015) Possible future projection of Indian Summer Monsoon Rainfall (ISMR) with the evaluation of model performance in Coupled Model Inter-comparison Project Phase 5 (CMIP5). Glob Planet Change 129:92-106

Seetha CJ, Varikoden H, Babu CA, Kuttipurath J (2020) Significant changes in the ENSO-monsoon relationship and associated circulation features on multidecadal timescale. Clim Dyn 54:1491-1506

Sengupta D, Goswami BN, Senam R (2001) Coherent intraseasonal oscillations of Ocean and atmosphere during the Asian summer monsoon. Geophys Res Lett 28:4127-4130

Sharmila S, Joseph S, Sahai AK, Abhilash S, Chattopadhyay R (2015) Future projection of Indian summer monsoon variability under climate change scenario: An assessment from CMIP5 climate models. Glob Planet Change 124:62-78

Shukla J, Paolino DA (1983) The Southern Oscillation and long-range forecasting of the summer monsoon rainfall over India. Mon Weather Rev 111:1830-1837

Sikka DR (1980) Some aspects of the large scale fluctuations of summer monsoon rainfall over India in relation to fluctuations in the planetary and regional

scale circulation parameters. Proc Indian Acad Sci (Earth Planet Sci) 89:179-195

Sinha A, Belkerhammer M, Stott L, Mudelsee M, Cheng H (2011) The leading mode of Indian Summer Monsoon precipitation variability during the last millennium. Geophys Res Lett. http://doi.org/10.1029/2011GL047713

Slingo JM (1987) The development and verification of a cloud prediction scheme for the ECMWF model. Q J R Meteorol Soc 113:899–927

Slingo JM, Annamalai H (2000) 1997: The El Nino of the century and the response of the Indian Summer Monsoon. Mon Weather Rev 128:1778-1797

Sreekanth TS, Varikoden H, Resmi EA, Mohankumar G (2019) Classification and seasonal distribution of rain types based on surface and radar observations over a tropical coastal station. Atmos Res 218:90-98

Stachnik JP, Schumacher C (2011) A comparison of the Hadley circulation in modern reanalyses. Geophys Res Lett. http://doi.org/10.1029/2011JD016677

Sudeepkumar BL, Babu CA, Varikoden H (2018) Future projections of active-break spells of Indian summer monsoon in a climate change perspective. Glob Planet Change 161:222-230.

Suhas E, Goswami BN (2008) Regime shift in Indian summer monsoon climatological intraseasonal oscillations. Geophys Res Lett. http://doi.org10.1029/2008GL035511

Suhas E, Neena JM, Goswami BN (2012) Interannual variability of Indian summer monsoon arising from interactions between seasonal mean and intraseasonal oscillations. J Atmos Sci 69:1761-1774

Sun F, Hall A, Qu X (2011) On the relationship between low cloud variability and lower tropospheric stability in the Southeast Pacific. Atmos Chem Phys 11:9053-9065

Suthinkumar PS, Babu CA, Varikoden H (2019) Spatial Distribution of Extreme Rainfall Events During 2017 Southwest Monsoon over Indian Subcontinent. Pure Appl Geophys 176:5431-5443

Swapna P, Krishnan R, Wallace JM (2014) Indian Ocean and monsoon coupled interactions in a warming environment. Clim Dyn 42:2439-2454

Taraphdar S, Mukhopadhyay P, Goswami BN (2010) Predictability of Indian summer monsoon weather during active and break phases using a high resolution regional model. Geophys Res Lett. http://doi.org/10.1029/2010GL044969

Taylor KE (2001) Summarizing multiple aspects of model performance in a single diagram. J Geophys Res 106:7183-7192

Taylor KE, Stouffer RJ, Meehl GA (2009) A Summary of the CMIP5 Experiment Design, available at http://cmippcmdi.llnl.gov/cmip5/experimentdesign.html, 33pp.

Taylor KE, Stouffer RJ, Meehl GA (2012) An overview of CMIP5 and the experiment design. Bull Amer Meteorol Soc 93:485-498

Thomson AM, Calvin KV, Smith SJ, Kyle GP, Volke A, Patel P, Delgado-Arias S, Bond-Lamberty B, Wise MA, Clarke LE, Edmonds JA (2011) RCP 4.5: a pathway for stabilization of radiative forcing by 2100. Clim Change 109:77-94

Trenberth KE, Hurrell JW (1994) Decadal atmosphere-ocean variations in the Pacific. Clim Dyn 9:303-319

Trenberth KE, Stepaniak DP, Caron JM (2000) The global monsoon as seen through the divergent atmospheric circulation. J Clim 13:3969-3993

Ummenhofer CC, Sen Gupta A, Li Y, Taschetto AS, England MH (2011) Multi-decadal modulation of the El Niño–Indian monsoon relationship by Indian Ocean variability. Environ Res Lett. http://doi.org/10.1088/1748-9326/6/3/034006

Van Vuuren DP, Edmonds J, Kainuma M, Riahi K, Thomson A, Hibbard K, Hurtt GC, Kram, T, Krey V, Lamarque JF Masui T (2011) The representative concentration pathways: an overview. Clim Change 109:5-31

Varikoden H, Babu CA (2015) Indian summer monsoon rainfall and its relation with SST in the equatorial Atlantic and Pacific Oceans. Int J Climatol 35:1192-1200

Varikoden H, Harikumar R, Vishnu R, Sasi Kumar V (2011) Observational study of cloud base height and its frequency over a tropical station, Thiruvananthapuram, using a ceilometers. Int J Remote Sens 32:8505-8518

Varikoden H, Kumar KK, Babu CA (2013) Long term trends of seasonal and monthly rainfall in different intensity ranges over Indian subcontinent. Mausam 64:481-488

Varikoden H, Mujumdar M, Revadekar JV, Sooraj KP, Ramarao MVS, Sanjay J, Krishnan R (2018) Assessment of regional downscaling simulations for long term mean, excess and deficit Indian Summer Monsoons. Glob Planet Change 162:28-38

Varikoden H, Preethi B (2013) Wet and dry years of Indian summer monsoon and its relation with Indo-Pacific sea surface temperatures. Int J Climatol 33:1761-1771

Varikoden H, Revadekar JV (2019) On the extreme rainfall events during the southwest monsoon season in northeast regions of the Indian subcontinent. Meteorol Appl 27:1–13

Varikoden H, Revadekar JV, Kuttippurath J, Babu CA (2019) Contrasting trends in southwest monsoon rainfall over the Western Ghats region of India. Clim Dyn 52:4557-4566

Vinayachandran PN, Iizukabv S, Yamagata T (2002) Indian Ocean dipole mode events in an ocean general circulation model. Deep Sea Res Part II 49:1573–1596

Vishnu S, Francis PA, Shenoi SC, Ramakrishna SV (2018) On the relationship between the Pacific Decadal Osillation and monsoon depressions over the Bay of Bengal. Atmos sci Lett. http://doi.org/10.1002/asl.825

Wang B (2006) The Asian monsoon. Springer, Berlin Heidelberg.

Wang B, Fan Z (1999) Choice of South Asian summer monsoon indices. Bull Amer Meteorol Soc 80:629–638

Wang B, Lee JY, Xiang B (2015) Asian summer monsoon rainfall predictability: a predictable mode analysis. Clim Dyn 44:61-74

Wang B, Wu R, Li T (2003) Atmosphere–warm Ocean interaction and Its Impacts on Asian–Australian monsoon variation. J Clim 16:1195-1211

Wang B, Yim SY, Lee JY, Liu J, Ha KJ (2014) Future change of Asian-Australian monsoon under RCP 4.5 anthropogenic warming scenario. Clim Dyn 42:83-100

Webster PJ, Magana VO, Palmer TN, Shukla J, Tomas RA, Yanai MU, Yasunari T (1998) Monsoons: Processes, predictability, and the prospects for prediction. J Geophys Res 103:14451-14510

Webster PJ, Moore AM, Loschnigg JP, Leben RR (1999) Coupled ocean-atmosphere dynamics in the Indian Ocean during 1997–98. Nature 401:356–360

Wood R, Bretherton CS (2006) On the relationship between stratiform low cloud cover and lower tropospheric stability. J Clim 19:6425-6431

Wood R, Hartmann DL (2006) Spatial variability of liquid water path in marine boundary layer clouds: The importance of mesoscale cellular convection. J Climate 19:1748-1964

Wu R, Kirtman BP (2004) Impacts of the Indian Ocean on the Indian summer monsoon –ENSO relationship. J Clim 17:3037-3054

Xavier PK, Marzin C, Goswami BN (2007) An objective definition of the Indian summer monsoon season and a new perspective on the ENSO-monsoon relationship. Q J R Meteorol Soc133:749-764

Yamagata T, Behera SK, Luo JJ, Masson S, Jury MR, Rao SA (2004) Coupled ocean-atmosphere variability in the tropical Indian Ocean. Geophys Monogr Ser. http://doi.org/10.1029/147GM12

Yamagata T, Behera SK, Rao SA, Guan Z, Ashok K, Saji HN (2003) Comments on ‘dipoles, temperature gradients, and tropical climate anomalies. Bull Amer Meteorol Soc 84:1418-1421

Yatagai A, Kamiguchi K, Arakawa O, Hamada A, Yasutomi N, Kitoh, A (2012) APHRODITE: Constructing a long-term daily gridded precipitation dataset for Asia based on a dense network of rain gauges. Bull Amer Meteorol Soc 93:1401-1415

Zhang Y, Stevens B, Medeiros B, Ghil M (2009) Low-cloud fraction, lower tropospheric stability and large scale divergence. J Clim 22:4827-4844

****